To the Graduate Council:

I am submitting herewith a dissertation written by John R. White entitled "Conceptual Development of a Complete LWR Reload Design Methodology Based on Generalized Perturbation Theory." I have examined the final copy of this dissertation for form and content and recommend that it be accepted in partial fulfillment of the requirements for the degree of Doctor of Philosophy, with a major in Nuclear Engineering.

H. L. Dodds Jr., Major Professor

We have read this dissertation
and recommend its acceptance:

Accepted for the Council:

Vice Provost
and Dean of the Graduate School

CONCEPTUAL DEVELOPMENT OF A COMPLETE LWR RELOAD DESIGN METHODOLOGY BASED ON GENERALIZED PERTURBATION THEORY

A Dissertation

Presented for the

Doctor of Philosophy

Degree

The University of Tennessee, Knoxville

John R. White

March 1987

ACKNOWLEDGEMENTS

The author wishes to express his appreciation for the support and encouragement of Dr. H. L. Dodds Jr., his major professor, and the University of Tennessee faculty who served on his Graduate Committee.

The author would also like to thank several graduate students at the University of Lowell for their patience and willingness to listen to the author talk about the development and application of perturbation theory methods for countless hours. He would also like to single out Mr. David Chapman and Mr. Byron Frank for their direct assistance in parts of the work presented here. In particular, Mr. Chapman is the main author of the code that interfaces the VENTURE-generated sensitivity library to the BBMIP optimization algorithm, and Mr. Frank is currently implementing and testing the new GPT formulation developed as part of this work. The explicit contributions and many hours of discussion with these two University of Lowell students are greatly appreciated.

Last but not least, the author would like to express his sincere affection and gratitude to his wife, Joan, and his children, April and Amy, for their patience, sacrifice, and moral support during the several years that it took to complete this research. Hopefully we can start living a normal life again!

This research was supported in part by Westinghouse Electric Corporation.

ABSTRACT

A new approach for the physics design and analysis of LWR reload cores is developed and demonstrated through several practical applications. This new design philosophy uses first- and second-order response derivatives to predict the important reactor performance characteristics (power peaking, reactivity coefficients, etc.) for any number of possible material configurations (assembly shuffling and burnable poison loadings). The response derivatives are computed using generalized perturbation theory (GPT) techniques.

This report describes in detail an idealized GPT-based design system. The idealized system would contain individual modules to generate the required first-order and higher-order sensitivity data. It would also contain at least two major application codes; one for core design optimization and the other for evaluation of several safety parameters of interest in off-normal situations. This ideal system would be fully automated, user-friendly, and quite flexible in its ability to provide a variety of design and analysis capabilities.

Three major components of the system are discussed in detail. First, a GPT-based optimization algorithm is developed, implemented, and illustrated in several applications. The extremely good results obtained in these demonstrations clearly show the potential of the overall methodology. Next, a new first-order GPT formulation that includes macroscopic depletion, k-reset via soluble boron control, and poison and thermal-hydraulic feedback effects is developed. The feedback treatment in the adjoint mode is verified through analytical and numerical illustrations. Finally, several aspects of a practical approach to higher-order GPT are addressed. In particular, a formal second-

order GPT formulation is developed and three promising techniques for calculating the required flux derivatives are identified.

The information gained from these three studies gives a good foundation for the development of a complete integrated design package. The initial testing and applications documented herein verify the feasibility of the basic concept and illustrate the unique capabilities and overall potential of the GPT-based design methodology. The actual implementation of a production-oriented GPT-based design system is identified as the logical follow-up to this work.

TABLE OF CONTENTS

SECTION	PAGE
I. INTRODUCTION/OVERVIEW	1
II. THE GPT-BASED DESIGN SYSTEM	5
III. GPT-BASED FUEL MANAGEMENT OPTIMIZATION	10
III.1 Introduction	10
III.2 Problem Formulation	16
III.3 Illustrative Applications	24
A. The Tools	24
B. Reference Model	26
C. Direct Perturbations	29
D. BP Optimization	35
E. Combined Optimization	38
III.4 Summary Comments	41
IV. DEVELOPMENT OF LWR-COMPATIBLE GPT METHODS	44
IV.1 Historical Perspective	44
IV.2 General GPT Formulation	49
IV.3 Solution of the Flux Equations	62
IV.4 Verification of Method	64
A. Analytical Example	65
B. Numerical Examples	68
IV.5 Summary	73
V. IN SEARCH OF HIGHER-ORDER ACCURACY	76
V.1 Introduction	76
V.2 Basic Problem Description	77

V.3 Second-Order GPT 81
V.4 Calculation of the Flux Derivatives 86
A. Choice of Independent Variables 86
B. Solution Schemes 88
V.5 Summary 95
VI. CONCLUSIONS AND FUTURE WORK 97
VI.1 Conclusions 97
VI.2 Future Work 102
LIST OF REFERENCES 105
APPENDIXES 114
APPENDIX A DERIVATION OF SECOND-ORDER GPT USING A DIFFERENTIAL APPROACH 115
APPENDIX B LOCAL VERSUS GLOBAL EFFECTS 119
APPENDIX C VERIFICATION OF GREEN'S FUNCTION PERTURBATION METHOD 124
VITA 128

LIST OF TABLES

TABLE		PAGE
3.1	Representative Sampling of Fuel Management Optimization Studies	12
3.2	Material Perturbations Used to Evaluate Accuracy of GPT/DPT Formulation	30
3.3	GPT/DPT Versus Direct Calculations for the K_{eff} Responses	32
3.4	GPT Versus Direct Calculations for Selected BOC Relative Power Responses	33
3.5	Summary of Overall Accuracy of BOC GPT Predictions	34
4.1	Comparison of GPT Estimates With and Without Feedbacks Versus Direct Computations	71
4.2	Comparison of Explicit and Implicit Components of GPT Predictions	73
B.1	GPT Estimates for Several Responses for the Rod-Insertion Problem in the 2-D IAEA Configuration	122
B.2	GPT Estimates for Several Responses for the Rod-Ejection Problem in the 2-D IAEA Configuration	123
C.1	Comparison of Delta Flux Predictions for Rod Insertion in Central Zone of Simple 1-D Model	125
C.2	Delta Flux Convergence Rates for Rod Insertion in Central Zone of Simple 1-D Model	126

LIST OF FIGURES

FIGURE		PAGE
2.1	Schematic Diagram of GPT-Based Design System	7
3.1	VENTURE Quarter-Core Configuration	27
3.2	Eighth-Core Map with Results for Reference Core Configuration...	28
3.3	Eighth-Core Map with GPT versus Direct Results for BP Optimization Case with $P_{max} = 1.27$	37
3.4	Eighth-Core Map with GPT versus Direct Results for Combined Optimization Case	39
4.1	Outline of Calculational Procedure for Solution of Adjoint Depletion Equations	60
4.2	Quarter-Core IAEA PWR Benchmark Configuration	69

I. INTRODUCTION / OVERVIEW

Generalized Perturbation Theory (GPT) is a technique used to estimate changes in various reactor performance parameters arising from changes in the core material configuration. GPT methods use adjoint sensitivity theory in which the response derivatives (or sensitivities) are independent of the system perturbations. This fact makes first-order perturbation methods very cost effective when many material variations must be evaluated (as in reload design analyses).

GPT methods have been available for many years, but there has been relatively little application of these techniques outside the field of cross section sensitivity and uncertainty analysis.[1-10] The present author has been involved extensively in the development and application of GPT methods for several years, including the development and implementation of Depletion Perturbation Theory (DPT).[11-25] During the last three years, this involvement has focused on the application of GPT methods for the design and optimization of Light Water Reactor (LWR) reloads.[26-29] In particular, the basis for a complete GPT-based LWR reload design methodology has evolved during this time. The current document will present this new approach to core design.

The main emphasis of the present research is the evaluation of GPT techniques for use in the LWR in-core fuel management design process. The process of determining a suitable loading pattern is manpower intensive since many trial and error computations are required to identify a potentially acceptable pattern. There are several semi-automated procedures available to aid the engineer in his quest for the best loading scheme, but many of these tools only solve some simplified problem or in some way fall short of the

intended goal (see Ref. 30 for example). The preliminary investigations into GPT-based optimization methods performed as part of this work suggest that perturbation techniques just might be able to fill the gap that currently exists in this area. A comprehensive GPT sensitivity library, coupled with a standard integer programming package or a specially designed algorithm for evaluating numerous loading patterns, may provide the designer with an invaluable analysis tool.

A related (but secondary) objective of the current research effort is the evaluation of GPT methods as a tool for estimating several of the safety parameters that must be determined for each new design. Once an acceptable reload configuration and burnable poison (BP) pattern are established, the engineer must insure that this fuel management scheme will satisfy plant technical specifications under a wide range of operational conditions. The computations required to verify that the safety requirements are met are repetitious and tedious in nature. They involve the evaluation of several core configurations that represent variations from the reference full-power all-rods-out (ARO) core design. The new configurations are simply perturbations upon some reference state; thus GPT methods may indeed be a powerful tool here.

The key ingredient in the above discussion is the ability to generate a comprehensive GPT sensitivity library. Both applications, the use of GPT-based optimization methods and the prediction of the safety parameters, require complete, easy-to-use, and accurate response derivatives that are consistent with standard procedures used in the forward design process. These derivatives will be generated via the adjoint functions of first-order GPT. In addition, some applications (especially for the evaluation of the

safety parameters) may require higher accuracy than can be obtained with first-order GPT. Thus, there is also a need to develop an easy-to-use higher-order correction technique to be utilized in conjunction with first-order GPT.

The above brief discussion summarizes the overall goals of this dissertation research. In particular, several items that require considerable research and development were identified as follows:

1. Development of a complete GPT-based design philosophy,
2. Development of an efficient GPT-based optimization algorithm,
3. Development of a first-order LWR-compatible GPT formulation (with thermal-hydraulic feedback, criticality reset, etc.), and
4. Investigation of realistic approaches to higher-order GPT.

The objectives of this dissertation research are to address the theoretical aspects of each of these items in detail and to integrate (conceptually) each component within a complete design system. The accomplishment of these goals is documented in the remainder of this report. Section II first presents an overview of the basic concept of a GPT-based design system. Here the emphasis is on the major building blocks of the complete system and on the interfacing and designer interaction with the various modules. The key components are a GPT-based optimization module, a safety parameter predictive tool, and two blocks for the generation of the first- and higher-order response derivatives that make up the required sensitivity library.

Section III presents the GPT-based optimization algorithm and some illustrative applications which highlight the overall potential of the method. Sections IV and V then discuss the generation of the first-order sensitivities and higher-order corrections to first-order GPT, respectively. These GPT methods are fully compatible with current LWR design practices (which

include macro depletion models, thermal-hydraulic and poison feedbacks, and a criticality reset mechanism). Finally, Section VI summarizes this research effort and suggests areas requiring further study. The overall GPT-based design concept as well as the theory for the specific components of the complete system (discussed separately in Sections III - V) represent original contributions to the field. The reader will discover that there is still much work to be done towards developing a practical GPT-based design package. However, much of this work will be the actual implementation of a production-oriented system, since the research presented here provides a good theoretical foundation and verification of the basic concept.

II. THE GPT-BASED DESIGN SYSTEM

Before discussing the theoretical details of optimization methods and first- and higher-order GPT for LWR applications, it is appropriate to outline how these new developments will interface with existing LWR design procedures. The previous section has hinted at the construction of a complete GPT-based design system, but some of the details still may be a bit vague. Thus, the purpose of this section is to describe the system in detail, with special emphasis on how the individual components contribute to the overall capability.

Simply stated, the long-term goal of this overall effort is the development and application of a GPT-based core design software package. The package will consist of some standard neutronics design tools presently available, plus several additional modules to determine the first- and higher-order response derivatives and to perform the optimization applications and safety analyses. It is assumed that the main forward design tool will be a state-of-the-art code which will be based on either the finite difference scheme or on some nodal approximation. Thus, any GPT development work should be general enough to be compatible with either approach. The specific coding details and notation for a nodal-based GPT method would be different than an adjoint method based on the finite-difference technique. However, the base theoretical formulation (with all equations written in a general operator notation) should be the same. The important point here is that the GPT capability must be fully compatible with the forward design code.

The applications portions of the overall system should not be sensitive to the details of the GPT formulation, since they rely solely on the availability of

a response sensitivity library; not on the details of how the library was generated. The optimization applications package can be quite general, since determining fuel shuffling patterns and burnable poison (BP) loadings subject to given constraints is a fairly standard (but tedious) procedure. The safety evaluation model on the other hand, may require some specialization, since specific procedures for generating the required data may be tied to the forward design methodology.

A rough sketch of the GPT-based design system proposed here is given in Figure 2.1. The emphasis in this schematic is on portraying the big picture, with special attention given to the designer interaction with the system and to the interfacing of the various modules. There are two boxes containing GPT methods. The first-order capability is integrated as part of the forward design code and the higher-order correction terms are calculated in a separate module.

The desired response derivatives output from the GPT modules are directed to the Sensitivity Library. This library is really the focal point or heart of the GPT-based system. Most of the computational power of the proposed system is expended in generating this resource. Once a comprehensive set of accurate response derivatives is prepared, operation of the application packages becomes quite straightforward. At this point, a simple truncated Taylor series expansion (using the response derivatives) is utilized to estimate the new responses for a variety of perturbations to the reference configuration. In both the optimization applications and the safety analyses, the evaluation of many new configurations is the name of the game. The ease with which these evaluations can be made is the main advantage of the GPT approach. An initial investment is made in computer resources for

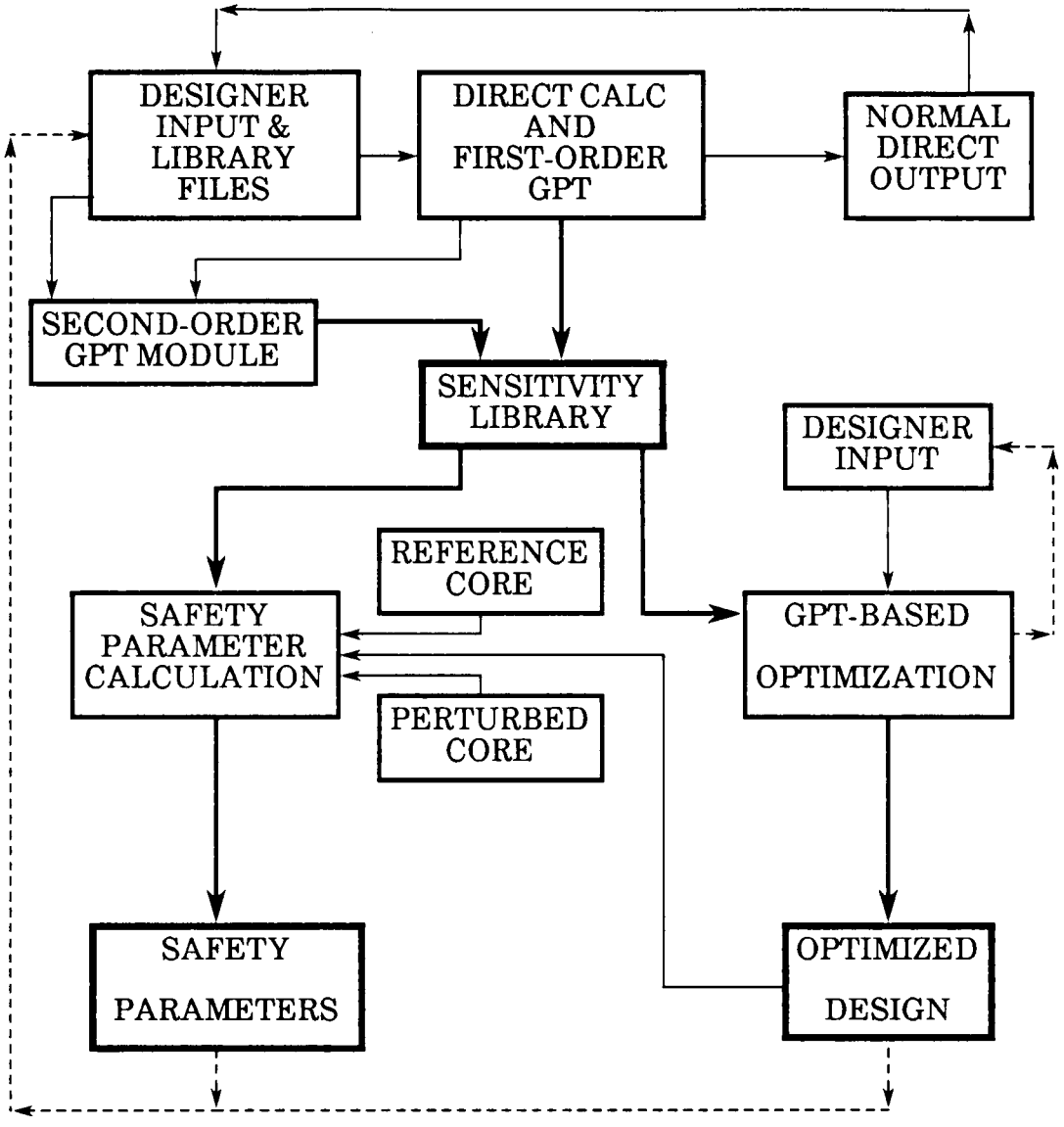


Figure 2.1 Schematic Diagram of GPT-Based Design System

the preparation of the sensitivity library and the payback comes in the ease, efficiency, and the flexibility of the application packages.

The designer can interact with the system in several ways. First the engineer must define the so-called reference configuration. Once defined, a simple switch would then turn on the first-order GPT capability within the standard design code and generate part of the sensitivity library. There will be an outer loop within the code so that the desired derivatives for several responses can be determined in a single code access. The higher-order correction terms could then be determined in a separate step, using the first-order sensitivity functions and some calculated estimate of the perturbed flux distribution. The higher-order derivatives are added to the sensitivity library to complete the first step of this analysis. In an ideal system, generation of the sensitivity library could be performed within a few days. A couple of computer runs to generate the first-order data and another few automated sequences to compute the higher-order corrections would be the only requirements. These computations would be computer intensive but, if properly automated, they would require little manual intervention. This could represent a considerable savings in manpower costs and actual calendar time for the complete design process.

Within this system the designer has considerable flexibility since access to the sensitivity library makes it very easy to estimate the performance of any new configuration. The iterative design process can be manual within an interactive design tool or it can be automated within a sophisticated optimization software package. In practice, both options are desirable.

Once a potentially acceptable design configuration is obtained the designer would exercise the safety analysis package to evaluate the

performance of the given configuration under a variety of operational conditions. Each new condition represents a perturbation to the reference state. By determining the change in the reference macroscopic cross sections associated with the given perturbation, one can easily estimate the new response behavior by using up to two terms in the Taylor series expansion. Using this simple procedure, one can investigate any number of operational conditions.

The design system proposed above, if automated in a user-friendly applications package, could represent a significant upgrade to current methods for performing reload analyses. The key to making this a reality is the development of an accurate and comprehensive GPT capability that incorporates all the features currently used in the forward design process (such as treating feedback effects and criticality reset). Development of the application packages is also very important. Although implementation of the optimization and safety analysis capability appears conceptually straightforward, actual programming of production versions of these packages may prove to be quite challenging.

III. GPT-BASED FUEL MANAGEMENT OPTIMIZATION

To illustrate the overall potential of the proposed GPT-based design system, it is appropriate to describe in detail the use of GPT-based methods in a specific area of application. The inherent complexity of the in-core fuel management process makes this application a suitable candidate for demonstration of the power of the GPT methodology. Thus, this section will define the task at hand, develop a formal GPT-based algorithm for solution of the fuel management problem, and present several actual applications of the method.

III.1 Introduction

In fuel reload design, the desired end product is a fuel shuffling pattern and BP loading scheme that satisfies all design criteria (peaking factor limits, shutdown margins, cycle energy requirements, etc.). In addition, it would be nice if the final scheme also represented the best configuration in terms of cost versus performance. In practice, the difficulty involved in finding a single feasible solution (one which satisfies all constraints) dominates the design philosophy. Thus, the reload engineer is usually satisfied with a feasible solution, and he is not really concerned with the question of choosing the best or optimal design. His main concerns lie in the ease-of-use of the various software packages used in the design process and in the availability of a design methodology that can guide him in his search for a good feasible reload configuration.

With this philosophy, it is understandable that a considerable amount of work has gone into automating the fuel management design process. Much of this work was done by the engineers and computer applications personnel

directly involved in the actual design process. This work involved interfacing several individual codes, providing automated calculational sequences, and developing user-friendly input and output interfaces (data base management systems, interactive graphics, etc.). These improvements have made the reload design process much less tedious (and almost bearable). Examples of several specific efforts in this area are contained in Ref. 30.

In parallel with this automation effort, researchers have investigated a variety of techniques that can aid the engineer in choosing a suitable reload pattern. These fuel management optimization studies have used a variety of techniques (linear, integer, quadratic, and dynamic programming, gradient projection methods, and direct search algorithms), and some authors have even coupled in the use of perturbation methods.[31-75] Most of these schemes have had partial success, but typically they have been restricted to specific applications, simplified models, multistage optimization, etc. In practice, there does not appear to be a general purpose algorithm that tackles the full complexity of the complete fuel management problem. It is hoped that the GPT-based formulation outlined in this work will fill this gap.[26-27]

Table 3.1 contains a representative sampling of the many fuel management optimization studies that have been performed over the last twenty years. An attempt has been made to classify the various studies into several broad categories. This classification scheme is quite arbitrary and the boundaries of each group are quite flexible.

Table 3.1 serves several functions. First, it gives a concise chronological presentation of the various contributions to the field and the major areas that were addressed. The work in the late 60's and early 70's concentrated on the ex-core fuel management problem, where simple core models were sufficient

TABLE 3.1 Representative Sampling of Fuel Management Optimization Studies

Author	Ref.	Date	Model[a]	Multi-Stage	Pert.[b] Theory	Obj.[c] Func.	BPs
Wall & French	31	1965	1, 2			1	
Melice	33	1969	1, 2		3	2	
Suzuki & Kiyose	36	1971	1, 2			1	
Sauar	37	1971	1, 2			1	
Wade & Terney	38	1971	1		3	5	
Naft & Sesonske	39	1972	1, 3			5	
Stout & Robinson	40	1973	3			4	
Federowicz & Stover	43	1973	3		1	4	
Chitkara et al.	45	1974	2a, 3		1	1	
Mingle	46	1975	1, 3	X	2	1,5	
Motoda et al.	47	1975	1, 2, 3	X		1	
Huang & Levine	50,51	1978	2, 3		1	4,2	
Sekimizu	53	1978	1, 3	X		3	
Lin et al.	54	1979	2a, 3		1	1	
Terney et al.	56	1982	3		3	5	
Ho & Rohach	58	1982	3		2	4	
Ho & Sesonske	60	1982	1, 2, 3			4	X
Chang & Sesonske	67	1984	3			2	X
Ahn & Levine	69	1985	1, 2, 3	X	1	1	X
Hobson & Turinsky	72	1986	3		1	2	
Morita et al.	73	1986	3			6	X
Downar & Kim	75	1986	3	X		6	X
White et al.	27	1986	3		3	6	X

[a]Model 1 simple model
2 multicycle
2a equil. cycle
3 detailed core loading

[b]Pert. Theory 1 Direct Method
2 Standard Pert. Theory
3 Gen. Pert. Theory

[c]Obj. Func. 1 cost or amount of fuel
2 reactivity
3 burnup
4 power peaking
5 flexible with soft constraints
6 flexible with hard constraints

for calculating inventory and enrichment requirements and fuel costs over several cycles. Since the early 70's, an extensive effort has been ongoing to determine the detailed placement of the individual assemblies within the core (what this author calls in-core fuel management).

The general in-core problem is so complex that many simplifying arguments were required. For example, Stout and Robinson[40] utilized a relatively rigid set of logical shuffling rules and several authors (see Table 3.1) have broken the full problem into separate stages, each nearly independent of the other. The most common simplification in the multistage optimization studies is the zoning of the new and partially burnt fuel into several regions and then determining the placement of individual assemblies within each region.

Of specific interest in this study is the use of perturbation theory methods for fuel management optimization. As can be seen in Table 3.1, this idea has intrigued several researchers over the years. Many studies have used direct perturbation techniques, standard perturbation theory, and static generalized perturbation theory methods. All of these efforts use a linearized iteration scheme where the size of the perturbation is limited to minimize nonlinear effects. New response derivatives are computed each iteration until no further improvement is obtained.

These perturbation-based schemes have two basic drawbacks; the high cost of repetitively calculating the required derivatives (either by direct or adjoint methods) and the specificity of the optimization problem that is solved. The second concern is probably the most limiting since many months (or years) of development effort and engineering analysis can go into the production of a specific tool; only to find out that it is too rigid to be useful in

an ever-changing design environment. The current emphasis on techniques that handle the burnable poison (BP) problem in addition to fuel shuffling (see Table 3.1) is evidence of the shifting needs of the designer. With increased interest in extended fuel cycles and low-leakage cores, the use of BPs has become a necessity. This has made many of the earlier rigid methods that were based on out-in or checkerboard loading schemes somewhat outdated.

Another major concern with rigid fuel management tools is that there is no universally accepted criteria for choosing the best core design. Some authors maximize burnup, some minimize power peaking, some maximize BOC or EOC reactivity, and others try to optimize fuel-cycle costs directly. This author contends that there is no one solution to this dilemma; the complete fuel reload design process is just too complex for any simple answer. Thus, maximum flexibility should be a primary consideration in the development of any fuel management design tool. This has been the trend in most recent studies (see last three entries in Table 3.1).

The above considerations have influenced the current development of a GPT-based optimization algorithm. The experience gained from the studies listed in Table 3.1 has been extremely useful. In addition, the works of Gandini[32] and Rozon et al.[55] were particularly pertinent to this study. Although they did not address explicit LWR applications, they do introduce the formal connection between the use of generalized perturbation theory and the design optimization process (for LMFBRs and CANDUs, respectively). Terney and Williamson's optimal control approach[56] is also very relevant, and their work does concentrate on LWR design. However, their studies promote the linearized iteration technique (which this author feels is not necessary) and they utilize soft constraints within the definition of the objective function.

This latter procedure is sometimes called the penalty function approach for treating constraints.[76] In general, this technique only allows a qualitative analysis of the problem.

The trade-off here should be clear. If an iterative scheme is used, a large number of adjoint computations each iteration becomes infeasible. Therefore, one must combine several key constraints into a global (nonphysical) performance index that gives a qualitative measure of the system behavior. On the other hand, if a once-through optimization scheme is employed, the important constraints (peaking factors, reactivity, etc.) can be treated explicitly, since the appropriate importance functions will only have to be computed once (and saved within the sensitivity library). This author feels that the second approach is a more direct attack on the given problem and it should help alleviate much of the highly nonlinear behavior that was observed with the penalty function technique.[56]

Based on the above discussions, the criteria set forth in this work are,

1. Flexibility in choice of objective function and constraints,
2. Overall ease of use,
3. Cost effectiveness in terms of the manual design process (with emphasis on manpower required), and
4. Emphasis on feasible rather than optimal solutions.

Flexibility, user-friendliness, and cost-effectiveness are common goals of any code development effort. The concept of feasible rather than optimal designs is somewhat unique. However, in light of the dilemma as to what is optimum, this terminology is justified.

Although somewhat abstract, these criteria have impacted the choice of a once-through GPT-based scheme. The GPT-based design system described in

Section II meets these criteria. GPT allows a flexible choice of the objective function and constraints on the system. Once the sensitivity library is generated, the optimization applications package can be developed to be extremely user-friendly. Also, since the development of the sensitivity library can be completely automated, there should be considerable savings in manpower (and possibly computer) costs relative to the currently used manual iteration process. Finally, since the ultimate goal is a good feasible reload scheme, a little inaccuracy in the first-order GPT response predictions is tolerable, as long as the final detailed design computations verify the feasibility of the final fuel and BP loadings.

The key premise here is the suggestion that a non-iterative first-order Taylor series approximation for the important design parameters will be sufficiently accurate to serve as the basis for an automated design tool. Clearly one must demonstrate the validity of this hypothesis. The remainder of this section is devoted to this task.

III.2 Problem Formulation

In fuel shuffling studies the desired responses are complex functions of the reload pattern and, in general, a new solution of the few-group two-dimensional diffusion equation is required for each combination of independent variables. Because of the large number of possibilities, a direct assault on this problem is not practical due to time and cost considerations. However, if these responses can be written as algebraic functions of the independent variables with the use of GPT sensitivity functions, then one can take advantage of standard linear optimization theory principles. If a set of first-order derivatives is available in library format (from previous GPT calculations), then an efficient algorithm can be developed.

A major difficulty in formulating an appropriate optimization scheme is related to the discrete nature of the fuel shuffling process. The change in the independent variables (burnup, BP loading, etc.) is not a continuous function, since only discrete assembly interchanges and BP additions are allowed. A solution to this problem is to use some form of integer programming in which the independent variables are forced to have discrete (integer) values.[77-78] This type of optimization scheme is more complicated than continuous linear programming, but software is available that treats the IP problem.

To illustrate the level of difficulty involved in the reload design process, consider the following problem description: "Given the present end-of-cycle (EOC) configuration and the number and enrichment of fresh fuel assemblies for the next cycle, determine the beginning-of-cycle (BOC) reload pattern that maximizes the cycle length (i.e. maximize EOC K_{eff}) subject to the constraints that all safety-related criteria (peaking factors, shutdown margins, moderator temperature coefficients, etc.) are satisfied." The solution to this problem is very complex in practice, but conceptually, it is a straightforward description of a constrained optimization problem. The objective function is the cycle length (or EOC K_{eff}) and the nuclear constraints are the safety parameters. This problem can be stated mathematically as

maximize $\quad F(y_n)$

subject to $\quad b_{kl} \leq C_k(y_n) \leq b_{ku}$

where both the objective function F and the constraints C_k are functions of the independent variables, y_n. The b_k's are the upper and lower bounds on the constraints. In addition to the nuclear constraints, physical limitations on the independent variables are usually necessary and these are treated in a similar manner.

There is a large number of optimization techniques for the solution of constrained problems of this type.[77-78] These procedures require several functional evaluations of the objective function and constraints for various possible combinations of the independent variables for the problem. Since solution of the few-group diffusion equation for each set of functional evaluations is not practical, an alternative formulation is required. This is where the application of the GPT sensitivity functions becomes important. If the independent variables are denoted as y_n, and the first-order GPT derivatives are available, then

$$F' = F_o + \sum_n \frac{\partial F}{\partial y_n} (y_n - y_{no}) \tag{3.1}$$

and

$$C'_k = C_{ko} + \sum_n \frac{\partial C_k}{\partial y_n} (y_n - y_{no}) \qquad k = 1, 2, \ldots K \tag{3.2}$$

where the subscript o indicates the reference state. Thus F' and the C'_k's can be evaluated easily for any combination of independent variables y_n. If these perturbation expressions are accurate (depends on the accuracy of the first-order approximation), then the solution from the optimization algorithm should represent an optimal reload configuration that not only maximizes the desired objective function but also satisfies all safety criteria.

A critical area that needs to be addressed is associated with the definition of the independent variables for the system. Special care needs to be taken here to attempt to reduce the problem complexity as much as possible. The important parameters (decision variables) in reload analyses are the locations of the individual assemblies and the number of burnable poison (BP) rods in each assembly. These decision variables need to be written in terms of the independent parameters y_n. y_{no} may represent, for example, the average

burnup of the assembly in zone n for the reference state. Interchanging two assemblies produces a discrete change in the average exposure in location n and this discrete behavior must be treated in the resultant algorithm.

A specific choice of independent variables that is compatible with the discrete fuel management formulation has been made. Consider the variables X_{ij} and Y_i which are defined as

$$X_{ij} = \begin{cases} 0 & \text{assembly j is not in location i} \\ 1 & \text{assembly j is in location i} \end{cases}$$

Y_i = number of burnable poison (BP) sets in location i

Physical constraints on the shuffling variable X_{ij} restrict each assembly to be placed in one location, and each location to contain only one assembly. These constraints can be written as,

$$\sum_i X_{ij} = 1 \qquad \text{for all j} \tag{3.3}$$

and

$$\sum_j X_{ij} = 1 \qquad \text{for all i} \tag{3.4}$$

In addition, the BP variable has user-defined upper and lower limits.

A simple algebraic formulation for the objective function and nuclear constraints can be written in terms of these variables and the GPT derivatives. Denoting the desired response as R (either the objective function or some neutronic constraint) and using only first-order GPT for the moment, the first-order estimate of the perturbed response is

$$R' = R_o + \sum_i \frac{\partial R}{\partial BU_i} \Delta BU_i + \sum_i \frac{\partial R}{\partial N_{BP_i}} \Delta N_{BP_i} \tag{3.5}$$

But the variation in burnup and BP density in location i can be written as

$$\Delta BU_i = \sum_j BU_j X_{ij} - \sum_j BU_j \delta_{ij} = \sum_j (BU_j - BU_i) X_{ij} \tag{3.6}$$

and

$$\Delta N_{BP_i} = mN_{BP}(Y_i - Y_{io}) \tag{3.7}$$

where

N_{BP} = assembly-averaged BP density per rod (fixed), and

m = integer multiplier that forces discrete movement of m rods.

The first term on the right hand side of eqn. (3.6) represents the burnup of the assembly shuffled into location i and the second term is the burnup of the assembly initially in position i (δ_{ij} is the Kronecker delta function). Therefore, ΔBU_i is simply the difference between the average exposure in location i before and after the shuffling operation.

Substituting eqns. (3.6) and (3.7) into eqn. (3.5) gives

$$R' = a_o + \sum_{ij} c_{ij}X_{ij} + \sum_{i} a_i Y_i \tag{3.8}$$

where

$$a_o = R_o - \sum_{i} a_i Y_{io} \tag{3.9}$$

$$a_i = \frac{\partial R}{\partial N_{BP_i}} mN_{BP} \tag{3.10}$$

$$c_{ij} = \frac{\partial R}{\partial BU_i} (BU_j - BU_i) \tag{3.11}$$

Equation (3.8) is the final form of the objective function and constraint formulation. Its simplicity is its main feature. The c_{ij}'s and a_i's are derived using first-order GPT. Then, for any combination of decision variables X_{ij} and Y_i, the nuclear response functional can be estimated via eqn. (3.8). Each response would be characterized by its own set of coefficients which would require an independent GPT computation. These coefficients can be stored for several responses in a sensitivity library and then used within an optimization code as needed. The potential benefits of such capability is

enormous if eqn. (3.8) is an accurate representation of how R' varies with respect to burnup and BP density.

Although the primary concern for the in-core fuel management problem is the application of first-order GPT methods, second-order expressions consistent with the above response/constraint formulation will be derived for completeness. If second-order accuracy is desired, eqn. (3.5) becomes

$$R' = R_o + \sum_i \frac{\partial R}{\partial BU_i} \Delta BU_i + \sum_i \frac{\partial R}{\partial N_{BP_i}} \Delta N_{BP_i} \tag{3.12}$$

$$+ \sum_{pq} \frac{\partial^2 R}{\partial BU_p \partial BU_q} \Delta BU_p \Delta BU_q \qquad \text{(Term A)}$$

$$+ \sum_{pq} \frac{\partial^2 R}{\partial N_{BP_p} \partial N_{BP_q}} \Delta N_{BP_p} \Delta N_{BP_q} \qquad \text{(Term B)}$$

$$+ \sum_{pq} \frac{\partial^2 R}{\partial BU_p \partial N_{BP_q}} \Delta BU_p \Delta N_{BP_q} \qquad \text{(Term C)}$$

Using eqns. (3.6) and (3.7), the three second-order terms become

$$\text{Term A} = \sum_{pq} \frac{\partial^2 R}{\partial BU_p \partial BU_q} \left[\sum_j BU_j X_{pj} \sum_k BU_k X_{qk} \right. \tag{3.13}$$

$$\left. - BU_p \sum_k BU_k X_{qk} - BU_q \sum_j BU_j X_{pj} - BU_p BU_q \right]$$

$$\text{Term B} = (mN_{BP})^2 \sum_{pq} \frac{\partial^2 R}{\partial N_{BP_p} \partial N_{BP_q}} \left[Y_p Y_q - Y_p Y_{qo} - Y_{po} Y_q + Y_{po} Y_{qo} \right] \tag{3.14}$$

$$\text{Term C} = mN_{BP} \sum_{pq} \frac{\partial^2 R}{\partial BU_p \partial N_{BP_q}} \left[Y_q \sum_j BU_j X_{pj} - Y_{qo} \sum_j BU_j X_{pj} \right. \tag{3.15}$$

$$\left. - BU_p Y_q + BU_p Y_{qo} \right]$$

These second-order expressions account for the interaction of two individual perturbations in locations p and q. This level of detail requires that a full set of response derivatives be available. This subject will be treated in some detail in Section V. However, it is unlikely that all these derivatives will be necessary from a cost versus accuracy viewpoint. Not only are the derivatives difficult to compute, but they also complicate the expression for R'. Clearly, eqns. (3.13) - (3.15) are nonlinear with respect to the decision variables X_{ij} and Y_i. Thus, a nonlinear integer programming technique would be required to treat the full higher-order coupling.

A more likely result of a higher-order correction to first-order GPT is the computation of the higher-order effects of a single large localized perturbation to the reference system. This represents the case where p=q and the only second-order derivatives of interest are the $\partial^2 R/\partial BU_p^2$ and $\partial^2 R/\partial N_{BP_p}{}^2$ terms. Letting p = q = i, the second-order terms reduce to

$$\text{2nd-order terms} = \sum_i \frac{\partial^2 R}{\partial BU_i^2}\left[\sum_j BU_j X_{ij} \sum_k BU_k X_{ik} - 2BU_i \sum_j BU_j X_{ij} + BU_i^2\right] + (mN_{BP})^2 \sum_i \frac{\partial^2 R}{\partial N_{BP_i}^2}\left[Y_i^2 - 2Y_i Y_{io} + Y_{io}^2\right] \tag{3.16}$$

Since two different assemblies cannot be in location i, the first term on the right of eqn. (3.16) becomes

$$\sum_j BU_j X_{ij} \sum_k BU_k X_{ik} = \sum_j BU_j^2 X_{ij}^2 = \sum_j BU_j^2 X_{ij}$$

Also, since the goal here is to put the final result in linear form, one needs to linearize the Y^2_i term. Thus, let $Y^2_i \approx Y_i Y_{io}$ for simplicity. Using these

results, the second-order terms become

$$2\text{nd} - \text{order terms} = b_o + \sum_{ij} d_{ij} X_{ij} + \sum_{i} b_i Y_i \tag{3.17}$$

where

$$b_o = \sum_{i} \frac{\partial^2 R}{\partial BU_i^2} BU_i^2 + (mN_{BP})^2 \sum_{i} \frac{\partial^2 R}{\partial N_{BP_i}^2} Y_{io}^2 \tag{3.18}$$

$$b_i = -(mN_{BP})^2 Y_{io} \tag{3.19}$$

$$d_{ij} = \frac{\partial^2 R}{\partial BU_i^2}\left(BU_j^2 - 2BU_i BU_j\right) \tag{3.20}$$

Finally coupling these results for the second-order terms with the first-order relationship gives

$$R' = (a_o + b_o) + \sum_{ij} (c_{ij} + d_{ij}) X_{ij} + \sum_{i} (a_i + b_i) Y_i \tag{3.21}$$

This latter result is very important. Equation (3.21) implies that with the assumption of negligible contributions from the mixed derivative terms and with the approximation that $Y^2_i \approx Y_i Y_{io}$, the objective function and constraint formulation in the higher-order approximation is exactly the same form as the first-order estimate. Thus, the same linear optimization software can be used for both cases.

In summary, it should be emphasized that the main thrust here is to use first-order GPT as the basis for a fuel management optimization algorithm. For the first-order treatment, the objective function and constraint formulation is given by eqn. (3.8). If some limited higher-order derivatives are available, then greater accuracy can be achieved via eqn. (3.21), with no additional complexity in the optimization algorithm. Finally, if a full complement of higher-order derivatives is available, then eqns. (3.8) and

(3.13)-(3.15) would be used with a full nonlinear optimization routine. It is felt that this last level of complexity is not warranted.

III.3 Illustrative Applications

Since the individual pieces (the GPT and optimization software) were already available, a detailed numerical study of the feasibility of the GPT-based optimization algorithm was performed. The goals here were to gain some general experience in this area and to address the accuracy of using only the first-order response derivatives. We set out to answer the question, "Could such a simple straightforward approach to core design really work?"

III.3.A The Tools: Because of its availability, the Multi-Purpose Optimization System (MPOS)[79] was chosen as the optimization tool for initial applications-oriented work. MPOS is a software package that solves the linear, integer, and quadratic programming problems (LP, IP, and QP, respectively). In particular, there are three IP algorithms to handle pure, mixed, and zero-one integer programming problems.

To gain some experience with the use of the MPOS package, several simple optimization problems were executed. In this early testing, one algorithm stood out among the others as easier to use and it seemed to fit the overall requirements of the binary fuel shuffling problem. This specific algorithm is called BBMIP (for Branch and Bound Mixed-Integer Programming).[79] The BBMIP software uses continuous linear programming to obtain bounds on the solution space and then systematically imposes integrality constraints to obtain the desired integer feasible solution that optimizes the objective function. Although this package may not be the best, it has proved to be adequate for the testing and demonstration of the basic concepts.

Implementation of the basic GPT-based methodology has concentrated on interfacing the sensitivity library to the BBMIP software. The response derivatives for the library were generated with the VENTURE[80]/DEPTH-CHARGE[25] system. VENTURE is a modular computation system for nuclear reactor core analysis. Core neutronics problems are solved using multigroup finite difference diffusion theory techniques. Depletion calculations are possible and one-, two-, and three-dimensional geometries can be employed. VENTURE was developed mainly for the analysis of advanced reactor concepts (LMFBRs and HTGRs, etc.). However, thermal reactor calculations using a simplified cross section treatment can also be performed.*

The DEPTH-CHARGE modules were added to the overall computation system in the early 80's.[20] These modules, coupled with the VENTURE neutronics code, were designed to solve the adjoint equations of Depletion Perturbation Theory (DPT). The reader is referred to Refs. 13-25 for further details on DPT and on the workings of the VENTURE/DEPTH-CHARGE system.

An interfacing code was also written (see Ref. 81 for the details) to manipulate the VENTURE/DEPTH-CHARGE GPT/DPT derivatives and construct the required input for the BBMIP algorithm. The main function of the code is to translate user input, which gives the problem-specific objective

---

*It is recognized that VENTURE is not considered to be a standard LWR design tool since its fuel burnup and cross section treatments are not consistent with current LWR design procedures. However, with some effort, VENTURE can be made to approximate just about any situation. Thus, the existing GPT/DPT capability within the VENTURE/DEPTH-CHARGE system has been utilized to demonstrate the overall potential of the GPT-based optimization formulation. The inconsistencies of the current GPT capability and that required for production LWR design are discussed in detail in Section IV.

function and constraints, into data readable by the MPOS input processor. From a mathematical perspective, it simply constructs an initial tableau which contains the cost coefficients in the proper format. The cost coefficients are the a_i's and c_{ij}'s given in eqns. (3.8) - (3.11) for each specific problem.

III.3.B Reference Model: The core model chosen for demonstration of the method is a typical Westinghouse three-loop PWR. A two-dimensional, two-group, quarter-core model with 1/8-core symmetry was used. The VENTURE model, illustrating the location of zone assignments, is shown in Fig. 3.1. The reference BOC configuration contained fresh, once, and twice burnt fuel assemblies arranged in a low leakage pattern. With the fuel loading pattern fixed, a few manual iterations were made to specify the BP pattern so that the maximum assembly power was around 1.30. The resultant BP pattern and assembly power distribution are shown in Fig. 3.2. This BOC configuration represents the reference core model used in the rest of this work. This BOC state was then depleted for an average burnup of 15200 MWD/MTU. The EOC reference power profile is also shown in Fig. 3.2. For simplicity, the burnup calculations used a fixed boron letdown curve which kept K_{eff} close to unity ($\pm 0.5\%$).

The GPT capability within the VENTURE/DEPTH-CHARGE system was then used to generate the sensitivity library utilized in the subsequent perturbation and optimization runs. A complete set of derivatives was prepared for each BOC assembly relative power in the 1/8-core configuration. Importance data for BOC and EOC K_{eff} were also generated, where the latter response demonstrates the DPT capability mentioned previously. These 28 sensitivity profiles (26 assembly relative powers and the BOC and EOC K_{eff}),

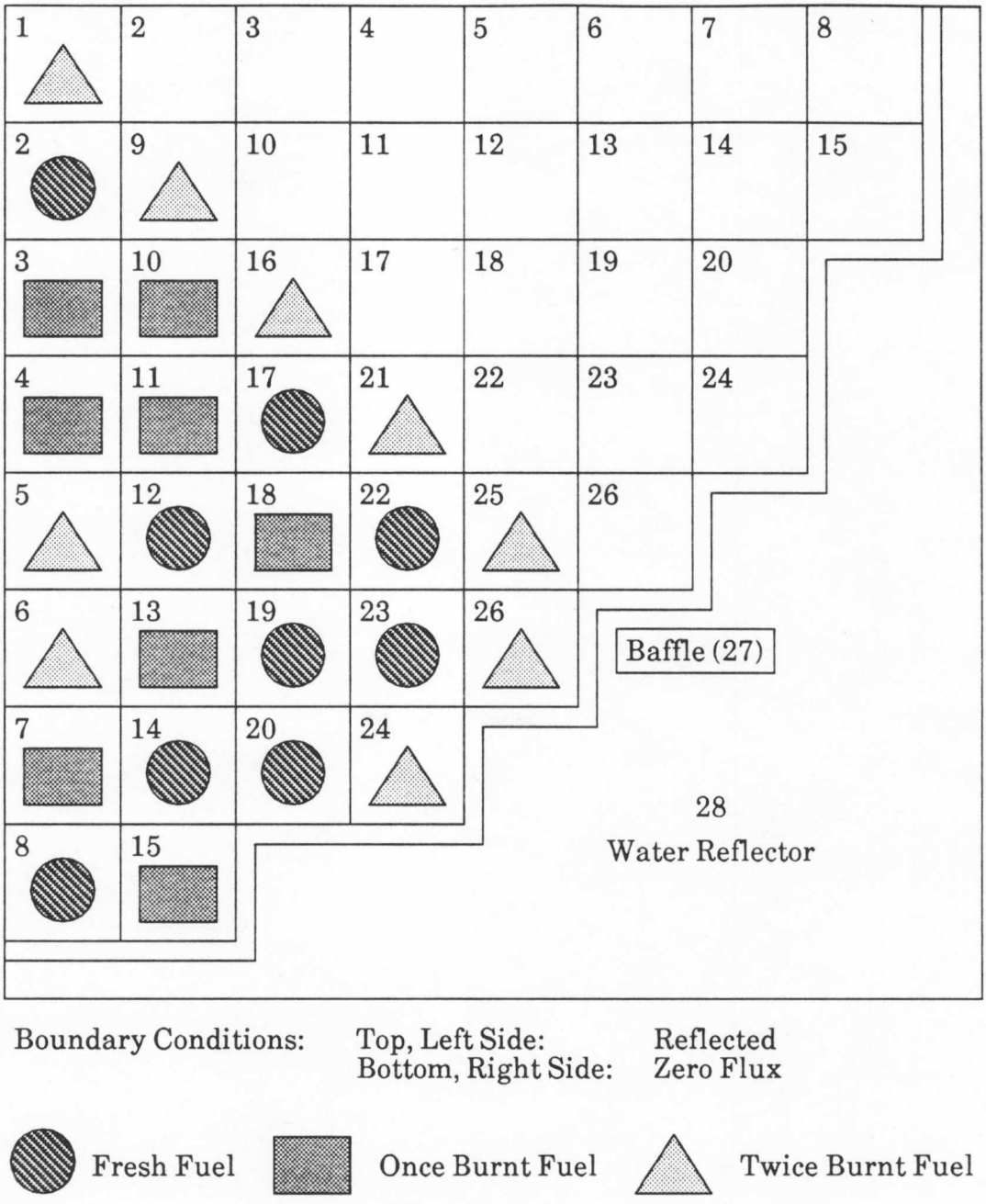


Figure 3.1 VENTURE Quarter-Core Configuration

1-1-0 0.903 0.873				
2-2-12 1.231 1.173	9-9-0 0.859 0.868			
3-3-0 1.126 1.043	10-10-8 0.996 1.058	16-16-0 0.781 0.974		
4-4-8 1.099 1.100	11-11-2 1.173 1.142	17-17-16 1.286 1.345	21-21-0 0.992 1.020	
5-5-0 0.907 0.935	12-12-20 1.285 1.341	18-18-0 1.208 1.162	22-22-16 1.263 1.280	25-25-0 0.683 0.744
6-6-0 0.848 0.889	13-13-0 1.136 1.086	19-19-24 1.303 1.350	23-23-0 1.234 1.083	26-26-0 0.368 0.413
7-7-0 1.026 0.976	14-14-10 1.176 1.109	20-20-0 1.079 0.955	24-24-0 0.448 0.461	
8-8-0 0.675 0.741	15-15-0 0.448 0.500			

Key: A-B-C A⇒Loc. B⇒Assy. C⇒BPs
D D⇒BOC Rel. Power
E E⇒EOC Rel. Power

Note: BOC K_{eff} = 0.9978
EOC K_{eff} = 1.0034
Total BPs = 848

Figure 3.2 Eighth-Core Map with Results for Reference Core Configuration

plus much of the reference data shown in Fig. 3.2, make up the sensitivity library for this core configuration.

III.3.C Direct Perturbations: Using the sensitivity library, several illustrative demonstrations were performed. As a first test, a relatively large set of arbitrary single and multiple perturbations were introduced into the reference system. Comparisons of perturbation theory estimates versus direct results (obtained from direct recalculation of the perturbed system) were made. The idea here was to obtain a database of experience concerning the accuracy of GPT/DPT methods for use in reload design applications.

Table 3.2 gives a list of the direct perturbations used in this study. The first set of runs was made to test the accuracy of a single binary shuffle with increasing change in exposure. Cases 9-12 illustrate variations in the number of BP rods, as single perturbations and in combination with fuel shuffling. Case 13 is the sum of six individual two-assembly interchanges (sum of Cases 1-3 and 5-7). Finally, Cases 14-17 represent realistic shuffling operations where several assembly movements take place simultaneously.

The complete set of 17 perturbations covers a wide range of potential situations, and as such, comparisons of GPT versus direct results for these cases should provide an adequate database from which to draw conclusions concerning the accuracy of GPT's prediction capability.

The responses chosen for this comparison were the BOC and EOC K_{eff} and several relative zone-average powers at BOC. The particular regions treated for the zone power comparisons were zones 2, 7, 10, 12, 15, 17, 19, 21, and 26, where the zone numbers correspond to the VENTURE configuration given in Fig. 3.1. These zones are distributed throughout the 1/8-core model and the reference relative powers cover the complete spectrum from low to

TABLE 3.2 Material Perturbations Used to Evaluate Accuracy of GPT/DPT Formulation

Case	Perturbation Description*	ΔExposure (MWD/MTU)
1	Shuffle (10,13)	2890
2	Shuffle (21,26)	4408
3	Shuffle (18,24)	7804
4	Sum of 1, 2, and 3	---
5	Shuffle (3,7)	1520
6	Shuffle (1,25)	3276
7	Shuffle (5,15)	8888
8	Sum of 5, 6, and 7	---
9	ΔBP in Zone 13 (0⇒8 rods)	---
10	Sum of 1 and 9	---
11	Sum of 4 and 9	---
12	ΔBP in Zone 19 (24⇒16 rods)	---
13	Sum of 4 and 8	---
14	Shuffle (3,18), (4,11), (9⇒15⇒16⇒9)	---
15	Shuffle (3,18), (4⇒10⇒11⇒4), (6⇒15⇒16⇒9⇒6)	---
16	Shuffle (3⇒13⇒4⇒10⇒11⇒18⇒3), (15,16)	---
17	Shuffle (3⇒4⇒11⇒10⇒18⇒6⇒15⇒3), (13,16)	---

*(A,B) indicates that assemblies A and B are interchanged, A⇒B⇒C indicates that assembly A is shuffled into location B, assembly B into location C, etc.

high values (0.37 to 1.30). Thus, the comparisons of predicted versus direct calculations for these responses for 17 different perturbations (total of 170 BOC experimental data points; 10 responses times 17 perturbations) should provide a good evaluation of GPT methods.

Selected results from these comparisons are given in Tables 3.3 and 3.4, and a summary table containing the root mean square (RMS) and maximum errors for each of the ten BOC responses is given in Table 3.5. In this latter table the RMS error is defined by

$$\text{RMS Error} = \sqrt{\frac{\sum_{i=1}^{N} \left(R_{GPT} - R_{Direct} \right)^2}{N}}$$

where the number of numerical experiments for each response is 17.

Concentrating first on the K_{eff} response, one sees that the EOC reactivity is predicted with higher accuracy than the BOC ΔK_{eff}. The maximum absolute deviation is 181 PCM ($181*10^{-5}$) at BOC and only 17 PCM at EOC. The RMS errors are 75 PCM and 10 PCM at BOC and EOC, respectively. The increased accuracy in the EOC versus BOC responses has been noted in previous work.[22] This phenomenon is the result of the smoothing nature of the burnup process.

Although the EOC ΔK_{eff} predictions are very good, the errors at BOC are quite high. Thus, it appears that some treatment of a higher-order correction for the static ΔK_{eff} predictions may be required for the BOC situation.

On the other hand, the GPT predictions of the relative assembly powers at BOC are extremely accurate. In fact, these power predictions are much better than anticipated. In over 150 separate estimates, the maximum error is

TABLE 3.3 GPT/DPT Versus Direct Calculations for the K_{eff} Responses

Case	Direct BOC ΔK (*10-5)	GPT BOC ΔK (*10-5)	Abs. Error	Direct EOC ΔK (*10-5)	DPT EOC ΔK (*10-5)	Abs. Error
1	96.	49.	47.	15.	18.	3.
2	-58.	-65.	7.	-28.	-32.	4.
3	-361.	-426.	65.	-218.	-231.	13.
4	-304.	-442.	138.	-228.	-245.	17.
5	17.	10.	7.	-3.	-4.	1.
6	-18.	-21.	3.	-31.	-31.	0.
7	149.	105.	44.	26.	14.	12.
8	162.	94.	68.	-8.	-21.	13.
9	-280.	-324.	44.			
10	-254.	-275.	21.			
11	-670.	-766.	96.			
12	348.	334.	14.			
13	-199.	-349.	150.			
14	325.	258.	67.			
15	304.	239.	65.			
16	419.	337.	82.			
17	99.	-82.	181.			

Reference Responses: BOC K_{eff} = 0.99778
EOC K_{eff} = 1.00340

TABLE 3.4 GPT Versus Direct Calculations for Selected BOC Relative Power Responses

Case	Zone 2 Rel. Power		Zone 15 Rel. Power		Zone 19 Rel. Power	
	Direct	GPT	Direct	GPT	Direct	GPT
1	1.010	0.988	0.490	0.493	1.379	1.386
2	1.233	1.235	0.455	0.455	1.311	1.311
3	1.307	1.325	0.479	0.480	1.290	1.284
4	1.049	1.086	0.534	0.534	1.384	1.376
5	1.330	1.326	0.423	0.422	1.280	1.281
6	1.306	1.301	0.446	0.447	1.292	1.293
7	1.256	1.271	0.344	0.325	1.279	1.281
8	1.426	1.436	0.324	0.299	1.245	1.249
9	1.365	1.374	0.418	0.417	1.258	1.255
10	1.134	1.131	0.462	0.462	1.336	1.338
11	1.194	1.229	0.505	0.503	1.338	1.328
12	1.069	1.074	0.457	0.458	1.485	1.466
13	1.261	1.291	0.387	0.385	1.324	1.322
14	1.235	1.244	0.316	0.288	1.296	1.300
15	1.247	1.252	0.328	0.306	1.295	1.299
16	1.057	1.035	0.353	0.343	1.352	1.363
17	1.212	1.251	0.310	0.284	1.266	1.262

Reference Responses: P2 = 1.231
P15 = 0.448
P19 = 1.303

TABLE 3.5 Summary of Overall Accuracy of BOC GPT Predictions

	Reference Response	RMS Error	Max. Error
ΔK_{eff} Response ($*10^{-5}$)	---	75.	181.
Relative Power Responses			
Zone 2	1.231	0.020	0.039
Zone 7	1.026	0.010	0.023
Zone 10	0.996	0.010	0.022
Zone 12	1.285	0.004	0.009
Zone 15	0.448	0.013	0.028
Zone 17	1.286	0.005	0.013
Zone 19	1.303	0.007	0.019
Zone 21	0.992	0.006	0.012
Zone 26	0.368	0.004	0.008

approximately 0.04 and the RMS error for the complete set is only 0.01. Although this maximum deviation is too large for final design computations, the general nature of the GPT predictions is quite acceptable. From the data presented here it is clear that these estimates are sufficiently accurate to allow determination of fuel loading patterns that should meet design specifications. Since the first objective of any loading pattern search is to satisfy the power constraints, it appears that GPT may be a useful tool in such analyses.

The next step in the verification process was the demonstration of the GPT technique in some actual optimization applications. Several such cases have been performed and two specific cases will be described here: one that

optimizes only the BP loading, and a second case that illustrates a combined BP loading and fuel shuffling problem. For further demonstrations beyond those given here, the reader is referred to Ref. 81.

III.3.D BP Optimization: The reference core described previously is far from ideal. The maximum BOC assembly relative power of 1.303 is a little high, and the use of 848 BP rods in the full-core model to obtain this peaking is somewhat excessive. Therefore, as a first test of the GPT-based optimization scheme, it was decided to try to increase the thermal margin (reduce peaking) and also reduce the total number of BP rods while maintaining the same fuel loading pattern. The total number of BP rods was chosen as the objective function and the relative assembly powers were used as constraints. The specifications are:

Case 1 minimize number of BP rods subject to $P_i \leq P_{max}$ for all assemblies,

BOC $K_{eff} \geq 1.0$, and

EOC $K_{eff} \geq 1.0$

with a. reference loading pattern fixed, and

b. no BPs allowed in central or in control locations.

With these specifications, three similar runs were made with P_{max} varying from 1.29 to 1.27 to 1.25. The original BP pattern was modified greatly and all cases gave improved core performance relative to the reference pattern. A brief summary of the GPT results from these computer runs is given below:

Specified P_{max}	Calc. P_{max}	BP Rods	BOC K_{eff}	EOC K_{eff}
1.29	1.287	528	1.0125	1.0033
1.27	1.269	632	1.0075	1.0034
1.25	1.250	744	1.0019	1.0035

The first observation to note here is that in all cases the constraints were satisfied. Also of note is the large decrease in the number of BP rods (compared to the reference value of 848). Even for the case where the assembly peaking is reduced from 1.303 to 1.250, over one hundred BP rods were removed. A final observation is the trade-off made between thermal margin and the number of BP rods needed to obtain the increased margin. The greater the margin the greater the BP requirement, and the relationship is nonlinear. There is a point of diminishing returns where the extra reduction in peaking is too costly in terms of the number of BPs required.

If we choose the case where $P_{max} = 1.27$ as the optimum configuration, we then need to evaluate the GPT-predicted core performance against direct computations. This verification is given in Fig. 3.3, where the predicted and direct power distributions are compared. The main point to be made from these data is the good accuracy of the GPT-calculated powers. The maximum absolute error is .016 in location 10. This is not bad considering the size of the perturbations made to the reference configuration. The actual maximum peaking occurs in zone 14 with a value of 1.273. This is only .003 higher than the specified constraint. As for the eigenvalue comparison, the predicted BOC K_{eff} is low by about 80 PCM. The EOC K_{eff} was not checked since previous perturbation cases have shown that the EOC reactivity is predicted very

1-1-0 0.907 0.913				
2-2-12 1.268 1.272	9-9-0 0.907 0.913			
3-3-0 1.204 1.212	10-10-0 1.120 1.136	16-16-0 0.803 0.807		
4-4-2 1.199 1.204	11-11-0 1.225 1.229	17-17-16 1.253 1.250	21-21-0 0.949 0.943	
5-5-2 0.878 0.879	12-12-18 1.269 1.266	18-18-0 1.157 1.151	22-22-12 1.233 1.223	25-25-0 0.644 0.639
6-6-2 0.809 0.810	13-13-0 1.110 1.109	19-19-22 1.262 1.225	23-23-0 1.154 1.146	26-26-0 0.339 0.336
7-7-0 1.042 1.045	14-14-2 1.264 1.273	20-20-0 1.056 1.054	24-24-0 0.418 0.416	
8-8-0 0.683 0.684	15-15-0 0.460 0.461			

Key: A-B-C A⇒Loc. B⇒Assy. C⇒BPs
D D⇒GPT Rel. Power
E E⇒Direct Rel. Power

Note: GPT BOC K_{eff} = 1.0075
Direct BOC K_{eff} = 1.0083
Total BPs = 632

Figure 3.3 Eighth-Core Map with GPT Versus Direct Results for BP Optimization Case with P_{max} = 1.27

accurately with the DPT derivatives. Overall, these results are quite encouraging.

III.3.E Combined Optimization: As a second example of the potential of the GPT-based method, consider the combined optimization problem that attempts to find the optimal fuel shuffling and BP loading in a single calculation. This problem is extremely complex since the number of possible shuffling patterns and BP loadings is enormous. Although the GPT-based method is sufficiently general to treat this problem completely, the MPOS system has an operational limitation on the number of independent variables that can be used. Therefore, to stay within the limits of the MPOS system, the initial testing of the combined problem treats a more specific problem. In particular, the second application will try to fine tune the Case 1 design by allowing shuffling only within individual fuel batches. The objective function and constraints are the same as for Case 1 but now fuel shuffling as well as BP variations are allowed. The specific problem definition is:

Case 2 minimize number of BP rods

subject to $P_i \leq 1.27$ for all assemblies,

BOC $K_{eff} \geq 1.0$, and

EOC $K_{eff} \geq 1.0$

with
a. fresh fuel and central assembly are fixed,
b. maintain 1/8-core symmetry,
c. allow shuffling among once burnt fuel and among twice burnt fuel, and
d. no BPs allowed in central or control locations.

The results from the optimization run with these specifications are given in Fig. 3.4. The number of BP rods is reduced another 80 rods relative to the

1-1-0 0.898 0.894				
2-2-14 1.249 1.253	9-6-0 0.932 0.938			
3-7-0 1.258 1.270	10-10-0 1.135 1.150	16-5-0 0.791 0.792		
4-4-0 1.250 1.265	11-11-0 1.241 1.244	17-17-14 1.263 1.257	21-9-0 0.903 0.892	
5-21-0 0.925 0.925	12-12-18 1.267 1.263	18-15-0 1.143 1.135	22-22-10 1.236 1.223	25-16-0 0.633 0.625
6-25-0 0.824 0.824	13-18-0 1.063 1.064	19-19-20 1.263 1.255	23-23-0 1.145 1.134	26-26-0 0.334 0.330
7-3-0 1.000 1.006	14-14-0 1.267 1.281	20-20-0 1.048 1.047	24-24-0 0.412 0.410	
8-8-0 0.678 0.681	15-13-0 0.476 0.480			

Key: A-B-C A⇒Loc. B⇒Assy. C⇒BPs
D D⇒GPT Rel. Power
E E⇒Direct Rel. Power

Note: GPT BOC K_{eff} = 1.0101
Direct BOC K_{eff} = 1.0114
Total BPs = 552

Figure 3.4 Eighth-Core Map with GPT Versus Direct Results for Combined Optimization Case

BP optimization case with P_{max} = 1.27, and the resultant fuel shuffling pattern is

3⇒7⇒3

5⇒16⇒25⇒6⇒9⇒21⇒5

13⇒15⇒18⇒13

where the notation A⇒B⇒C indicates that assembly A is shuffled into location B, assembly B into C, etc. Thus, by performing the indicated fine tuning, additional performance (relative to the desired objective function) can be obtained while maintaining roughly the same thermal margin (assembly peaking around 1.27).

This combined optimization problem is significantly more difficult than the Case 1 design since the number of independent variables is greatly increased. However, even with the large number of perturbations to the reference configuration, the GPT-predicted assembly powers are still quite accurate. This can be seen by comparing the GPT and Direct results in Fig. 3.4. The worse case absolute errors are only .015 in locations 4 and 10. These errors are relatively small considering that 8 BPs were removed from both locations. The actual peak occurs in zone 14 where 10 BPs were removed. This time, the directly calculated peaking is .011 greater than the specified maximum of 1.27. However, an assembly peak of 1.281 is acceptable, and the objective function is improved considerably.

Concerning the BOC eigenvalue comparisons, Fig. 3.4 shows that the error in the GPT BOC K_{eff} value is about 130 PCM. This error is relatively large. Unfortunately, reactivity responses demand high accuracy, and it appears that, in most cases, the expected errors will be in the range of 50-150 PCM. This may not be acceptable for some applications. Clearly some further

study is required here. In any case, the current applications only imposed a greater-than inequality for K_{eff}; thus, the above results are completely acceptable.

III.4 Summary Comments

To conclude this section, a brief summary is in order. This section has presented the development and demonstration of a powerful GPT-based optimization algorithm. The key to this method is a simple algebraic formulation for the objective function and neutronic constraints. The method is extremely flexible since the number and choice of responses is limited only by the availability of the appropriate GPT derivatives. This formulation can also take advantage of recent developments in time-dependent perturbation methods. The use of GPT/DPT and the overall flexibility of the problem specification are distinguishing features of this approach relative to previous work in this area.

The method has been tested by using the GPT/DPT capability of the VENTURE/DEPTH-CHARGE system and an integer programming algorithm from the MPOS package. Although this capability does not represent a production-oriented design package, it does allow demonstration of the overall methodology.

The examples in Section III.3 were designed to illustrate some of the power and flexibility of the GPT-based system. As such they may not represent the best choice of objective function or constraints. The point to emphasize, however, is that these specifications can be easily modified with the GPT-based method. Each designer can determine the specifications that are most appropriate for his particular problem.

The problem size was also restricted somewhat by the limitations of the BBMIP algorithm, but this in no way limits the generality of the basic approach. Even with the use of the MPOS package, some relatively complicated and realistic design problems can be addressed.

The results of the two example optimization problems were quite impressive, especially when considering that the power distributions and eigenvalues were estimated with first-order GPT. These results are typical for a wide class of problems. In fact, it appears that if realistic constraints are imposed upon the system, then excellent results can be expected. It is the realistic constraints that eliminate the possibility of gross changes in the global flux and power distributions. If these changes are small, first-order GPT works quite well. Thus, it appears that the first-order approximation is well suited for the fuel shuffling and BP loading problems; especially for the prediction of assembly powers.

With the successful demonstration of the basic concept, emphasis now needs to be shifted toward the development of a production analysis tool that is compatible with current LWR design methods. This will require the development and implementation of GPT/DPT capability into existing LWR design codes. This subject is treated in detail in the next section. In addition, further work is required to identify or develop a robust integer programming package that can treat larger problems (relative to the BBMIP algorithm). This topic has not been treated in detail in this work since the emphasis of the current effort is the theoretical development of the overall methodology. However, if a production design tool is eventually developed, this subject will definitely require more attention. Finally, completion of a production design tool requires coupling of the GPT and optimization formulations into a user-

friendly package. This development represents a relatively major undertaking, but the potential benefits of the GPT-based scheme clearly warrant that this effort be made.

IV. DEVELOPMENT OF LWR-COMPATIBLE GPT METHODS

The previous section has established the viability of the proposed GPT-based design methodology. To make such a system attractive for realistic applications, it must be fully compatible with current LWR design practices. This section will present a GPT/DPT methodology that fulfills this requirement.

IV.1 Historical Perspective

Before proceeding with the development of an LWR-compatible time-dependent (depletion) perturbation theory, it is appropriate to provide a brief perspective of how GPT methods developed over the last 15-20 years. Static perturbation methods have evolved from the early work of Lewins,[82-85] Usachev,[86] Gandini,[87-89] and others.[90-96] These methods can be utilized in time-independent critical reactor applications and in the analysis of reactor shield design. These first-order methods have been utilized extensively in the evaluation of nuclear data files, in the analysis of experimental results, and in the sensitivity and uncertainty analysis of integral performance parameters, especially for fast reactor studies.[1-10]

Perturbation methods incorporating time-dependence also have an interesting history. Gandini[97] proposed the use of time-dependent perturbation theory for the neutron field in connection with the analysis of reactor kinetic experiments. Starting from a generalized perturbation formulation in the neutron field, he later showed[98] that the perturbation expressions for the nuclide field could be derived by analogy. For this analysis he simply replaced the neutron and precursor densities with a nuclide concentration vector and utilized the buildup and decay matrix in place of the Boltzmann operator.

Komata[99] also showed that a time-dependent perturbation theory formulation similar to Gandini's could be derived using both a formal mathematical procedure as used in standard perturbation theory and a variational principle technique as suggested by Pomraning.[90]

Gandini[100] and Tondinelli[101] have applied these new perturbation theory techniques for the nuclide field to burnup and buildup problems during the reactor operating history and to sensitivity analyses of actinide production estimates. Williams[11] also implemented a similar capability into the ORIGEN[102] isotope generation and depletion code and has applied the theory to compute the plutonium production in a thermal reactor with an emphasis on sensitivity and uncertainty analyses.

The above studies, however, did not consider the nonlinear interaction between the neutron and nuclide fields. The neutron flux field was assumed unchanged when a nuclide or data perturbation was made. Kallfelz[103] addressed this problem by linking time-dependent perturbation theory for the nuclide field with static generalized perturbation theory for the flux field. Using this method he was able to calculate the indirect effect of a nuclide perturbation. However, the theory was still somewhat limited in scope and could not be applied to typical reactor depletion problems.

Other developments in this area can be attributed to Wade and Terney[38] and co-workers,[104] and to Harris and Becker.[105] Wade and Terney's work dealt mainly with the optimal control of nuclear reactors over time. Much of their formulation, however, had the same basic approach as the more general development of William's Depletion Perturbation Theory[12-15] (which was developed some six or more years later). Harris' work was somewhat

specialized in that he concentrated on adjoint sensitivity theory for fuel cycle cost and treated relatively simplistic spatial models.

In the late 70's Williams pieced together much of the earlier work and developed a generalized coupled neutron/nuclide depletion perturbation theory that was sufficiently general to be applicable to fuel cycle problems of arbitrary complexity.[12-15] His theoretical framework, derived using a variational principle, is compatible with conventional quasi-static methods for solving realistic reactor depletion problems. It has been shown that three adjoint equations (for the flux shape, flux normalization, and nuclide density) are required to fully account for variations in both the neutron and nuclide fields arising from variations in initial conditions and nuclear data. The nuclide density adjoint equation in this coupled formulation is identical to that obtained in the previously mentioned uncoupled formulations.[11,101] Additionally, it should be noted that the coupled formulation reduces to the uncoupled case when zero flux normalization and shape variations are assumed.

The final-value problem comprising this coupled set of adjoint equations defines a sensitivity function which relates changes in some specified integral response function to variations in the material concentrations initially loaded in the reactor. Once this importance function has been calculated, the effect of an initial condition perturbation can be estimated by the evaluation of a simple integral expression. Since the importance function is independent of the specific perturbation, a single adjoint calculation allows one to investigate the effects of any number of initial condition variations.

Williams' derivation of the nuclide adjoint equations assumed that the forward nuclide densities were continuous across the time boundaries of the

quasi-static approximation. In general, this assumption is not valid since typical depletion calculations include simulated control rod movement or nuclide (fuel or poison) concentration searches at each step during the depletion cycle. At cycle boundaries, fuel assembly shuffling and discharge or the addition of makeup feed also result in large nuclide discontinuities. Thus the original theory of Williams, although very general in most aspects, is somewhat restricted by the continuous nuclide field assumption.

White et al.[16-18] addressed this deficiency in the original development and modified Williams' formulation to include nuclide field discontinuities. White[20,25] also implemented this multicycle coupled neutron/nuclide perturbation theory within two new modules of the VENTURE/BURNER modular system. The two new modules, coupled with the existing VENTURE code, have been named the VENTURE/DEPTH-CHARGE system. The DEPTH module (coupled with VENTURE) solves for the three adjoint functions of DPT and calculates the desired time-dependent derivatives of the response with respect to the nuclide concentrations and nuclear data utilized in the reference model. The CHARGE code is a collection of utility routines for general data manipulation and input preparation and it considerably extends the usefulness of the system through the automatic generation of adjoint sources, estimated perturbed responses, and relative data sensitivity coefficients. The system provides a complete generalized first-order perturbation/sensitivity theory capability for both static and time-dependent analyses of realistic multidimensional fast reactor models.

The early development of DPT methods into the DEPTH-CHARGE code was performed as part of the current author's Master's thesis work at the University of Tennessee.[18] Since the initiation of that work several additional

theoretical contributions have been made in the field of GPT/DPT development. Cacuci et al.[106-107] and Greenspan et al.[108] have added additional generalizations to the basic theory so that a single development (if viewed from a broad perspective) can treat any application of interest. Gandini,[109-110] Dubi,[111] and Palmiotti[52] have also addressed the question of higher-order perturbation theory and their work might be useful for future extensions to the basic first-order formulation. The subject of higher-order GPT will be treated in more detail in Chapter V of this document.

In the area of applications of GPT/DPT methods, it appears that the DEPTH-CHARGE capability is unique in the United States (see Refs. 113-114 for a current Japanese paper on this subject) and therefore, applications have been limited by the availability of the VENTURE system. Also, since VENTURE was designed primarily for fast reactor applications, there has not been much effort in the analysis of thermal systems. Bowman[115-116] did implement a similar DPT formulation into the SIMULATE LWR nodal code,[117] but his work did not include the development of a production design tool. This is somewhat unfortunate because SIMULATE is used quite extensively in the LWR industry, and the development and application of DPT methods within an LWR nodal code could have initiated further use of the overall capability for the analysis of thermal systems. This overall research effort endeavors to stimulate further GPT applications in the area of LWR reload design.

Although limited in scope, there have been several static and time-dependent applications of the original DEPTH-CHARGE capability. The major emphasis of these applications has been in the analysis of data sensitivities and uncertainties for LMFBR core physics parameters. The

interested reader may consult Refs. 7-8 and 19-24 for more information concerning specific applications.

At this point the reader should have a good historical perspective of the developments leading up to this work. The goal here is to develop a GPT/DPT methodology that is compatible with standard practices used in the physics design of LWR reload cores. In particular, three key features that are not available in the current version of the VENTURE/DEPTH-CHARGE system are

1. Macroscopic depletion,
2. Criticality reset, and
3. Poison and thermal-hydraulic feedback.

Macro depletion and cross section feedbacks are specific to LWR design codes. Thus these features were not even considered in the development of GPT methods for fast reactor applications. Criticality reset has been treated by a few authors, but usually not as a primary consideration. The GPT/DPT methods developed as part of this work will integrate all three of these features. Realistic applications of GPT methods in the reload design process demand that the adjoint procedure be 100% compatible with existing design codes. The GPT/DPT formulations given in subsequent subsections will satisfy this requirement. This new capability should open the door for the use of GPT in realistic LWR applications.

IV.2 General GPT Formulation

In this section a complete time-dependent formulation is developed that includes macroscopic burnup, thermal-hydraulic and poison feedback, and a criticality reset mechanism. The approach taken here is to define a variational principle that includes these considerations as constraint

equations appended to the response functional using Lagrange multipliers. Using this technique (see Refs. 14 and 18), it is possible to define the following K-functional:

$$K(\Sigma_{xg}, PS, \psi, BU_m, N_j, C, FS, RP, \Sigma^M_{xg}) = \tag{4.1}$$

$$R(\Sigma_{xg}, PS, \psi, BU_m, N_j, C) \qquad \text{Response}$$

$$- \sum_n \langle \Gamma^*(L - \lambda F)\psi \rangle \Big|^n \qquad \text{Diffusion Equation}$$

$$- \sum_n \sum_{xg} \langle E^*_{xg} \left| \Sigma_{xg} - \left(\Sigma^o_{xg} + \sum_{l=1}^{L_x} \Sigma^l_{xg} \right) SF_{xg} \right| \rangle \Big|^n \qquad \text{Feedback Effects}$$

$$- \sum_n C^* \left| \lambda - \frac{\langle \psi^* L \psi \rangle}{\langle \psi^* F \psi \rangle} \right| \Big|^n \qquad \text{k-Reset}$$

$$- \sum_n FN^* \left| FS - W_1 \right| \Big|^n \qquad \text{Flux Norm.}$$

$$- \sum_n PN^* \left| PS - W_2 \right| \Big|^n \qquad \text{Power Norm.}$$

$$- \sum_n \sum_m \langle B^{*n}_m \left| BU^n_m - f^n_m(BU^{n-1}_m, \psi^{n-1}, PS^{n-1}, \psi^n, PS^n) \right| \rangle \qquad \text{Fuel/BP Burnup}$$

$$- \sum_n \sum_{xg} \langle E^*_{xg} SF_{xg} \left| \Sigma^o_{xg} - \sum_m \left(h_{xgm}(BU_m) + \Sigma^M_{xgm} \right) \right| \rangle \Big|^n \qquad \Sigma^o_{xg} \text{ vs Burnup}$$

$$- \sum_n \sum_j \langle N^{*n}_j \left| N^n_j - y^n_j(N^{n-1}_j, \psi^{n-1}, PS^{n-1}, \psi^n, PS^n) \right| \rangle \qquad \text{Xe/Sm Depletion}$$

$$- \sum_n \sum_{xg} \langle E^*_{xg} SF_{xg} \sum_j \left(\Sigma^j_{xg} - Z_{xgj}(N_j) \right) \rangle \Big|^n \qquad \Sigma^j_{xg} \text{ vs Density}$$

where the boldface matrix notation represents the multigroup energy dependence and much of the remaining notation is standard.

The descriptive phrase to the right of each term defines the interpretation and justification for each expression. The response functional is

a reaction rate or reaction rate ratio. In general it may be a direct function of several variables, including the feedback-corrected cross section, Σ_{xg} (type x and group g), the flux distribution, Ψ, the criticality control variable, C, and the power normalization term, PS (for power scaling). In addition, R may be dependent on these parameters at each time point (denoted by the n superscript) since the response can be a discrete integral over time.

The second term in eqn. (4.1) includes the constraint that the time-dependent diffusion equation must be satisfied at each time step. The operator notation used here allows for easier manipulation of the equations and it is general enough to include both a nodal or finite difference solution scheme. The particular technique chosen would affect the implementation of the method, but the development of the basic formulation would not be altered significantly.

The feedback-corrected macroscopic data are functions of the uncorrected data, Σ°_{xg} any feedback effects, Σ^{l}_{xg}, and possibly a spectrum correction term, SF_{xg}. The feedbacks (l = xenon, samarium, boron, Doppler, water, etc.) and the spectrum correction are functions of the flux distribution and the absolute power normalization. Thus, variations made to the initial material distribution (represented by Σ^{M}_{xgm}) or to the reactor power, RP, cause direct perturbations to the system as well as the indirect perturbations due to changes in the feedback cross sections. Treating this indirect effect within the GPT formulation is one of the primary concerns of this development work.

The variational principle given above accounts for criticality reset via the fourth term on the right hand side of eqn. (4.1). In this expression, Ψ^* represents an importance function used to evaluate the eigenvalue, λ. The

defining equation for Ψ^* can be derived by appropriate manipulation of the K-functional (to be discussed shortly). The control variable used here is either the eigenvalue (which indicates no reset) or the concentration in parts per million (PPM) of soluble boron. The use of the PPM variable is specific to PWRs, but it is utilized in a general sense here to represent the mechanism most readily used to control criticality. Thus the specification of C = PPM does not limit the generality of our development.

The fifth and sixth terms in eqn. (4.1) are generalized flux and power normalization constraints. The symbol FS (PS) represents a flux (power) scaling factor and $W_1(W_2)$ gives the explicit dependence of FS (PS) on the fission cross section and flux distribution. The exact representation for these terms (as well as Σl_{xg} and SF_{xg}) may be slightly different depending on the particular physics design code. With appropriate adjustment of the definition of these parameters, the above variational principle can be made compatible with most LWR design codes.

The last four terms in eqn. (4.1) define the macroscopic depletion process. The first of these indicates the functional dependence of the burnup distribution at time point n (BU^n) on several parameters evaluated at n-1 and at n. In particular, $f^n{}_m$ shows explicit dependence on BU, Ψ, and PS at n-1 as well as on Ψ and PS at n. This is done for generality since some codes evaluate the burnup and flux distributions simultaneously during the iterative process. The additional m subscript has been included to account for different burnup relationships for fuel and burnable poison (BP) depletion.

The next term in eqn. (4.1) simply shows the dependence of the feedback-free cross sections on the burnup distribution and any new makeup material ($\Sigma^M{}_{xgm}$) at that time. In particular, each LWR code uses slightly different

correlating schemes to represent the variation of Σ°_{xg} versus burnup. In any given application, h_{xgm} would be specialized to the particular code of interest.

The last two terms in the K-functional have exactly the same form as the previous two terms. These expressions are designed to model xenon and samarium depletion in a manner similar to the way that fuel and BP depletion were treated. In this case, however, the actual densities, N_j, are followed versus time and then an expression (denoted by Z_{xgj}) is used to relate the density to the poison feedback macroscopic cross section Σ^{j}_{xg}.

The above macroscopic burnup formulation, coupled with the feedback and k-reset constraints, defines the forward problem solved in most LWR depletion applications. To define a time-dependent adjoint formulation consistent with the forward problem, one must force the K-functional to be stationary with respect to the dependent parameters. The dependent variables are Σ_{xg}, C, PS, Ψ, BU_m, and N_j and the independent parameters are Σ^{M}_{xgm}, RP, and FS. Forcing the dependent parameter variations to zero results in a set of simultaneous equations that defines all the adjoint functions (or Lagrange multipliers), Γ^*, E^*_{xg}, C^*, FN^*, PN^*, B^*_m, and N^*_j and the weight function Ψ^*. The perturbation equation, on the other hand, is derived by taking the variation with respect to the independent parameters. Typically, the flux scaling factor FS is used only to define precisely the normalization on the flux distribution and it does not change. Therefore, the independent parameters of interest in this work are the feed macros, Σ^{M}_{xgm}, and the reactor power, RP, at each time point.

Taking the variation of eqn. (4.1) with respect to Σ^{M}_{xgm} and RP gives:

$$\Delta R = \sum_{n} \left[\sum_{xg} \langle E^{*}_{xg} SF_{xg} \sum_{m} \delta\Sigma^{M}_{xgm} \rangle + PN^{*} \frac{\partial W_2}{\partial RP} \delta RP \right] \Bigg|^{n} \qquad (4.2)$$

This expression is the perturbation formulation of interest in this work. Knowledge of the importance functions, E^*_{xg} and PN^*, at all time points allows one the ability to estimate values of ΔR due to perturbations in the makeup feed or reactor power at any time. Estimates of ΔR can be obtained by the evaluation of a simple integral expression for any number of potential material or power variations. This efficient predictive capability is the main advantage of GPT methods.

To benefit from the use of eqn. (4.2) one must be able to calculate the desired importance functions. To derive these, one forces the first variation of the K-functional with respect to the dependent parameters to vanish. Taking one term at a time, one has

1. Setting $\sum_n \langle \frac{\partial K}{\partial \Sigma_{xg}} \delta\Sigma_{xg} \rangle \Big|^n$ to zero gives:

$$E^*_{xg}\Big|^n = \left[\frac{\partial R}{\partial \Sigma_{xg}} - \Gamma^* \frac{\partial}{\partial \Sigma_{xg}}(\mathbf{L} - \lambda \mathbf{F})\boldsymbol{\psi} + \frac{\mathbf{C}^*}{\langle \boldsymbol{\psi}^* \mathbf{F} \boldsymbol{\psi} \rangle} \left(\boldsymbol{\psi}^* \frac{\partial}{\partial \Sigma_{xg}}(\mathbf{L} - \lambda \mathbf{F})\boldsymbol{\psi} \right) \right. \tag{4.3}$$

$$\left. + FN^* \frac{\partial W_1}{\partial \Sigma_{xg}} + PN^* \frac{\partial W_2}{\partial \Sigma_{xg}} \right] \Big|^n$$

2. Setting $\sum_n \langle \frac{\partial K}{\partial PS} \delta PS \rangle \Big|^n$ to zero gives:

$$PN^*\Big|^n = \frac{\partial R}{\partial PS}\Big|^n + \sum_{xg} \langle E^*_{xg} A^{PS1}_{xg} \rangle \Big|^n + \sum_m \langle B^{*n}_m \frac{\partial f^n_m}{\partial PS^n} + B^{*n+1}_m \frac{\partial f^{n+1}_m}{\partial PS^n} \rangle \tag{4.4}$$

$$+ \sum_j \langle N^{*n}_j \frac{\partial y^n_j}{\partial PS^n} + N^{*n+1}_j \frac{\partial y^{n+1}_j}{\partial PS^n} \rangle$$

where

$$A^{PS1}_{xg}\Big|^n = \left[\Sigma^{SF}_{xg} \frac{\partial SF_{xg}}{\partial PS} + \left(\sum_l \frac{\partial \Sigma^l_{xg}}{\partial PS} \right) SF_{xg} \right] \Big|^n \tag{4.5}$$

and $$\Sigma^{SF}_{xg}\Big|^{n} = \left[\Sigma^{o}_{xg} + \sum_{l}\Sigma^{l}_{xg}\right]\Big|^{n} = \frac{\Sigma_{xg}}{SF_{xg}}\Big|^{n} \tag{4.6}$$

3. Setting $\sum_{n}\langle\frac{\partial K}{\partial \psi}\delta\psi\rangle\Big|^{n}$ to zero gives:

$$(L - \lambda F)^{*}\Gamma^{*}\Big|^{n} = S^{*}\Big|^{n} \tag{4.7}$$

where

$$S^{*}\Big|^{n} = \left[\frac{\partial R}{\partial \psi} + \sum_{xg}E^{*}_{xg}A^{\psi 1}_{xg} + FN^{*}\frac{\partial W_{1}}{\partial \psi} + \frac{C^{*}}{\langle\psi^{*}F\psi\rangle}\Big((L-\lambda F)^{*}\psi^{*}\Big) + PN^{*}\frac{\partial W_{2}}{\partial \psi}\right]\Big|^{n} \tag{4.8}$$

$$+\sum_{m}\left[B^{*n}_{m}\frac{\partial f^{n}_{m}}{\partial \psi^{n}} + B^{*n+1}_{m}\frac{\partial f^{n+1}_{m}}{\partial \psi^{n}}\right] + \sum_{j}\left[N^{*n}_{j}\frac{\partial y^{n}_{j}}{\partial \psi^{n}} + N^{*n+1}_{j}\frac{\partial y^{n+1}_{j}}{\partial \psi^{n}}\right]$$

and $$A^{\psi 1}_{xg}\Big|^{n} = \left[\Sigma^{SF}_{xg}\frac{\partial SF_{xg}}{\partial \psi} + \Big(\sum_{l}\frac{\partial \Sigma^{l}_{xg}}{\partial \psi}\Big)SF_{xg}\right]\Big|^{n} \tag{4.9}$$

4. Setting $\sum_{n}\langle\frac{\partial K}{\partial BU_{m}}\delta BU_{m}\rangle\Big|^{n}$ to zero gives:

$$B^{*}_{m}\Big|^{n} = \left[\frac{\partial R}{\partial BU_{m}} + \sum_{xg}E^{*}_{xg}SF_{xg}\frac{\partial h_{xgm}}{\partial BU_{m}}\right]\Big|^{n} + B^{*n+1}_{m}\frac{\partial f^{n+1}_{m}}{\partial BU^{n}_{m}} \tag{4.10}$$

5. Setting $\sum_{n}\langle\frac{\partial K}{\partial N_{j}}\delta N_{j}\rangle\Big|^{n}$ to zero gives:

$$N^{*}_{j}\Big|^{n} = \left[\frac{\partial R}{\partial N_{j}} + \sum_{xg}E^{*}_{xg}SF_{xg}\frac{\partial Z_{xgj}}{\partial N_{j}}\right]\Big|^{n} + N^{*n+1}_{j}\frac{\partial y^{n+1}_{j}}{\partial N^{n}_{j}} \tag{4.11}$$

6. Setting $\sum_{n}\langle\frac{\partial K}{\partial C}\delta C\rangle\Big|^{n}$ to zero gives:

$$C^{*}\frac{\partial \lambda}{\partial C}\Big|^{n} = \left[\frac{\partial R}{\partial C} + \langle\Gamma^{*}F\psi\rangle\frac{\partial \lambda}{\partial C} + \sum_{xg}\langle E^{*}_{xg}SF_{xg}\Big(\sum_{l}\frac{\partial \Sigma^{l}_{xg}}{\partial C}\Big)\rangle\right]\Big|^{n} \tag{4.12}$$

When the eigenvalue is the control variable eqn. (4.12) reduces to

$$\left.\frac{C^*}{\langle \psi^* F \psi \rangle}\right|^n = \left.\left(\frac{\partial R/\partial \lambda + \langle \Gamma^* F \psi \rangle}{\langle \psi^* F \psi \rangle}\right)\right|^n \tag{4.13}$$

When the PPM of soluble boron is the control variable eqn. (4.12) reduces to

$$\left.\frac{\partial R}{\partial PPM}\right|^n = -\left.\sum_{xg} \langle E^*_{xg} SF_{xg} \frac{\partial \Sigma^{Boron}_{xg}}{\partial PPM} \rangle\right|^n \tag{4.14}$$

This last expression, coupled with eqn. (4.3), can be used to define precisely the value of C* for this case,

$$\left.\frac{C^*}{\langle \psi^* F \psi \rangle}\right|^n = \frac{-\left|\frac{\partial R}{\partial PPM} + \sum_{xg}\left(\langle \frac{\partial R}{\partial \Sigma_{xg}} SF_{xg} \frac{\partial \Sigma^{Boron}_{xg}}{\partial PPM} \rangle - \langle \Gamma^* \frac{\partial}{\partial \Sigma_{xg}} (L - \lambda F)\psi SF_{xg} \frac{\partial \Sigma^{Boron}_{xg}}{\partial PPM} \rangle\right)\right|}{\sum_{xg} \langle \psi^* \frac{\partial}{\partial \Sigma_{xg}} (L - \lambda F)\psi SF_{xg} \frac{\partial \Sigma^{Boron}_{xg}}{\partial PPM} \rangle} \tag{4.15}$$

where we have assumed that W_1 and W_2 are not functions of the control cross sections.

7. Additional Relationships:

It should be noted that eqn. (4.7) indicates that the adjoint source is orthogonal to the forward flux. That is,

$$\langle \psi S^* \rangle = 0 \tag{4.16}$$

This condition, with S* represented by eqn. (4.8), defines the FN* function,

$$FN^*\Big|^n = -\langle \psi \frac{\partial W_1}{\partial \psi} \rangle^{-1} \left|\langle \psi \frac{\partial R}{\partial \psi} \rangle + \sum_{xg} \langle \psi E^*_{xg} A^{\psi 1}_{xg} \rangle\right|^n + PN^* \langle \psi \frac{\partial W_2}{\partial \psi} \rangle\Big|^n \tag{4.17}$$

$$+ \sum_m \left(\langle B^{*n}_m \psi^n \frac{\partial f^n_m}{\partial \psi^n} \rangle + \langle B^{*n+1}_m \psi^n \frac{\partial f^{n+1}_m}{\partial \psi^n} \rangle\right) + \left|\sum_j \left(\langle N^{*n}_j \psi^n \frac{\partial y^n_j}{\partial \psi^n} \rangle + \langle N^{*n}_j \psi^n \frac{\partial y^{n+1}_j}{\partial \psi^n} \rangle\right)\right|$$

Equations (4.3)-(4.17) define a relatively complicated set of coupled adjoint equations. The equations in their present form are quite cumbersome to deal with since they contain multiple interdependencies on several of the

other importance functions. After considerable algebraic manipulation, the following more-refined set of defining equations is obtained:

$$E^*_{xg}\Big|^n = \left[\frac{\partial R}{\partial \Sigma_{xg}} - \Gamma^*_N \frac{\partial}{\partial \Sigma_{xg}}(L - \lambda F)\psi + FN^* \frac{\partial W_1}{\partial \Sigma_{xg}} + PN^* \frac{\partial W_2}{\partial \Sigma_{xg}}\right]\Big|^n \tag{4.18}$$

$$\Gamma^*_N\Big|^n = \left[\Gamma^* - \frac{C^*}{\langle \psi^* F \psi \rangle}\psi^*\right]\Big|^n \tag{4.19}$$

$$FN^*\Big|^n = \frac{-1}{\langle \psi S^*_4 \rangle}\left[\langle \psi S^*_1 \rangle + PN^* \langle \psi S^*_3 \rangle + \frac{C^*}{\langle \psi^* F \psi \rangle}\langle \psi S^*_2 \rangle\right]\Big|^n \tag{4.20}$$

$$PN^*\Big|^n = \frac{1}{ZN}\left[PN^*_R - \frac{C^*}{\langle \psi^* F \psi \rangle} PN^*_\lambda\right]\Big|^n \tag{4.18}$$

where C^* is defined in eqn. (4.13) or (4.15) depending on the choice of control variable.

These expressions contain the regular and generalized adjoint fluxes which are defined by:

$$(L - \lambda F)^* \psi^*\Big|^n = S^*_\lambda\Big|^n \tag{4.22}$$

$$S^*_\lambda\Big|^n = \left[-S^*_2 + S^*_4 \frac{\langle \psi S^*_2 \rangle}{\langle \psi S^*_4 \rangle} + \frac{PN^*_\lambda}{ZN}\left(S^*_3 - S^*_4 \frac{\langle \psi S^*_3 \rangle}{\langle \psi S^*_4 \rangle}\right)\right]\Big|^n \tag{4.23}$$

$$(L - \lambda F)^* \Gamma^*\Big|^n = S^*_R\Big|^n \tag{4.24}$$

$$S^*_R\Big|^n = \left[S^*_1 + S^*_4 \frac{\langle \psi S^*_1 \rangle}{\langle \psi S^*_4 \rangle} + \frac{PN^*_R}{ZN}\left(S^*_3 - S^*_4 \frac{\langle \psi S^*_3 \rangle}{\langle \psi S^*_4 \rangle}\right)\right]\Big|^n \tag{4.25}$$

with

$$S^*_1\Big|^n = \frac{\partial R}{\partial \psi}\Big|^n + \sum_{xg} A^\psi_{xg}\left[\frac{\partial R}{\partial \Sigma_{xg}} - \Gamma^* \frac{\partial}{\partial \Sigma_{xg}}(L - \lambda F)\psi\right]\Big|^n \tag{4.26}$$

$$+ \sum_m \left[\frac{\partial R}{\partial BU_m}\frac{\partial f_m}{\partial \psi}\Big|^n + B^{*n+1}_m\left(\frac{\partial f^{n+1}_m}{\partial BU^n_m}\frac{\partial f^n_m}{\partial \psi^n} + \frac{\partial f^{n+1}_m}{\partial \psi^n}\right)\right]$$

$$+ \sum_j \left[\frac{\partial R}{\partial N_j} \frac{\partial y_j}{\partial \psi} \right]^n + N_j^{*n+1} \left(\frac{\partial y_j^{n+1}}{\partial N_j^n} \frac{\partial y_j^n}{\partial \psi^n} + \frac{\partial y_j^{n+1}}{\partial \psi^n} \right) \Bigg|$$

$$S_2^* \Big|^n = \sum_{xg} A_{xg}^{\psi} \left[\psi^* \frac{\partial}{\partial \Sigma_{xg}} (L - \lambda F) \psi \right] \Big|^n \tag{4.27}$$

$$S_3^* \Big|^n = \left[\frac{\partial W_2}{\partial \psi} + \sum_{xg} A_{xg}^{\psi} \frac{\partial W_2}{\partial \Sigma_{xg}} \right] \Big|^n \tag{4.28}$$

$$S_4^* \Big|^n = \left[\frac{\partial W_1}{\partial \psi} + \sum_{xg} A_{xg}^{\psi} \frac{\partial W_1}{\partial \Sigma_{xg}} \right] \Big|^n \tag{4.29}$$

where

$$A_{xg}^{\psi} = A_{xg}^{\psi 1} + A_{xg}^{\psi 2} + A_{xg}^{\psi 3} \tag{4.30}$$

$$A_{xg}^{\psi 2} = SF_{xg} \sum_m \frac{\partial h_{xgm}}{\partial BU_m} \frac{\partial f_m}{\partial \psi} \tag{4.31}$$

$$A_{xg}^{\psi 3} = SF_{xg} \sum_j \frac{\partial Z_{xgj}}{\partial N_j} \frac{\partial y_j}{\partial \psi} \tag{4.32}$$

$$A_{xg}^{PS} = A_{xg}^{PS1} + A_{xg}^{PS2} + A_{xg}^{PS3} \tag{4.33}$$

$$A_{xg}^{PS2} = SF_{xg} \sum_m \frac{\partial h_{xgm}}{\partial BU_m} \frac{\partial f_m}{\partial PS} \tag{4.34}$$

$$A_{xg}^{PS3} = SF_{xg} \sum_j \frac{\partial Z_{xgj}}{\partial N_j} \frac{\partial y_j}{\partial PS} \tag{4.35}$$

$$ZN = 1 - \sum_{xg} \langle A_{xg}^{PS} \frac{\partial W_2}{\partial \Sigma_{xg}} \rangle + \sum_{xg} \langle A_{xg}^{PS} \frac{\partial W_1}{\partial \Sigma_{xg}} \rangle \frac{\langle \psi S_3^* \rangle}{\langle \psi S_4^* \rangle} \tag{4.36}$$

where $A^{\psi 1}{}_{xg}$, $A^{PS1}{}_{xg}$ and $\Sigma^{SF}{}_{xg}$ are defined by eqns. (4.9), (4.5), and (4.6) respectively, and

$$PN_\lambda^* \Big|^n = - \sum_{xg} \langle A_{xg}^{PS} \left[\psi^* \frac{\partial}{\partial \Sigma_{xg}} (L - \lambda F) \psi \right] \rangle \Big|^n + \sum_{xg} \langle A_{xg}^{PS} \frac{\partial W_1}{\partial \Sigma_{xg}} \rangle \frac{\langle \psi S_2^* \rangle}{\langle \psi S_4^* \rangle} \Big|^n \tag{4.37}$$

$$PN_R^* \Big|^n = \frac{\partial R}{\partial PS}\Big|^n - \sum_{xg} \langle A_{xg}^{PS} \frac{\partial W_1}{\partial \Sigma_{xg}} \rangle \frac{\langle \psi S_1^* \rangle}{\langle \psi S_4^* \rangle}\Big|^n \tag{4.38}$$

$$+ \sum_{xg} \langle A_{xg}^{PS} \Big| \frac{\partial R}{\partial \Sigma_{xg}} - \Gamma^* \frac{\partial}{\partial \Sigma_{xg}} (L - \lambda F)\psi \Big| \rangle \Big|^n$$

$$+ \sum_{m} \Big[\langle \frac{\partial R}{\partial BU_m} \frac{\partial f_m}{\partial PS} \rangle \Big|^n + \langle B_m^{*n+1} \Big(\frac{\partial f_m^{n+1}}{\partial BU_m^n} \frac{\partial f_m^n}{\partial PS^n} + \frac{\partial f_m^{n+1}}{\partial PS^n} \Big) \rangle \Big|$$

$$+ \sum_{j} \Big[\langle \frac{\partial R}{\partial N_j} \frac{\partial y_j}{\partial PS} \rangle \Big|^n + \langle N_j^{*n+1} \Big(\frac{\partial y_j^{n+1}}{\partial N_j^n} \frac{\partial y_j^n}{\partial PS^n} + \frac{\partial y_j^{n+1}}{\partial PS^n} \Big) \rangle \Big|$$

and the expressions for $B^{*n}{}_m$ and $N^{*n}{}_j$ remain the same as those given in eqns. (4.10) and (4.11), respectively.

The above equations define a complete time-dependent adjoint GPT formulation that is compatible with most LWR depletion codes. These equations describe a backward adjoint depletion problem. The process is initiated with a final-time source which represents the derivative of the response with respect to several variables evaluated at the final time t_f. At this time point all terms evaluated at $n+1 = N+1$ are zero. Starting with this source, the adjoint equations are solved backwards in time until the initial time (in the forward sense) has been reached. The time-dependent importance functions that result can then be utilized in the perturbation expression in eqn. (4.2). This overall calculational procedure is summarized in Fig. 4.1.

The procedure outlined in Fig. 4.1 is conceptually straightforward and it is similar to the algorithm developed for the original DEPTH-CHARGE code. The adjoint depletion steps [eqns. (4.10) and (4.11)] are quite simple but the S^*_R and S^*_λ terms are more complicated than in the original development.

I. Perform Reference Forward Depletion Calculation

Begin loop over time (initial to final)

A. Do normal forward calculation

B. Perform regular adjoint calculation (eqns. 4.22 and 4.23)

C. Save Ψ and Ψ^* for subsequent Γ^* calculations

D. Do forward burnup calculation

E. Go to I.A or exit loop if end of cycle

End time loop

II. Perform Adjoint Depletion Calculation

Begin loop over number of responses

A. Define desired response

B. Set terms with N + 1 superscripts to zero

Begin loop over time (final to initial)

C. Calculate generalized adjoint flux (eqns. 4.24 and 4.25)

D. Sweep out fundamental mode (during iteration as defined in eqn. 4.19)

E. Calculate E^*_{xg}, FN^*, and PN^* importance functions (eqns. 4.18, 4.20, and 4.21)

F. Do adjoint depletion calculation (eqns. 4.10 and 4.11)

G. Let n = n-1 and go to II.C or exit loop if beginning of cycle

End time loop

H. Save adjoint functions for this response

I. Go to II.A or exit response loop

End of response loop

Figure 4.1 Outline of Calculational Procedure for Solution of Adjoint Depletion Equations

The added complexity is due primarily to the feedback correction terms. Another new feature of this development is the k-reset mechanism, which manifests itself as the generalized sweeping procedure in eqn. (4.19)-(4.21).

It is important to note that the above formulation is quite general; yet it can be specialized to be consistent with most current design codes. The somewhat abstract notation used for the feedback and normalization terms ($\Sigma l_{xg}/SF_{xg}$ and W_1/W_2, respectively) and for the functions that correlate macro cross sections to burnup and Xe/Sm densities to macro cross sections (h_{xgm} and Z_{xgj}, respectively) would require specialization to the forward design code of interest. Once this is done, one can evaluate explicitly the many derivative terms ($\partial\Sigma l_{xg}/\partial\Psi$, $\partial\Sigma l_{xg}/\partial PS$, $\partial h_{xgm}/\partial BU_m$, $\partial\Sigma_{xgj}/\partial N_j$, etc.) that appear in the above formulation. Examples of specific feedback correlations and normalization models are contained in most code documentation.[117]

Thus, the computation of the derivative terms is a straightforward task. Many of the feedback correlations are simple linear functions of the dependent variables, making computation of the desired derivatives relatively easy. One function of special interest, however, is $h_{xgm}(BU_m)$. This function correlates the macroscopic cross sections to burnup. Some codes treat this correspondence through relatively complicated table-lookup procedures (with appropriate interpolation routines). If this procedure is used in the forward code, then the derivatives of the function with respect to the BU_m variable will have to be computed via a finite difference procedure. In practice, this procedure poses no great difficulty except that the data handling aspects are slightly more complicated. Finally, with known derivative terms, the solution procedure for the adjoint functions will follow the outline given in Fig. 4.1.

The actual implementation of the complete time-dependent adjoint formulation is beyond the scope of the current effort. The main emphasis here is the theoretical development of a comprehensive LWR-compatible adjoint formulation; and this goal has been accomplished. However, to get a better feel for the potential applications of this new theory, some further discussion and illustration of the main features of the new formulation are appropriate.

IV.3 Solution of the Flux Equations

The complete time-dependent GPT formulation given in the previous section includes, as a subset, a static GPT method that can be used in the analysis of steady-state design problems. The static formulation is applicable to a wide class of problems of interest and it is much simpler to comprehend. It still contains the main features of interest in this development: the thermal-hydraulic and poison feedback treatment and the k-reset capability. Thus, the static GPT formulation will be utilized in further discussions of these features. This simplification is not really necessary, but it does remove the complexity associated with the burnup terms. Also, in the natural evolution of methods development, we need to address the static case before treating the time-dependent burnup problem. In addition, it should be noted that Bowman[115-116] has already addressed the adjoint macroscopic depletion problem within the SIMULATE code; thus, this aspect of the formulation has already been solved.

The main expressions of interest in the static formulation are the regular and generalized adjoint flux equations. The steady-state assumption eliminates the dependence on time point n and simplifies the general formulation by canceling all the burnup-related terms (functions of f_m, h_{xgm}, y_j, and Z_{xgj}). The remaining expressions for the adjoint sources, S^*_λ and S^*_R, are still quite complicated, but manageable.

The adjoint flux equations derived here are similar to those solved within VENTURE (Ref. 80). For comparison purposes, VENTURE solves the generalized expression

$$(\mathbf{L} - \lambda\mathbf{F})^*\Gamma^* = \mathbf{S}^* = \frac{\partial R}{\partial \psi} \tag{4.39}$$

along with a sweeping procedure identical to eqn. (4.19). The only difference between eqn. (4.22) and eqn. (4.39) is the additional terms in the adjoint source formulation. These additional terms are the result of the incorporation of feedback effects in the current GPT methodology. When feedback effects are ignored, $\mathbf{S}^*_R$ reduces to $\partial R/\partial\Psi$ and $\mathbf{S}^*_\lambda$ goes to zero. The extra terms in eqns. (4.25) and (4.23) in the current development account for the indirect change in the cross sections through the dependence of the feedbacks on the flux distribution and power normalization. The dependence on Ψ is inherent in the terms containing $\mathbf{A}^{\Psi}_{xg}$ and the normalization dependence is treated within the terms containing A^{PS}_{xg}.

Since the additional source terms are functions of the quantity of interest, they will enter into the iterative calculation. For illustration, consider the Ψ^* expression. The first source term in eqn. (4.23) contains Ψ^* as a distributed parameter and the other terms have Ψ^* within an integral expression. The first contribution can be written in a generic way as some matrix operator $\mathbf{H}^*$ operating on Ψ^*. Thus, the Ψ^* equation can be rewritten as

$$(\mathbf{L} - \lambda\mathbf{F})^*\psi^* = -\mathbf{H}^*\psi^* + \mathbf{S}^*_4\frac{\langle \psi \mathbf{H}^*\psi^*\rangle}{\langle \psi \mathbf{S}^*_4\rangle} + \frac{PN^*_\lambda}{ZN}\left(\mathbf{S}^*_3 - \mathbf{S}^*_4\frac{\langle \psi \mathbf{S}^*_3\rangle}{\langle \psi \mathbf{S}^*_4\rangle}\right) \tag{4.40}$$

where $\mathbf{H}^*$ is defined through the correspondence with the $\mathbf{S}^*_2$ expression. An explicit representation of $\mathbf{H}^*$ could be made, but it would require several new

definitions and further discussion. The real point of interest here is the form of eqn. (4.40), not the precise definition of H^*.

Rearranging eqn. (4.40) slightly gives

$$(L - \lambda F + H)^*\psi^* = S_4^* \frac{\langle \psi H^* \psi^* \rangle}{\langle \psi S_4^* \rangle} + \frac{PN_\lambda^*}{ZN}\left(S_3^* - S_4^* \frac{\langle \psi S_3^* \rangle}{\langle \psi S_4^* \rangle} \right) \tag{4.41}$$

This form of the equation suggests that part of the adjoint feedback effect can be treated as a cross section correction to the reference forward feedback-corrected cross sections. The rest of the feedback contribution is contained in a fixed-source term that is computed and updated during the iterative scheme. Thus, eqn. (4.41) is more representative of how the iterative computations will proceed.

The above discussion applies to the Γ^* as well as ψ^* equation. If these two importance functions can be determined, then the desired response derivatives can be computed. At present, some specific coding for the solution of the static ψ^* and Γ^* equations with feedback is being implemented within a proprietary Westinghouse design code. This code development work is not complete as yet, but some preliminary results are available that illustrate the key features of the method and verify the completeness of the theoretical development. The following subsection will summarize some of the important data obtained in this preliminary testing phase.

IV.4 Verification of Method

The new aspect of the GPT formulation developed in the previous subsection is the implicit treatment of thermal-hydraulic and poison feedback effects within the adjoint flux equations. Two relatively simple problems (one analytical and the other numerical) have been performed to verify the theoretical development and to illustrate some of the interesting features of

the feedback treatment. This subsection will present the major results of these sample problems.

IV.4.A Analytical Example: Consider a simple 1-D slab, 1-group, bare homogeneous reactor problem where the only feedback mechanism is a reactivity dependence on the reactor power level. This can be modeled by letting the absorption cross section be linearly dependent on the flux normalization. The defining equations for such a system are:

$$\frac{d^2}{dx^2}\psi(x) + B^2\psi(x) = 0 \qquad \text{Flux Distribution} \qquad (4.42)$$

$$B^2 = \frac{\lambda\nu\Sigma_f - \Sigma_a}{D} \qquad \text{Material Buckling} \qquad (4.43)$$

$$\Sigma_a = \Sigma_a^o + C_1 PS \qquad \text{Cross Section Feedback} \qquad (4.44)$$

$$\nu\Sigma_f = \nu\Sigma_f^o$$

$$D = D^o$$

$$FS = 1 = \frac{1}{\nu\Sigma_f \langle\psi\rangle} \qquad \text{Flux Normalization} \qquad (4.45)$$

$$PS = \alpha_p = \frac{1}{\kappa\Sigma_f \langle\psi\rangle} \qquad \text{Power Normalization} \qquad (4.46)$$

where P represents reactor power and PS and FS are the power scaling and flux scaling factors discussed previously. C_1 is a coefficient that specifies the magnitude of the feedback component. The right hand side of eqns. (4.45) and (4.46) are specific examples of the W_1 and W_2 functions introduced in eqn. (4.1).

For a homogeneous system that has a reflective boundary condition at the center of the reactor and a zero flux condition at an extrapolated length a/2, it can be shown that the solution to eqn. (4.42) is given by

$$\phi(x) = a_p \psi(x) = \frac{P\pi}{\kappa\Sigma_f a} \cos\frac{\pi x}{a} \tag{4.47}$$

and

$$\lambda = \frac{DB^2 + \Sigma_a}{\nu\Sigma_f} = \frac{DB^2 + \Sigma_a^o}{\nu\Sigma_f} + \frac{C_1 PS}{\nu\Sigma_f} = \lambda^o + \frac{C_1 P}{\kappa\Sigma_f} \tag{4.48}$$

Therefore,

$$\frac{\partial\lambda}{\partial\Sigma_a^o} = \frac{1}{\nu\Sigma_f} \tag{4.49}$$

and

$$\frac{\partial\lambda}{\partial P} = \frac{C_1}{\kappa\Sigma_f} \tag{4.50}$$

Equations (4.49) and (4.50) are the desired results of the forward analysis. Now, one should be able to get identical derivatives using the formal GPT expressions given previously. For the case of interest, the perturbation formula given in eqn. (4.2) can be expressed as

$$\Delta R = \langle E_a^* \delta\Sigma_a^o \rangle + PN^* \frac{\partial W_2}{\partial P} \delta P \tag{4.51}$$

and since the desired response is λ and the perturbation is constant throughout the core, then

$$\frac{\partial\lambda}{\partial\Sigma_a^o} = \langle E_a^* \rangle \tag{4.52}$$

and

$$\frac{\partial\lambda}{\partial P} = PN^* \frac{\partial W_2}{\partial P} \tag{4.53}$$

Thus we need to show that eqns. (4.49) and (4.50) are identical to eqns. (4.52) and (4.53), respectively.

In showing this result it should be noted that for the static case when the general response R becomes λ (and the control variable C is λ), then the generalized adjoint flux, Γ^*, and the regular adjoint flux, ψ^*, are identical.

Under these conditions, eqn. (4.13) reduces to

$$\frac{C^*}{\langle \psi^* F \psi \rangle} = \frac{1 + \langle \psi^* \nu\Sigma_f \psi \rangle}{\langle \psi^* \nu\Sigma_f \psi \rangle} \tag{4.54}$$

and eqn. (4.19) becomes

$$\Gamma_N^*(x) = \frac{-\psi^*(x)}{\langle \psi^* \nu\Sigma_f \psi \rangle} \tag{4.55}$$

Finally, if we normalize ψ^* such that the integral in the denominator of eqn. (4.55) is -1, then the importance function of interest is simply the normalized ψ^*.

Now to determine this function note that the adjoint source, S^*_λ, reduces to zero for this case. This can be shown as follows. First eqn. (4.5) reduces to $A^{PS1}{}_x = \partial\Sigma_a/\partial PS$ for x = absorption and zero otherwise, and eqn. (4.9) becomes $A^{\psi 1}{}_x = \partial\Sigma_x/\partial\psi = 0$ for all cross section types. With these results, the S^*_λ expression simplifies to

$$S^*_\lambda = PN^*_\lambda \left[\frac{\partial W_2}{\partial \psi} - \frac{\partial W_1}{\partial \psi} \frac{\langle \psi (\partial W_2/\partial\psi) \rangle}{\langle \psi (\partial W_1/\partial\psi) \rangle} \right] \tag{4.56}$$

Performing the indicated operations gives

$$S^*_\lambda = PN^*_\lambda \left[-\frac{\alpha_P \kappa\Sigma_f}{\kappa\Sigma_f \langle \psi \rangle} + \frac{\nu\Sigma_f}{\nu\Sigma_f \langle \psi \rangle} \left(\frac{-\alpha_P}{-1} \right) \right] = 0 \tag{4.57}$$

Since the adjoint source reduces to zero, the adjoint flux simplifies to the standard case and, after appropriate normalization, this becomes

$$\Gamma_N^*(x) = \frac{-\psi^*(x)}{\langle \psi^* \nu\Sigma_f \psi \rangle} = -\frac{4}{\pi} \cos\frac{\pi x}{a} \tag{4.58}$$

With this last expression, $\partial\lambda/\partial\Sigma^o_a$ becomes

$$\frac{\partial\lambda}{\partial\Sigma^o_a} = \langle E^*_a \rangle = -\langle \Gamma^*_N \frac{\partial}{\partial\Sigma_a} (L - \lambda F)\psi \rangle = -\langle \Gamma^*_N \psi \rangle = \frac{\langle \psi^* \psi \rangle}{\langle \psi^* \nu\Sigma_f \psi \rangle} = \frac{1}{\nu\Sigma_f} \tag{4.59}$$

and PN* becomes

$$PN^* = -\langle \Gamma^*_N \frac{\partial}{\partial\Sigma_a} (L - \lambda F)\psi \rangle \frac{\partial\Sigma_a}{\partial PS} = \frac{C_1}{\nu\Sigma_f} \tag{4.60}$$

Finally, from eqn. (4.53) we have

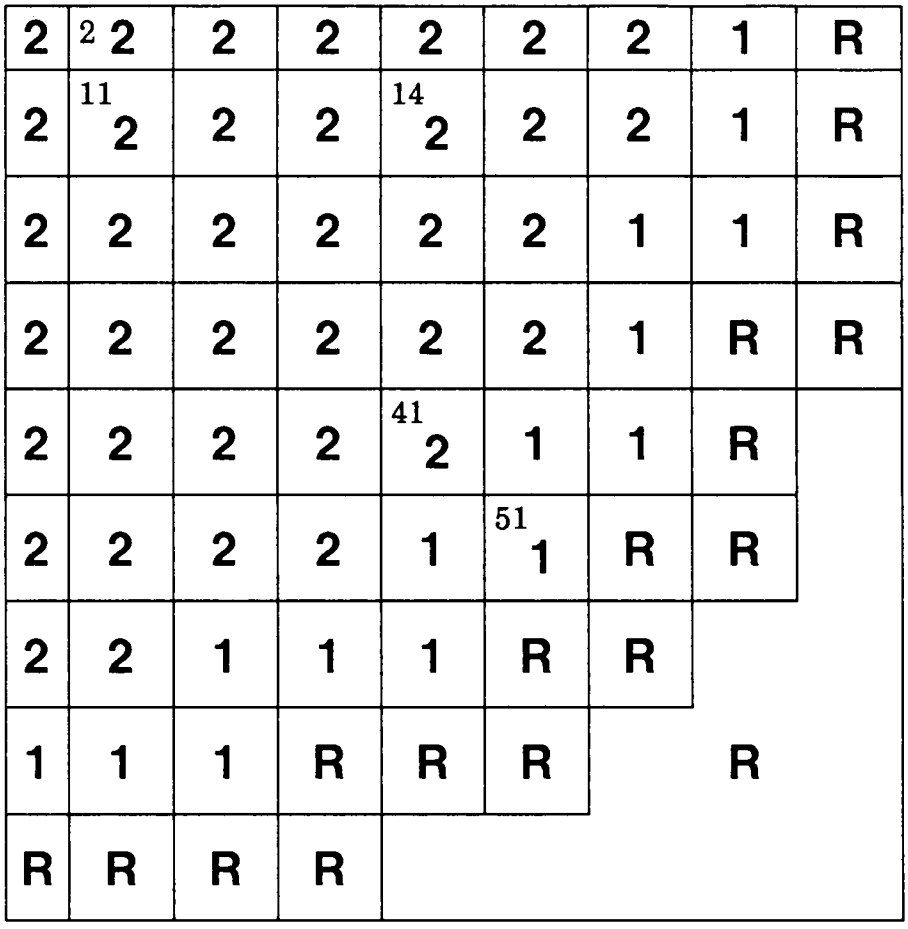
$$\frac{\partial\lambda}{\partial P} = \frac{C_1}{\nu\Sigma_f}\left(\frac{\nu\Sigma_f}{\kappa\Sigma_f}\right) = \frac{C_1}{\kappa\Sigma_f} \tag{4.61}$$

Thus, it has been shown that the adjoint formulation gives the expected results. The forward and adjoint derivatives are identical due to the simple geometric configuration and the linear feedback relationship (which is independent of the flux shape). In practical situations, the geometric model and feedback dependence are considerably more complicated.

In the above model the feedback coefficient, C_1, is zero when feedback is not treated and C_1 is nonzero when it is treated. Equation (4.61) is proportional to C_1 and thus there would be no variation in reactivity with power if C_1 is assumed zero. Previous GPT formulations simply ignore these effects. Thus, the inclusion of these phenomena within the adjoint formulation has added a new dimension to the usefulness of perturbation theory methods.

IV.4.B Numerical Examples: As indicated previously, the static portion of the new GPT formulation with feedback is currently being implemented into a proprietary Westinghouse finite difference neutronics code. This work is still in the early development stage, but the initial verification of the overall method for the K_{eff} response has been completed.

The model used for this numerical verification study is based on the 2-D 2-group IAEA PWR benchmark problem.[118] The basic quarter-core configuration is given in Fig. 4.2. The model has two fuel enrichments, with the higher enrichment located on the core periphery. The benchmark model as given in Ref. 118 has been modified to include a water density calculation based on the inlet enthalpy and the local enthalpy rise (which is a function of the local power density). The end result is a node-wise value of water density



1 Fuel Type 1 **2** Fuel Type 2 **R** Reflector

Boundary Conditions: Top, Left Side: Reflected
Bottom, Right Side: Zero Flux

Figure 4.2 Quarter-Core IAEA PWR Benchmark Configuration

that varies around an average value which is consistent with the core-average enthalpy. When a perturbation is made to the reference cross section data, the core power distribution is altered and the local water density profile is also perturbed. These changes in water density represent implicit perturbations to the reference model and these are inherent in any real reactor system. The so-called thermal-hydraulic feedback treatments used in current design codes are an attempt to approximate this behavior.

In the present study, 300 PPM of soluble boron were added to the fuel regions. Thus, the node-wise absorption cross section varies slightly depending on the local water density (which is a function of local power). Several direct (explicit) perturbations were made to the reference system and the corresponding reactivity changes (ΔK in PCM) were tabulated. Two adjoint flux computations were also made; one case included the new adjoint feedback formulation [i.e. S^*_λ given by eqn. (4.23)] and the other calculation ignored the feedback effect by simply setting S^*_λ to zero. A detailed comparison of the GPT estimates (with and without feedback) versus the direct computation of ΔK should provide a good benchmark for the new methodology.

Summary results for several of these comparisons are given in Table 4.1. The top three cases model an explicit 1% increase in the thermal absorption cross section in various zones, the middle set has an explicit 1% increase in $\nu\Sigma_{f2}$, and the last four cases model power reductions of increasing magnitude. Note that for the power perturbations there are no explicit variations in the reference feedback-free cross sections.

The distinction between explicit and implicit cross section variations is important. The explicit perturbations are under user control. For example, a

TABLE 4.1 Comparison of GPT Estimates With and Without Feedbacks Versus Direct Computations

Perturbation	ΔK_{Direct}	No Feedback		With Feedback	
		ΔK_{GPT}	Abs. Error	ΔK_{GPT}	Abs. Error
1% $\Delta\Sigma_{a2}$ Zone 11	-49.7	-49.7	0.0	-52.1	2.4
1% $\Delta\Sigma_{a2}$ Zone 51	-4.7	-5.7	1.0	-5.3	0.6
1% $\Delta\Sigma_{a2}$ Zone 11 & 51	-55.2	-55.4	0.2	-57.4	2.2
1% $\Delta\nu\Sigma_{f2}$ Zone 11	56.3	51.5	4.8	54.0	2.3
1% $\Delta\nu\Sigma_{f2}$ Zone 51	5.9	6.0	0.1	5.6	0.3
1% $\Delta\nu\Sigma_{f2}$ Zone 11 & 51	61.7	57.5	4.2	59.6	2.1
-1% ΔP	-2.6	0.0	2.6	-2.7	0.1
-5% ΔP	-13.4	0.0	13.4	-13.6	0.2
-10% ΔP	-26.8	0.0	26.8	-27.4	0.6
-50% ΔP	-128.7	0.0	128.7	-136.8	8.1

Note: Units of ΔK are PCM = 1.0×10^{-5}

simple interchange of two assemblies represents an explicit material or cross section variation. However, the original perturbation has a secondary affect on all the other unperturbed locations. In trying to predict the influence of the single assembly interchange, the user does not know *a priori* all these other implicit perturbations. Thus, the adjoint importance functions must be smart enough to account for both the explicit and implicit cross section variations to the reference configuration.

Getting back to Table 4.1, one sees good agreement between the GPT estimates and the direct calculations except for the power perturbation cases where feedback was ignored. In these cases, standard GPT indicates that

there is no reactivity change since a power perturbation only has an implicit effect on the cross sections (through the feedback treatment). In contrast, with the new adjoint formulation that includes the feedback effect, one sees excellent agreement.

In the first six cases, the differences between the GPT estimates with and without feedback are not significant. This is because the effect of the direct perturbations is much larger than the influence of the implicit variations for these cases. To quantify this statement and to further verify the correctness of the theoretical development, several auxiliary computations were performed. The goal here was to isolate the explicit and implicit contributions to ΔK.

This goal was achieved by editing the feedback-corrected macroscopic cross sections for the reference case and for each of the direct perturbation runs. In this way, detailed delta cross sections by node could be determined. Since the explicit perturbations are known, these data can be used to separate the explicit and implicit variations. Finally, these delta cross sections were used with the standard (no feedback) adjoint flux to get an estimate of the two components of ΔK.

The results of this exercise are summarized in Table 4.2. Here it is confirmed that the implicit component of ΔK is only a small part of the total reactivity change (less than 10% for these cases). Also it is important to note that the GPT estimates that include the adjoint feedback treatment are almost identical to the combined explicit and implicit ΔK values. Thus, we see that the feedback-corrected adjoint functions are indeed smart enough to automatically account for the implicit feedback effects.

TABLE 4.2 Comparison of Explicit and Implicit Components of GPT Predictions

Perturbation	No Feedback			With Feedback
	Explicit ΔK	Implicit ΔK	Total ΔK	Total ΔK
1% $\Delta\Sigma_{a2}$ Zone 11	-49.7	-2.3	-52.0	-52.1
1% $\Delta\Sigma_{a2}$ Zone 51	-5.7	0.4	-5.3	-5.3
1% $\Delta\Sigma_{a2}$ Zone 11 & 51	-55.4	-1.9	-57.3	-57.4
1% $\Delta\nu\Sigma_{f2}$ Zone 11	51.5	2.7	54.2	54.0
1% $\Delta\nu\Sigma_{f2}$ Zone 51	6.0	-0.4	5.6	5.6
1% $\Delta\nu\Sigma_{f2}$ Zone 11 & 51	57.5	2.3	59.8	59.6

Note: Units of ΔK are PCM = 1.0×10^{-5}

The above results clearly verify the theoretical development of GPT with thermal-hydraulic feedback. They provide the proof-of-principle of the basic idea. However, additional numerical testing for a variety of different configurations and other feedbacks (Doppler, xenon, etc.) is also underway. In addition, the capability to treat generalized responses (other than just K_{eff}) is being implemented. Future documentation of these applications-oriented studies will be contained as part of a University of Lowell Master's Thesis (by Byron R. Frank). This effort will address and illustrate the realistic application of the first-order GPT methods developed as part of the present research.

IV.5 Summary

In completing this section, a few summary remarks are appropriate. This complete section documents the development and verification of a

comprehensive GPT formulation that is compatible with current LWR design practices. The section begins by giving a brief historical overview of the development and application of GPT methods prior to the initiation of the present study. Here it is shown that the main emphasis to date has been the application of GPT for the sensitivity and uncertainty analysis of fast reactor performance characteristics. A deficiency in the state-of-the-art capability for the analysis of LWR systems was noted, primarily in the treatment of thermal-hydraulic and poison feedback effects in few-group problems.

To remedy this deficiency, a complete time-dependent GPT formulation was developed that includes macroscopic burnup, thermal-hydraulic and poison feedback, and a criticality reset mechanism. The derivation uses a variational approach that includes these considerations as constraint equations appended to the response functional. Detailed expressions were derived and a complete calculational algorithm for the solution of the resultant adjoint depletion equations was outlined.

Emphasis then shifted toward solution of the adjoint flux equations, with focus on the adjoint feedback effect. It was shown that the feedback treatment in the adjoint mode manifests itself as new components in the adjoint source description. This behavior complicates the iterative solution technique only slightly.

Two examples (one analytical and the other numerical) were performed as a test of the theoretical development and as an illustration of the key features of the feedback treatment. The results of these problems have confirmed the basic theoretical formulation and they have highlighted how the feedback-corrected (smart) adjoint functions can automatically account for implicit cross section variations associated with a user-defined (explicit)

perturbation. There is much more application-oriented work that needs to be performed (as future work), but the basic proof-of-principle has been established.

V. IN SEARCH OF HIGHER-ORDER ACCURACY

V.1 Introduction

The emphasis of the present work has been the development of an LWR core design methodology that is based on first-order generalized perturbation theory methods. The previous three sections of this document form the basis of this development effort. The basic design philosophy was expounded, first-order GPT was shown to be sufficiently accurate for design optimization studies, and a new LWR-compatible GPT formulation was developed.

The limitation of GPT's first-order accuracy has been noted, and it appears that much of the method's success to date is due to the rigid constraints imposed on the power distribution. It is the realistic power constraints that eliminate the possibility of gross variations in the global flux and power profiles relative to a reasonable reference core configuration. Thus, the first-order GPT approximation seems to be well suited for the fuel shuffling and BP loading problems under normal steady-state full power operation.

However, the final reload analysis is not complete with the determination of a fuel management scheme that satisfies peaking factor and reactivity constraints in the all-rods-out (ARO) full power condition. In practice, once an acceptable reload configuration has been determined, the reload design engineer must insure that this fuel management scheme will satisfy all plant technical specifications for a wide range of operational conditions. In fuel shuffling and BP loading studies, the size of the material perturbations is limited by physical and operational restrictions. In contrast, when performing safety computations, one is usually interested in off-normal

conditions, where the material or cross section variations from reference may be quite large. In these cases first-order GPT will not be sufficiently accurate and some simple higher-order correction will be required for successful implementation of a GPT-based safety analysis applications package (see Fig. 2.1 on page 7).

Thus, a related (but secondary) objective of the current research effort is the investigation of higher-order GPT methods as a mechanism for predicting many of the safety parameters (peaking factors, shutdown margins, reactivity coefficients, etc. in off-normal situations) that must be determined for each new design. An applications-oriented higher-order GPT technique would significantly enhance the power of the overall GPT-based design methodology.

This section will address some of the key issues associated with the development of a realistic higher-order methodology. This is a relatively complex subject and the goal here is only to identify some potentially interesting approaches that should resolve most of the problems associated with the search for higher-order accuracy.

V.2 Basic Problem Description

The development of higher-order perturbation methods has received attention over the years (see Refs. 92-94, 109-112, and 119-122), but to date there has not been much success in terms of realistic applications of the methods. The techniques are either too cumbersome, impractical from the perspective of the large number of complex calculations required, or simply not developed to the point where routine computations are possible.

There are two basic approaches for obtaining higher-order accuracy, both of which rely on obtaining some estimate of the perturbed flux distribution. In the first method, one attempts to determine the perturbed flux

explicitly to some higher-order approximation. This estimate of the perturbed distribution function is then used to predict any integral response of interest. The basic approach is to represent the perturbed flux as

$$\psi' = \sum_{n} \Phi^{(n)}$$

where n refers to the order of the perturbation series and the $\Phi^{(n)}$ functions are successive higher-order approximations. The above expression is substituted into the diffusion equation which results in defining expressions for the $\Phi^{(n)}$s. The most common technique for approximating the $\Phi^{(n)}$s is to expand these functions in terms of the higher harmonics of the diffusion equation (the lambda or omega eigenfunctions). Saito[92-94] and Gandini's "Standard Method"[110,121] use variations on this theme.

These modal techniques appear to have potential, but the basic approach is limited by the availability of the harmonic expansion functions. The forward and adjoint higher harmonics are relatively easy to compute in one-dimensional geometry,[112,123-124] but convergence difficulties and the requirement for sweeping out contamination from the lower harmonics complicate computations in realistic two-dimensional configurations. There has been some success in this area,[125] but the desired computations are by no means routine.

Numerical studies[93,112] using 1-D reactor models illustrate the potential of the basic method. Palmiotti's[112] recent application of Gandini's Standard Method is particularly interesting. In this study, several 1-D fast reactor models were considered. Excellent results were obtained for large perturbations using 13 harmonics and an order of approximation of about 5 (more in some cases).

The major advantage of the Standard Method is its explicit formulation. This means that once the higher harmonics are known, the perturbed flux for any material or cross section variation can be easily determined. The computational effort required for evaluation of each new configuration is relatively small. This feature is shared with first-order GPT methods and it is what makes the technique so attractive. However, as mentioned previously, determining the required forward and adjoint eigenfunctions is the major drawback at present. Thus, with the presently available technology, this method is not really practical for multidimensional analysis.

Dubi and Dudziak[111,122] have developed a similar method for source driven systems. Their approach determines the $\Phi^{(n)}$s (which are related to higher-order flux derivatives, $\partial^n\psi/\partial\Sigma^n$) using a Green's function formulation. Their technique is also explicit, but they also have a similar problem; namely, how to calculate the desired Green's functions for realistic geometries. Thus, although these explicit formulations look attractive, they are not really practical since methods for the efficient computation of the required Green's functions or higher harmonics for 2-D models are not readily available.

The second approach for obtaining higher-order accuracy in perturbation methods uses a formal derivation of second-order GPT. This technique couples the importance functions of first-order GPT with an expression for the first derivative of the flux with respect to the perturbed quantity. In this formulation, the first-order GPT adjoint functions are dependent on the response of interest and the first-order flux derivatives are a function of the particular perturbation. Thus, if there are N_R responses (requiring one adjoint calculation for each response) and N_P independent variables that may be perturbed (requiring one flux derivative computation for each independent

variable), then a total of $N_R + N_P$ diffusion theory computations are required if a complete set of first- and second-order derivatives is to be obtained. In general, this technique can require a large set of calculations and, at first glance, this approach does not appear to be very attractive. Indeed, it has always been the large number of computations that has limited the practical use of a formal second-order GPT method.

However, considering the efficiency of today's large scale computers, it is appropriate to reconsider the potential usefulness of a formal second-order perturbation methodology. The whole premise of the GPT-based design system proposed here is to divide the design process into two parts:

1. a computationally demanding, but automated, sequence of calculations to generate the sensitivity library, and
2. a flexible and user-friendly integrated applications package that would allow the quick and efficient evaluation of alternate designs.

The main advantages of this approach are the efficient use of manpower and an overall reduction in the real time necessary to perform a complete design analysis. In addition, the proposed GPT-based design process may produce a better reload design with the use of formal optimization tools and the ability to evaluate more alternatives than the standard trial and error manual approach.

Thus, it appears that a formal second-order GPT formulation may fit in nicely with our overall design framework. Clearly, the cost of performing N_P computations for the flux derivatives is still a major concern. Minimizing both the cost per calculation and the number of calculations required is very important.

The following subsections first develop the theoretical basis for the second-order GPT method and then address some alternatives for generating the required flux derivatives. The key concerns here are related to the cost per calculation and the number of calculations required. These issues, in turn, are related to how the second-order terms will be used. The remainder of this section will address these questions and identify the pros and cons of each alternative.

V.3 Second-Order GPT

Greenspan et al.[120] has derived a formal second-order GPT formulation for source driven systems using the differential sensitivity theory notation of Oblow.[126] Using an approach based on Greenspan's work, a similar formulation for the critical reactor problem is derived in detail in Appendix A. The essential result of that development is the second-order derivatives of the response R with respect to the independent data perturbations, $\delta\Sigma_j$ and $\delta\Sigma_i$:

$$\frac{\partial^2 R}{\partial\Sigma_j\partial\Sigma_i} = \frac{\partial^2 f}{\partial\Sigma_j\partial\Sigma_i} + \frac{\partial\lambda}{\partial\Sigma_i}\int_\eta \Gamma^* \frac{\partial F}{\partial\Sigma_j}\psi\, d\eta + \frac{\partial\lambda}{\partial\Sigma_j}\int_\eta \Gamma^* \frac{\partial F}{\partial\Sigma_i}\psi\, d\eta \tag{5.1}$$

$$+ \int_\eta \left(\frac{\partial^2 f}{\partial\psi\partial\Sigma_i} - \Gamma^*\frac{\partial}{\partial\Sigma_i}(L - \lambda F)\right)\frac{\partial\psi}{\partial\Sigma_j}\, d\eta$$

where

$$R = \int_\rho f[\,\psi(\rho), \Sigma(\rho)\,]\, d\rho \tag{5.2}$$

and the remaining notation is defined completely in Appendix A. The first three terms can be evaluated using information from the reference and first-order GPT computations. These terms represent the second-order direct effects. If R is not a function of Σ_i or Σ_j, then the first term is zero. Also, if Σ_i or Σ_j is not $v\Sigma_f$, then the second and third terms are zero. The first part of the last

term is also a direct effect component even though it contains the flux derivative term. As apparent, this term vanishes if R is not a direct function of Σ_i.

The term of real interest in eqn. (5.1) is the one that contains both the generalized importance function and the derivative term $\partial\psi/\partial\Sigma_j$. This expression represents the second-order indirect effects; namely,

$$\left.\frac{\partial^2 R}{\partial\Sigma_j \partial\Sigma_i}\right|_{\text{indirect}} = -\int_\eta \Gamma^* \frac{\partial}{\partial\Sigma_i}(L - \lambda F)\frac{\partial\psi}{\partial\Sigma_j} d\eta \tag{5.3}$$

This term accounts for the fact that the flux distribution is altered when a material or cross section perturbation is made. This term is assumed to be zero in the first-order GPT approximation. When the given perturbation has a significant effect on the flux (ie. when $\partial\psi/\partial\Sigma_j$ is large), then eqn. (5.3) becomes a significant component.

An alternate, more intuitive, derivation of the second-order terms can also be performed. This second approach avoids the complexity of differential sensitivity theory and it also illustrates some important characteristics of the higher-order terms. The exact indirect change in the response can be written in terms of the perturbed and reference fluxes, or in terms of the reference importance function and perturbed flux, giving

$$\Delta R_E = R' - R = \langle f(\Sigma', \psi')\rangle - \langle f(\Sigma,\psi)\rangle \qquad \text{Direct Method} \tag{5.4}$$

or

$$\Delta R_E = -\langle \Gamma^*(\Delta L - \lambda\Delta F - \Delta\lambda F)\psi'\rangle \qquad \text{Exact Perturbation Theory} \tag{5.5}$$

$$= -\underset{\text{local}}{\langle \Gamma^*(\Delta L - \lambda\Delta F)\psi'\rangle} + \Delta\lambda \underset{\text{global}}{\langle \Gamma^* F\psi'\rangle}$$

In these expressions, ΔR_E is the exact change in R (neglecting direct effects), ΔL and ΔF represent the independent perturbations to the loss and fission source operators, and $\Delta\lambda$ is the resultant change in the eigenvalue due

to the perturbation. The two terms in eqn. (5.5) are identified as local and global components. This terminology indicates that the local term is integrated only over the regions where the material perturbations are made. In contrast, the global term represents an integral over all regions containing fissionable material. This distinction may be used to advantage in certain situations. Appendix B discusses this point briefly.

Concentrating on the exact GPT expression for the moment, one sees that the perturbed flux is required to evaluate ΔR_E. Breaking ψ' into two components, $\psi' = \psi + \Delta\psi$, and substituting these in eqn. (5.5), gives

$$\Delta R_E = \Delta R_{FO} + \Delta R_{HO} \tag{5.6}$$

where

$$\Delta R_{FO} = -\langle \Gamma^*(\Delta L - \lambda \Delta F)\,\psi \rangle \tag{5.7}$$

$$\Delta R_{HO} = -\langle \Gamma^*(\Delta L - \lambda \Delta F)\,\Delta\psi \rangle + \Delta\lambda \langle \Gamma^* F \Delta\psi \rangle \tag{5.8}$$

Here ΔR_{FO} is the first-order estimate and ΔR_{HO} accounts for the remaining higher-order terms. Section IV of this report dealt exclusively with the computation of the GPT importance functions and the evaluation of a first-order expression similar to eqn. (5.7). In the development of a higher-order GPT method, on the other hand, one is concerned with the evaluation of eqn. (5.8). This expression contains second-order terms ($\Delta L \Delta\psi$ for example) and, when the flux variation is significant, some reasonable estimate of this contribution to ΔR_E will be necessary. The key to approximating ΔR_{HO} will be to estimate the $\Delta\psi$ distribution function.

Before addressing how $\Delta\psi$ might be computed, it is instructive to rewrite eqn. (5.8) in terms of the higher-order response derivatives [similar to eqn. (5.3)]. Denoting the independent group cross section for a particular reaction as Σ_i, the first-order derivative can be written as

$$\frac{\partial R}{\partial \Sigma_i(\rho)} = -\int_\eta \Gamma^*(\eta)\frac{\partial}{\partial \Sigma_i(\rho)}(L - \lambda F)\psi(\eta)d\eta \tag{5.9}$$

If the cross section variation is constant within zone z, then the first-order contribution to ΔR_E is given as

$$\Delta R_{FO} = \sum_{iz}\frac{\partial R}{\partial \Sigma_{iz}}\delta\Sigma_{iz} \tag{5.10}$$

where

$$\frac{\partial R}{\partial \Sigma_{iz}} = \int_{V_z}\frac{\partial R}{\partial \Sigma_i(\rho)}d\rho \tag{5.11}$$

The definition of the second-order derivatives can be made in a similar way, but these higher-order terms are somewhat complicated by the cross coupling of individual perturbations. A starting point is to approximate $\Delta\psi$ with a first-order Taylor series expansion,

$$\Delta\psi(\eta) = \sum_j\int_{\rho'}\frac{\partial\psi(\eta)}{\partial\Sigma_j(\rho')}\delta\Sigma_j(\rho')d\rho' \tag{5.12}$$

If the perturbation is homogeneous within a zone, then

$$\Delta\psi(\eta) = \sum_{jz'}\left[\frac{\partial\psi(\eta)}{\partial\Sigma_{jz'}}\delta\Sigma_{jz'}\right] \tag{5.13}$$

where

$$\frac{\partial\psi(\eta)}{\partial\Sigma_{jz'}} = \int_{V_{z'}}\frac{\partial\psi(\eta)}{\partial\Sigma_j(\rho')}d\rho' \tag{5.14}$$

Using this approximation, the ΔR_{HO} term can be written as

$$\Delta R_{HO} = -\sum_i\int_\rho\left[\int_\eta \Gamma^*(\eta)\frac{\partial}{\partial\Sigma_i(\rho)}(L - \lambda F)\Delta\psi(\eta)d\eta\right]\delta\Sigma_i(\rho)d\rho \tag{5.15}$$

$$= -\sum_{ij}\int_{\rho'}\int_\rho\left[\int_\eta \Gamma^*(\eta)\frac{\partial}{\partial\Sigma_i(\rho)}(L - \lambda F)\frac{\partial\psi(\eta)}{\partial\Sigma_j(\rho')}d\eta\right]\delta\Sigma_i(\rho)\delta\Sigma_j(\rho')d\rho d\rho'$$

$$= \sum_{ij}\int_{\rho'}\int_\rho\frac{\partial^2 R}{\partial\Sigma_i(\rho)\partial\Sigma_j(\rho')}\delta\Sigma_i(\rho)\delta\Sigma_j(\rho')d\rho d\rho'$$

where we see that $\partial^2 R/\partial\Sigma_i\partial\Sigma_j$ takes on exactly the same form as in eqn. (5.3).*

Writing this last expression in discrete form gives

$$\Delta R_{HO} = \sum_{iz}\sum_{iz'} \frac{\partial^2 R}{\partial\Sigma_{iz}\partial\Sigma_{jz'}}\delta\Sigma_{iz}\delta\Sigma_{jz'} \tag{5.16}$$

where

$$\frac{\partial^2 R}{\partial\Sigma_{iz}\partial\Sigma_{jz'}} = \int_{V_z}\int_{V_{z'}} \frac{\partial^2 R}{\partial\Sigma_i(\rho)\partial\Sigma_j(\rho')}d\rho d\rho' \tag{5.17}$$

Finally, if one assumes that the influence of one perturbation on another is small, then the cross derivatives can be eliminated, giving

$$\frac{\partial^2 R}{\partial\Sigma_i^2(\rho)} = -\int_\eta \Gamma^*(\eta)\frac{\partial}{\partial\Sigma_i(\rho)}(L-\lambda F)\frac{\partial\psi(\eta)}{\partial\Sigma_i(\rho)}d\eta \tag{5.18}$$

and

$$\Delta R_{HO} = \sum_{iz}\left[\int_{V_z}\frac{\partial^2 R}{\partial\Sigma_i^2(\rho)}d\rho\right]\delta\Sigma_{iz}^2 = \sum_{iz}\frac{\partial^2 R}{\partial\Sigma_{iz}^2}\delta\Sigma_{iz}^2 \tag{5.19}$$

The above expressions define a formal second-order GPT formulation that couples the first-order GPT importance functions with the first-order flux derivatives, $\partial\psi(\eta)/\partial\Sigma_i(\rho)$. The method can be derived using a formal differential sensitivity theory approach (see Appendix A) or using a more intuitive technique as just presented. Clearly, the key to the implementation of this methodology is the ability to compute the $\partial\psi/\partial\Sigma_i$ distribution functions. Some important considerations and possible approaches for estimating the flux derivatives are given in the next subsection.

---

*Detailed comparison of the current development and that given in Appendix A shows that a factor of 1/2 appears to be missing from the above indirect second-order terms. In addition, no assumption concerning the variation of Γ^* with respect to the data field is necessary in the current intuitive development. These slight inconsistencies are not completely understood and they have not been resolved as yet.

V.4 Calculation of the Flux Derivatives

The development of a practical higher-order GPT method for use in situations where first-order GPT breaks down is a complex undertaking. If one chooses the formal second-order GPT method as the basic approach, then the overall problem reduces to identifying some technique for estimating the flux perturbations that result from a change in the independent variables within the reactor system. Knowledge of the delta flux (or flux derivatives) associated with a particular perturbation would allow construction of the desired second-order response derivatives. However, it is important to emphasize that, for realistic applications, the computation of these derivatives must be as efficient and cost effective as possible.

V.4.A Choice of Independent Variables: In choosing a particular computational technique, several factors should be considered. Probably the most important consideration is the choice of independent parameters. If the number of independent variables is N_p, then a total of N_p computations is required for a full set of flux derivatives. The simplest and most flexible choice would be the macroscopic cross section for each reaction type x, each energy group g, and each zone z. In this case, N_p would equal X*G*Z (where the capital notation indicates the total number of reaction types X, total number of groups G, etc.). For realistic configurations, however, this number would be unreasonably large.

As a base for comparison, consider the 1/8 core model described in Section III.3.B. For that model G=2, Z=26, and the major reaction types were absorption, fission, and transport (ie. X=3). Therefore, in this case, N_p = 156, indicating that 156 computations would be required for a complete set of flux

derivatives, $\partial\psi/\Sigma_{xgz}$. This number of computations is too large for realistic applications.

With the experience gained from the optimization applications discussed in Section III, a second choice of independent variables might be a combination of the assembly burnup and the number of burnable poison or control rods in each location. In this case, $N_p = 2*Z$ (or 52 for the specific example given above). This number is still large, but it is becoming more manageable. This particular choice of variables would also be directly compatible with the optimization scheme developed earlier.

To reduce the number of independent parameters even further, it would be nice if a limit of one variable per assembly could be utilized. For LWR systems, the assembly-wise k_∞ has been used as a key parameter in correlating reactor performance to the individual assembly characteristics. For example, Chao et al.[74] states that "...the power distribution is essentially determined only by the reactivity distribution and vice versa." Thus, it appears that we may be able to reduce N_p such that $N_p = Z$ (or 26 for the above example). With an efficient calculational scheme, this number of computations becomes quite reasonable.

For 2-group theory, k_∞ is given by

$$k_\infty = \frac{\nu\Sigma_{f1}\Sigma_2 + \nu\Sigma_{f2}\Sigma_r}{\Sigma_1\Sigma_2} \tag{5.20}$$

where $\Sigma_r = \Sigma_{1\Rightarrow 2}$ and Σ_g is the total removal cross section in group g. The assembly-wise infinite multiplication factor is given by eqn. (5.20) with the cross sections averaged for the assembly of interest. A perturbation in the assembly characteristics (or cross sections) gives a corresponding change in $k_{\infty z}$. Likewise, assuming a one-to-one correspondence between performance

and reactivity, a delta $k_{\infty z}$ can also define a specific cross section perturbation. Note that some assumption about the variation in the data needs to be made. For example, one might fix the ratios $\nu\Sigma_{f1}/\Sigma_1$ and Σ_r/Σ_1, and only allow $\nu\Sigma_{f2}/\Sigma_2$ to vary with k_∞. This should be a good representation if the correspondence between power and reactivity is nearly exact.[74]

It should also be kept in mind that the goal of the present study is to find a simple higher-order correction to first-order GPT. As such, we are at liberty to make minor approximations as necessary, if the cost versus benefit is in our favor. One such approximation that is consistent with the above discussion may be the use of 1-group or modified 1-group theory as a tool for computing the desired flux derivatives. Equivalent 1-group constants can be obtained quite easily from the reference 2-group calculation. In addition, through analysis of many of the computations performed in this overall study, it has been noted that the fast-to-thermal flux ratio, ψ_1/ψ_2, is not changed significantly even when relatively large perturbations are made. Thus, a one-group representation for estimating the perturbed flux distribution may be in order. In this case, $k_\infty = \nu\Sigma_f/\Sigma_a$ and the correspondence between Δk_∞ and $\Delta\Sigma$ is straightforward.

V.4.B Solution Schemes: After choosing the independent variables to minimize N_p, consideration needs to be given to the solution technique for the flux derivatives. As given in eqn. (A.5), the form of the equation to be solved is

$$(L - \lambda F)\frac{\partial\psi(\eta)}{\partial\Sigma_i(\rho)} = -\left(\frac{\partial L(\eta)}{\partial\Sigma_i(\rho)} - \lambda\frac{\partial F(\eta)}{\partial\Sigma_i(\rho)} - \frac{\partial\lambda}{\partial\Sigma_i(\rho)}F(\eta)\right)\psi(\eta) \qquad (5.21)$$

where $\Sigma_i(\rho)$ represents a particular perturbation in the independent parameters in some phase space ρ. If a full 2-group formulation is used, then the L and F operators would be 2x2 matrix operators and the ψ and $\partial\psi/\partial\Sigma_i$

distributions would be 2-element vectors. If a 1-group scheme is used, then eqn. (5.21) would represent a single inhomogeneous differential equation.

The task at hand is the solution of eqn. (5.21) (or its equivalent). Three potential schemes have been identified in this work:

1. Direct Perturbation Method
2. Explicit Perturbation Method
3. Green's Function Perturbation Method

Each method represents a technique for computing the exact flux derivatives. However, as used in this work, the last two approaches will be presented as approximate solution methods. The approximations to be proposed are justified based on the premise that we are looking for a simple (in terms of cost and ease-of-use) second-order correction to first-order GPT.

In the Direct Perturbation Method one simply perturbs the system, solves the perturbed diffusion equation, and computes the desired flux derivatives via an approximate finite-difference scheme,

$$\frac{\partial\psi(\eta)}{\partial\Sigma_i} = \frac{\psi'(\eta) - \psi(\eta)}{\Delta\Sigma_i} \tag{5.22}$$

If the number of the independent variables N_p can be kept small, then the cost of such a scheme is manageable. The advantages of the direct approach are:

A. The method is conceptually straightforward and should be easy to automate,

B. The exact delta fluxes are obtained (for the given perturbation),

C. No new methods development is required, and

D. The method automatically treats thermal hydraulic and poison feedbacks since these effects are usually an integral part of the direct calculation scheme. However, treatment of these effects in a second-order theory should not be critical.

The only disadvantage of the technique is the cost of N_p direct flux computations. However, with efficient acceleration schemes and the use of high speed computers, the cost per flux calculation has been reduced considerably. Finite difference codes can solve the forward flux-eigenvalue problem in 2-D quarter-core geometry in a few minutes (or less) and a nodal solution scheme for the same system only takes on the order of several seconds (on most computer systems). Thus, it is not unreasonable to consider performing fifty or more computations to generate a second-order sensitivity library. The ease-of-use of the response derivatives should more than offset the cost of generating the initial library.

The Explicit Perturbation Method involves the direct solution of eqn. (5.21) for the desired flux derivatives. This expression represents a generalized fixed source problem similar to the generalized adjoint flux equation that results from first-order GPT. Thus, there is considerable experience in the solution of these types of problems.

One particular advantage of this solution method is the fact that the operator on the left hand side of eqn. (5.21) remains unchanged for each independent perturbation. Thus, only the source changes for each case and this behavior can be exploited to minimize the cost of performing N_p calculations. Huang et al.[61] have taken advantage of this result in their computation of the generalized importance function of first-order GPT. The procedure can be utilized here for the solution of eqn. (5.21) and also in the solution scheme for N_R adjoint importance functions (recall that N_R = the number of integral responses of interest).

Another potential cost saving feature of the Explicit Perturbation Method is a reduction in the convergence level of the flux derivatives that

result from the typical iteration procedure used to solve these types of problems. Since we only require an estimate of the flux derivatives, less accuracy during the numerical calculation should be sufficient. In contrast, the Direct Perturbation Method requires full accuracy for each perturbed flux calculation since the useful result may be the difference of two similar numbers. Thus, the number of iterations to converge the numerical solution of eqn. (5.21) may be significantly less than a typical flux calculation, which may result in additional cost savings relative to the direct approach.

The only disadvantage of the explicit perturbation approach is that new methods would have to be implemented into existing design codes. A routine for the calculation of the source terms and some modification of the iterative routines for the flux calculation would be required. In addition, some study and optimization of the scheme suggested in Ref. 61 would be necessary to obtain the full benefit of varying only the source for each of the flux derivative computations. Thus, the overall method appears to have potential and it should be investigated further in future studies.

The third method for solution of eqn. (5.21) is the Green's Function Perturbation Method. To illustrate the method, we first make the following definitions

$$\phi_\rho(\eta) = \frac{\partial\psi(\eta)}{\partial\Sigma(\rho)} \tag{5.23}$$

and

$$L = L^\circ + \Delta L \tag{5.24}$$

where L is the reference heterogeneous loss operator which is composed of a homogeneous (space-independent) component L° and a heterogeneous contribution ΔL. Substituting these expressions into eqn. (5.21) gives

$$L^\circ\phi_\rho^{m+1}(\eta) = S_\rho^m(\eta) \tag{5.25}$$

where

$$S_\rho^m(\eta) = -(\Delta L - \lambda F)\phi_\rho^m(\eta) - \frac{\partial}{\partial\Sigma(\rho)}(L - \lambda F)\psi(\eta) \tag{5.26}$$

The m superscript represents an iteration index. This notation indicates that eqn. (5.25) will be solved using an iterative scheme, since the desired flux derivative $\phi_\rho(\eta)$ appears on both sides of the equation.

The specific form of eqn. (5.25) was chosen because it represents a convenient format for solution via the Green's function approach.[127] In particular, the Green's function associated with a differential equation with space independent coefficients is easily determined. Using eqns. (5.25) and (5.26), the basic solution scheme for the present problem can be developed as follows.* The Green's function of the operator adjoint to L° is given as the solution to

$$L^{\circ *}(\eta)G^*(\eta,\eta') = \delta(\eta,\eta') \tag{5.27}$$

Multiplying eqn. (5.25) by the Green's function and integrating over η' one has

$$\int_{\eta'} G^*(\eta,\eta')L^\circ(\eta')\phi_\rho^{m+1}(\eta')d\eta' = \int_{\eta'} G^*(\eta,\eta')S_\rho^m(\eta')d\eta' \tag{5.28}$$

Using the definition of an adjoint operator, the left hand side (LHS) of this equation reduces to

$$\text{LHS} = \int_{\eta'} \left[L^{\circ *}(\eta')G^*(\eta,\eta')\right]\phi_\rho^{m+1}(\eta')d\eta' = \int_{\eta'} \phi_\rho^{m+1}(\eta')\delta(\eta,\eta')d\eta' = \phi_\rho^{m+1}(\eta) \tag{5.29}$$

---

*It should be noted that the use of Green's functions in multigroup computations is complicated by the fact that the Green's function assumes a matrix form. The details of the multigroup case have not been worked out as yet, so the formulation developed here will assume 1-group theory.

Therefore

$$\phi_\rho^{m+1}(\eta) = \frac{\partial\psi(\eta)}{\partial\Sigma(\eta)}\Bigg|^{m+1} = \int_{\eta'} G^*(\eta,\eta')S_\rho^m(\eta')d\eta' \tag{5.30}$$

After some algebraic manipulation, the iterative scheme defined in eqn. (5.30) can be shown to be equivalent to the following series solution,

$$\phi_\rho(\eta) = \sum_{j=0}^{\infty} \xi_j(\eta) \tag{5.31}$$

where

$$\xi_0(\eta) = \int_{\eta'} G^*(\eta,\eta')Q_\rho(\eta')d\eta' \tag{5.32}$$

$$\xi_j(\eta) = \int_{\eta'} G^*(\eta,\eta')B(\eta')\xi_{j-1}(\eta')d\eta' \tag{5.33}$$

with

$$Q_\rho(\eta') = -\frac{\partial}{\partial\Sigma(\rho)}(L - \lambda F)\psi(\eta') \tag{5.34}$$

$$B(\eta') = -\Big[\Delta L(\eta') - \lambda F(\eta')\Big] \tag{5.35}$$

In addition, the requirement that the reference and perturbed flux distributions have the same normalization indicates that the integral of the $\partial\psi(\eta)/\partial\Sigma(\rho)$ distribution be zero, or

$$\int_\eta \phi_\rho(\eta)d\eta = 0 \tag{5.36}$$

This orthogonality constraint gives a sweeping procedure similar to that required in the Γ^* solution discussed in Section IV. The expression that must be evaluated here is

$$\phi_{\rho N}(\eta) = \phi_\rho(\eta) - \frac{\langle\phi_\rho(\eta)\rangle}{\langle\psi(\eta)\rangle}\psi(\eta) \tag{5.37}$$

where $\phi_\rho(\eta)$ is the solution to eqn. (5.31), $\psi(\eta)$ is the reference unperturbed flux, and $\phi_{\rho N}$ is the desired $\partial\psi(\eta)/\partial\Sigma(\rho)$ distribution after decontamination.

Expressions (5.31)-(5.37) define the formal approach to the third technique for calculating the flux derivatives; namely, the Green's Function Perturbation Method. The zeroth source function $Q_\rho(\eta)$, which is used to calculate $\xi_o(\eta)$, is the first-order estimate of the change in the neutron source strength due to a perturbation in $\Sigma(\rho)$. $\xi_o(\eta)$ is the first-order $\partial\psi(\eta)/\partial\Sigma(\rho)$ distribution assuming that the reactor is a homogeneous non-multiplying medium. The higher-order terms $\xi_1(\eta)$, $\xi_2(\eta)$, . . . account for the fact that the system is really a multiplying heterogeneous configuration.

A small computer code was written to test the above procedure. The details of a simple, but illustrative, numerical benchmark are given in Appendix C. This benchmark verifies the overall solution methodology. In addition, it shows that using an approximate Green's function does not introduce significant error and that the series solution technique converges to an acceptable level quite rapidly. This is important since in practice the intent is to use the infinite homogeneous Green's function as an approximate solution to eqn. (5.27) and only a few terms will be used in the series expansion in eqn. (5.31). Also, for each position in η space, the integration over η' in eqns. (5.32) and (5.33) will be limited to 3-4 mean free paths (since the additional contribution to the integral should be small but expensive to compute).

Although some further study is required, this third solution scheme for obtaining the desired flux derivatives appears to have considerable potential. With suitable approximations, it could become a very cost effective procedure for estimating the desired flux derivatives. Thus, as in the second solution method, the only major problem with the current Green's function technique

is that it is new and it needs some methods development and further analysis before it can be put into a production design code.

V.5 Summary

In summarizing this section, it should be noted again that the development of a higher-order correction technique was not the primary goal of this overall research effort. On the other hand, the availability of the second-order response derivatives would enhance the usefulness of the sensitivity library and the complete GPT-based design concept. Thus, as a complement to the first part of this study, an effort was made to identify some of the problems associated with higher-order GPT, with the goal of suggesting possible approaches to overcome these difficulties.

A formal second-order GPT methodology was chosen as the only reasonable approach to computing perturbed responses with increased accuracy (relative to first-order GPT). A second-order formulation for the response derivatives was developed that combined the importance functions of first-order GPT with the $\partial\psi(\eta)/\partial\Sigma(\rho)$ distribution function, which represents how the flux profile changes with a given perturbation. Thus, the problem of calculating second-order response derivatives reduces to finding an efficient scheme for generating the desired flux derivatives.

The importance of reducing the number and cost of each flux derivative computation was emphasized. Three techniques for actually computing these functions were described. All three methods appear promising, but only the direct perturbation approach requires little or no new methods development. In contrast, the other two techniques have the potential of increased efficiency after some initial development. Thus, there appears to be a tradeoff in the ease of implementation and the long term cost reductions in the use of the final

product. In either case, the higher-order methodology presented here appears to be feasible in realistic applications. The eventual implementation of these methods in a production environment will probably depend on the industry's acceptance of the overall GPT-based design concept.

VI. CONCLUSIONS AND FUTURE WORK

VI.1 Conclusions

In summarizing this work, it is appropriate to outline the basic goals, accomplishments, and remaining concerns associated with this overall research effort. Section II of this report describes in some detail an idealized design system that is based on generalized perturbation methods. The package would contain individual modules to generate the required first-order and higher-order sensitivity data. It would also contain at least two major application codes; one for core design optimization and the other for evaluation of several safety parameters. This ideal system would be fully automated, user-friendly, and quite flexible in its ability to provide a variety of design and analysis capabilities.

The development, implementation, and application of this proposed design system are the ultimate goals of this work. In all honesty, however, the completion of such an enormous undertaking is several years in the future. Nevertheless, the work documented herein lays a concrete foundation for the future development of such a system. It has brought the overall GPT-based design concept much closer to reality.

In particular, the current work has attacked several major areas of concern relative to the practicality of the GPT-based design concept. The first question that needed to be answered concerned the ability of first-order GPT to accurately predict the important performance parameters (primarily relative power peaking) during normal full power operation. A relatively large database of arbitrary perturbations/response pairs was developed and

analyzed. This investigation indicated that the zone-average relative power profiles could be calculated quite accurately using first-order GPT.

With this initial encouragement, the emphasis of this project then shifted toward demonstrating the applications potential of the basic GPT design concept. The topic of fuel shuffling and BP loading optimization, for example, was addressed as a key area for application of the sensitivity library. As part of this demonstration a general GPT-based optimization algorithm was developed, implemented, and tested in several realistic design situations. This study utilized the GPT/DPT capability of the VENTURE/DEPTH-CHARGE system and an available branch and bound integer programming algorithm from the MPOS package.

The results of the optimization applications are quite impressive. Extremely good results were obtained when the GPT-predicted responses (mainly assembly relative powers) were compared to direct computations. This fact, coupled with the ease-of-use and flexibility of the system, clearly illustrates the potential of the overall methodology. The core reload designer can simply indicate the specifications (objective function and constraints) that are most appropriate for his particular problem, and the optimization algorithm will give the fuel shuffling and BP loading pattern that best satisfies the given criteria. And all of this is done in a single computer calculation at a relatively small cost!

The potential benefits of a production design system based on this design concept are enormous. The manpower costs and calendar time needed to determine feasible reload configurations could easily be reduced by a factor of two (or more). In addition, the potential benefits to be gained from improved designs also need to be considered. The ability to evaluate a large number of

near-optimal configurations (based on different objective function or constraint tradeoffs) gives the designer increased flexibility in determining the best design for each specific situation. This combination of flexibility and efficiency is the primary advantage of the proposed GPT-based design concept.

With the proof-of-principle of the basic concept clearly established, the next goal was to make the GPT part of the system fully compatible with standard LWR design codes. In particular, most current design codes treat macroscopic depletion, k-reset via soluble boron control (in PWRs), and poison and thermal-hydraulic feedback effects. These characteristics are specific to LWR design and, since much of the previous GPT development has been applied in fast reactor studies, these features are not available in current code packages with GPT capability. Thus, the emphasis of this part of the overall study was to remedy this situation.

Section IV of this document details the development and initial verification of an LWR-specific first-order GPT methodology. The main difference relative to standard GPT comes in the treatment of the feedbacks. The feedback effect in the adjoint computation manifests itself as new components in the adjoint source description. This behavior complicates the solution technique only slightly.

In general, once the theory has been turned into specific coding within a given design package, these additional features will be completely transparent to the user. The basic idea of the GPT approach is to determine a response derivative, $\partial R/\partial \Sigma_i$, that is independent of the specific perturbation Σ_i. The change in the response can then be estimated for any arbitrary (small) variation in Σ_i.

However, in few-group thermal reactor computations, a simple interchange of two assemblies, for example, has a secondary affect on all the other unperturbed locations. The original perturbation changes the local power density everywhere. This, in turn, causes local changes in the water density, xenon density, and neutron spectrum, and these variations are modeled through the various cross section feedback mechanisms. In trying to predict the influence of the single assembly interchange, the user does not know *a priori* all these other perturbations. Thus, the adjoint importance functions must be smart enough to account for the implicit variations as well as the explicit (user controlled) material perturbations. The GPT formulation developed here has this feature integrated within the overall methodology, and this new capability should be fully compatible with most LWR design codes. Thus, this development should open the door for the use of GPT in realistic LWR applications.

The final part of this research has addressed the topic of higher-order GPT. Although the primary emphasis of this study has dealt with the development and application of first-order perturbation methods, there are several practical applications where higher-order accuracy is required. Thus, this last subject was treated mainly for completeness in describing the full potential of the GPT-based design concept.

The study of promising approaches to higher-order GPT has concentrated on a formal second-order GPT formulation that combines the importance functions of first-order GPT with a first-order estimate of the change in the neutron flux distribution. Three techniques for calculating the $\partial\psi(\eta)/\partial\Sigma(\rho)$ distribution function, which quantifies how the flux profile changes with a given material variation, were described. Section V of this

report discusses the various advantages and disadvantages of each approach. Although further study is required before making a final selection, at present it appears that the simplest approach is the straightforward Direct Perturbation Method. The most efficient technique for computing a complete set of flux derivatives may be the Explicit Perturbation Method. If only local derivatives are desired then the Green's Function Perturbation Method appears most promising. These conclusions are rather qualitative at present and further study is needed to fully substantiate these statements.

Most importantly, second-order GPT methods appears to be feasible in a production design environment. No matter what method is chosen for computation of the flux derivatives, the key to this design concept is the automation of the whole process. A relatively large number of computations is required (one for each independent parameter), but if these calculations are completely automated then the full higher-order sensitivity library can be generated in a single (overnight) computer run. The modest cost of this single calculation will be more than offset by the ease-of-use of the GPT-based application packages that use the higher-order sensitivity library.

In summary, a new design philosophy has been introduced and several key ingredients of the method have been developed and demonstrated. The objective of the present study is to address the theoretical aspects and practicality of a GPT-based design system. This goal has been achieved and a clear picture of an idealized GPT-based design package that would significantly enhance current reload design capability has evolved.

The information gained from the three separate but related studies performed here (documented separately in Section III, IV, and V) has laid the foundation for the development of a complete integrated package. The initial

testing and applications documented herein have verified the feasibility of the method and they have clearly illustrated the unique capabilities and overall potential of the GPT-based design concept. The actual implementation of a production-oriented design system is the next step.

VI.2 Future Work

On the subject of future work, it should be emphasized that there is still much work to be done towards developing a practical user-friendly GPT-based design tool. However, much of this additional effort will be in the coding of a production-oriented system, since the research presented here provides a good theoretical foundation and verification of the basic concept.

In putting together a final design tool some care will be required to identify/develop a robust integer programming package that can handle a large number of independent variables and constraints. The BBMIP algorithm used in the optimization demonstrations in this work is not suitable for large-scale production applications. Problems with only 80-100 variables can be treated efficiently with BBMIP.

One technique that appears promising is the Monte Carlo integer programming method.[128] Hobson and Turinsky[66,72] have had some success with this method. To gain some first hand experience with this scheme, a small Monte Carlo optimization program was written. The BP optimization case described in Section III.3 was run and, after 100000 random choices for the BP loading, no feasible solutions were obtained. After several attempts, an iterative scheme (where the BP change per iteration is restricted) was finally chosen. This procedure was similar to that used in Ref. 72. Thus, it appears that a specially designed scheme for each class of problems can be worked out

that will converge to a near-optimal solution. Clearly further work is required, but the method does hold some promise.

In contrast to developing a special purpose algorithm (like the Monte Carlo scheme), another route to explore is to evaluate some of the commercially available optimization software. Several vendors support a large number of state-of-the-art algorithms that may be suitable for the fuel loading problem. Both options (specially designed versus canned optimization algorithms) should be explored in more detail.

Another area requiring further effort is the implementation and application of first-order GPT within existing LWR design codes. As indicated earlier, an effort is currently underway to implement the methods developed in Section IV into a proprietary finite-difference neutronics tool at Westinghouse Electric Corporation. This work is only in its early stages and much will be learned from this development work.

In addition, an effort should be made to develop and implement similar capability into non-proprietary code systems using both finite difference and various nodal schemes. Such an effort would be quite large, but it would allow maximum availability of the GPT capability. Implementation of the GPT formulation within a nodal simulator with thermal-hydraulic and poison feedbacks would be an interesting and challenging experience.

In the area of higher-order methods, there are significant challenges that still remain. Individual efforts in developing and fine-tuning the Explicit and Green's Function Perturbation Methods are needed. Once these have been performed, a systematic comparison of these methods with the Direct Perturbation Method would be appropriate. This evaluation could identify

quantitatively the best method for determining the flux derivatives that are required as part of the second-order GPT methodology.

Finally, the last major undertaking should be the integration of the various components into a user-friendly design package. This involves the implementation of automated sequences for the computation of the first- and second-order response derivatives and the coupling of the sensitivity library to the various application packages. The applications of primary interest are an automated optimization algorithm for fuel and BP loading, an interactive design tool for manual fuel reload analyses, and an automatic sequence of computations (using first- and second-order derivatives) for the evaluation of many of the safety parameters of interest in off-normal situations. The development of such a comprehensive system is a major undertaking, but the potential benefits of the GPT-based approach clearly warrant that this effort be made.

LIST OF REFERENCES

LIST OF REFERENCES

1. C. R. Weisbin, et al., "Application of FORSS Sensitivity and Uncertainty Methodology to Fast Reactor Benchmark Analysis," ORNL/TM-5563, Oak Ridge National Laboratory (1976).
2. J. H. Marable and C. R. Weisbin, "Performance Parameter Uncertainties for a Large LMFBR," *Trans. Am. Nucl. Soc.*, **26**, 542 (1977).
3. M. Salvatores, "Recent Developments in Cross Section Adjustment Procedures," *Proc. of Am. Nucl. Soc. Topical Mtg. on Adv. in Reactor Physics*, Gatlinburg, Tennessee (1977).
4. C. R. Weisbin, et al., Eds., *Proc. of Sem.-Workshop on the Theory and Application of Sensitivity and Uncertainty Analysis*, ORNL/RSIC-42, Oak Ridge National Laboratory (1979).
5. J. M. Kallfelz, et al., "Design and Sensitivity Analysis of a CDS-Type Heterogeneous Core," *ANS Topical Meeting 1980 Advances in Reactor Physics and Shielding*, Sun Valley, Idaho (1980).
6. J. H. Marable, C. R. Weisbin, and G. de Saussure, "Uncertainty in the Breeding Ratio of a Large LMFBR; Theory and Results," *Nucl. Sci. Eng.*, **75**, 30 (1980).
7. J. M. Kallfelz, et al., "Preliminary Analysis and Sensitivity Study of PHENIX Fuel Irradiation Experiments," ORNL/TM-7505, Oak Ridge National Laboratory (1981).
8. D. Biswas, J. M. Kallfelz, and J. R. White, "Depletion Analysis and Sensitivity Study of PHENIX Fuel Irradiation Experiments," *Trans. Am. Nucl. Soc.*, **38**, 673 (1981).
9. J. H. Marable, et al., "Sensitivities and Uncertainties of a Large LMFBR Using Adjusted Cross-Section Library ORACLE-1," *ANS Topical Meeting on Reactor Physics and Core Thermal Hydraulics*, Kiamesha Lake, New York (1982).
10. C. R. Weisbin, et al., "Sensitivity and Uncertainty Analysis of Reactor Performance Parameters," *Advances in Nucl. Sci. and Tech.*, Plenum Press, New York (1982).
11. M. L. Williams and C. R. Weisbin, "Sensitivity and Uncertainty Analysis for Functionals of the Time-Dependent Nuclide Density Field," ORNL-5393, Oak Ridge National Laboratory (1978).
12. M. L. Williams, et al., "Sensitivity Theory for Depletion Analysis," *Proc. of Sem.-Workshop on the Theory and Application of Sensitivity and Uncertainty Analysis*, Oak Ridge, Tennessee, ORNL/RSIC-42 (1978).
13. M. L. Williams, "Development of Depletion Perturbation Theory for Coupled Neutron/Nuclide Fields," *Nucl. Sci. Eng.*, **70**, 20, (1979).
14. M. L. Williams, "Perturbation and Sensitivity Theory for Reactor Burnup Analysis," Doctoral Dissertation, Nuclear Eng. Dept., Univ. of Tennessee (1979) also ORNL/TM-7096.

15. M. L. Williams, J. R. White, and T. J. Burns, "A Technique for Sensitivity Analysis of Space- and Energy-Dependent Burnup Calculations," *Trans. Am. Nucl. Soc.*, **32**,766 (1979).

16. J. R. White and T. J. Burns, "Development and Verification of Multicycle Depletion Perturbation Theory," *Trans. Am. Nucl. Soc.*, **34**, 824 (1980).

17. J. R. White, T. J. Burns, and M. L. Williams, "On the Implementation, Verification, and Application of Multicycle Depletion Perturbation Theory," *ANS Topical Meeting 1980 Advances in Reactor Physics and Shielding*, Sun Valley, Idaho (1980).

18. J. R. White, "The Development, Implementation, and Verification of Multicycle Depletion Perturbation Theory for Reactor Burnup Analysis," Master's Thesis, Nuclear Eng. Dept., Univ. of Tennessee (1980) also ORNL/TM-7305.

19. J. R. White, "Burnup Effects in Data Sensitivity Studies," *Trans. Am. Nucl. Soc.*, **35**, 587 (1980).

20. J. R. White, "The DEPTH-CHARGE Static and Time-Dependent Perturbation/Sensitivity System for Nuclear Reactor Core Analysis," ORNL/CSD-78, Oak Ridge National Laboratory (1981).

21. J. R. White and R. E. Schenter, "Analysis of Lumped Fission Product Uncertainty in CRBR," *Trans. Am. Nucl. Soc.*, **39**, 931 (1981).

22. J. R. White and M. L. Williams, "Application of Time-Dependent Generalized Perurbation Theory Methods in LWR Physics Analyses," *ANS Topical Meeting on Reactor Physics and Core Thermal Hydraulics*, Kiamesha Lake, New York (1982).

23. J. R. White, J. H. Marable, and R. E. Schenter, "Sensitivity Analysis of the Inherent Neutron Source Strength," *Trans. Am. Nucl. Soc.*, **43**, 723 (1982).

24. J. R. White, et al., "Sensitivity Analysis of the Doppler Coefficient in Heterogeneous LMFBRs," *Trans. Am. Nucl. Soc.*, **45**, 769 (1983).

25. J. R. White, "The DEPTH-CHARGE Static and Time-Dependent Peturbation/Sensitivity System for Nuclear Reactor Core Analysis, Revision I," ORNL/CSD-78R, Oak Ridge National Laboratory (1985).

26. J. R. White, D. M. Chapman, and D. Biswas, "Development of a GPT-Based Optimization Algorithm," *Trans. Am. Nucl. Soc.*, **50**, 83 (1985).

27. J. R. White, D. M. Chapman, and D. Biswas, "Fuel Management Optimization Based on Generalized Perturbation Theory," *Proc. of ANS Topical Meeting on Advances in Fuel Management*, Pinehurst, North Carolina (1986).

28. J. R. White and B. R. Frank, "Static Generalized Perturbation Theory with Feedback Effects and Criticality Reset," *Trans. Am. Nucl. Soc.*, **52**, 433 (1986).

29. J. R. White and B. R. Frank, "Generalized Perturbation Theory for LWR Depletion Analysis and Core Design Applications," *ANS Topical*

Meeting on Advances in Reactor Physics and Safety, Saratoga Springs, New York (Sept. 1986).

30. See *Proceedings of the ANS Topical Meeting on Advances in Fuel Management*, Pinehurst, North Carolina (1986).
31. I. Wall and H. Fenech, "The Application of Dynamic Programming to Fuel Management Optimization," *Nucl. Sci. Eng.*, **22**, 285 (1965).
32. A. Gandini, "Use of Generalized Perturbation Methods for Optimization of Reactor Design," *J. of Nucl. Energy*, **23**, 469 (1969).
33. M. Melice, "Pressurized Water Reactor Optimal Core Management and Reactivity Profiles," *Nucl. Sci. Eng.*, **37**, 451 (1969).
34. B. N. Naft and A. Sesonske, "A Direct Search Algorithm for Optimizing Fuel Loading Patterns," *Trans. Am. Nucl. Soc.*, **13**, 40 (1970).
35. P. Goldschmidt and J. Quenon, "Minimum Critical Mass in Fast Reactors with Bounded Power Density," *Nucl. Sci. Eng.*, **39**, 311 (1970).
36. A. Suzuki and R. Kiyose, "Application of Linear Programming to Refueling Optimization for Light Water Moderated Power Reactors," *Nucl. Sci. Eng.*, **46**, 112 (1971).
37. T. O. Sauar, "Application of Linear Programming to In-Core Fuel Management Optimization in Light Water Reactors," *Nucl. Sci. Eng.*, **46**, 274 (1971).
38. D. C. Wade and W. B. Terney, "Optimal Control of Nuclear Reactor Depletion," *Nucl. Sci. Eng.*, **45**, 199 (1971).
39. B. N. Naft and A. Sesonske, "Pressurized Water Reactor Optimal Fuel Management," *Nucl. Technol.*, **14**, 123 (1972).
40. R. B. Stout and A. H. Robinson, "Determination of Optimum Fuel Loadings in Pressurized Water Reactors Using Dynamic Programming," *Nucl. Technol.*, **20**, 86 (1973).
41. J. O. Mingle, "In-Core Fuel Management Using Perturbation Theory and Linear Programming," *Trans. Am. Nucl. Soc.*, **17**, 306 (1973).
42. H. Motoda, J. Herczeg, and A. Sesonske, "Optimization of Refueling Schedule for Light Water Reactors," *Trans. Am. Nucl. Soc.*, **17**, 307 (1973).
43. A. J. Federowicz and R. L. Stover, "Optimization of PWR Loading Patterns by Reference Design Perturbations," *Trans. Am. Nucl. Soc.*, **17**, 308 (1973).
44. W. P. Barthold, "Constrained Nuclear Design," *ANS Topical Meeting on Advanced Reactors; Physics, Design, and Economics*, Atlanta, Georgia (1974).
45. K. Chitkara and J. Weisman, "An Equilibrium Approach to Optimal In-Core Fuel Management for Pressurized Water Reactors," *Nucl. Technol.*, **24**, 33 (1974).
46. J. O. Mingle, "In-Core Fuel Management Via Perturbation Theory," *Nucl. Technol.*, **27**, 248 (1975).

47. H. Motoda, J. Herczeg, and A. Sesonske, "Optimization of Refueling Schedule for Light-Water Reactors," *Nucl. Technol.*, **25**, 477 (1975).

48. C. P. Tzanos, "Minimization of the Power Peak-to-Average Ratio," *Trans. Am. Nucl. Soc.*, **24**, 195 (1976).

49. S. R. Specker, et. al., "The BWR Control Cell Core Improved Design," *Trans. Am. Nucl. Soc.*, **30**, 336 (1978).

50. H. Y. Huang and S. H. Levine, "An Automated Optimal Multiple-Cycle PWR Fuel Management Code," *Trans. Am. Nucl. Soc.*, **30**, 338 (1978).

51. H. Y. Huang and S. H. Levine, "A New Method for Optimizing Core Reloads," *Trans. Am. Nucl. Soc.*, **30**, 339 (1978).

52. E. A. Williamson, et. al., "Interactive Fuel Management Using a CRT," *Trans. Am. Nucl. Soc.*, **30**, 341 (1978).

53. K. Sekimizu, "A Hierarchy Level Scheme for Quasi-Optimum Fuel Assembly Loading in Boiling Water Reactors," *Nucl. Technol.*, **37**, 296 (1978).

54. B. I. Lin, B. Zolotar, and J. Weisman, "An Automated Procedure for Selection of Optimal Refueling Policies for Light Water Reactors," *Nucl. Technol.*, **44**, 258 (1979).

55. D. Rozon, A. Hebert, and D. McNabb, "The Application of Generalized Perturbation Theory and Mathematical Programminmg to Equilibrium Refueling Studies of a CANDU Reactor," *Nucl. Sci. Eng.*, **78**, 211 (1981).

56. W. B. Terney and E. A. Williamson, Jr., "The Design of Reload Cores Using Optimal Control Theory," *Nucl. Sci. Eng.*, **82**, 260 (1982).

57. E. E. Pilat and R. J. Cacciapouti, "The Scope of Fuel Management Physics Calculations - Utility Needs Versus Present Realities," *Trans. Am. Nucl. Soc.*, **43**, 690 (1982).

58. L. Ho and A. F. Rohach, "Perturbation Theory in Nuclear Fuel Management Optimization," *Nucl. Sci. Eng.*, **82**, 151 (1982).

59. D. Chang and S. H. Levine, "Optimal Placement and Poison Control Depletion of Individual Fuel Assemblies Using the Gradient Projection Method," *Trans. Am. Nucl. Soc.*, **43**, 164 (1982).

60. A. L. B. Ho and A. Sesonske, "Extended Burnup Fuel Cycle Optimization for Pressurized Water Reactors," *Nucl. Technol.*, *58*, 422 (1982).

61. S. F. Huang, S. D. Suk, and M. Becker, "A Perturbation Theory Procedure for PWR Fuel Management," *Trans. Am. Nucl. Soc.*, **45**, 726 (1983).

62. J. P. Colletti, S. H. Levine, and J. B. Lewis, "Iterative Solution to the Optimal Poison Management Problem in Pressurized Water Reactors," *Nucl. Technol.*, **63**, 415 (1983).

63. C. R. Drumm and J. C. Lee, "Axial Gadolinium Burnable Absorber Optimization by the Method of Conjugate Gradients," *Trans. Am. Nucl. Soc.*, **46**, 83 (1984).

64. D. H. Ahn and S. H. Levine, "Direct Placement of Fuel Assemblies Using the Gradient Projection Method," *Trans. Am. Nucl. Soc.*, **46**, 123 (1984).

65. D. H. Ahn and S. H. Levine, "Automatic Optimized Reload and Depletion Method for a PWR," *Trans. Am. Nucl. Soc.*, **47**, 120 (1984).

66. G. H. Hobson and P. J. Turinsky, "Maximization of Core Reactivity Within Power and Burnup Constraints," *Trans. Am. Nucl. Soc.*, **47**, 117 (1984).

67. Y. C. Chang and A. Sesonske, "Optimization and Analysis of Low-Leakage Core Management for Pressurized Water Reactors," *Nucl. Technol.*, **65**, 292, (1984).

68. H. W. Bonin and A. Sesonske, "Optimal Thorium-Fueled CANDU Nuclear Reactor Fuel Management," *Nucl. Technol.*, **68**, 319 (1985).

69. D. H. Ahn and S. H. Levine, "Automatic Optimized Reload and Depletion Method for a Pressurized Water Reactor," *Nucl. Technol.*, **71**, 535, (1985).

70. G. H. Hobson, "Automatic Determination of Pressurized Water Reactor Core Loading Patterns Which Maximize End-of-Cycle Reactivity Within Peaking and Burnup Constraints," Ph.D. Thesis, Dept. of Nucl. Eng., North Carolina State University (1985).

71. T. J. Downar and Y. J. Kim, "A Reverse Depletion Method for PWR Core Reload Design," *Trans. Am. Nucl. Soc.*, **50**, 82 (1985).

72. G. H. Hobson and P. J. Turinsky, "Automatic Optimization of Core Loading Patterns to Maximize Cycle Energy Production within Operational Constraints," *Proc. Topical Meeting on Advances in Fuel Management*, Pinehurst, North Carolina, (1986).

73. T. Morita et al., "LPOP: Loading Pattern Optimization Program," *Trans. Am. Nucl. Soc.*, **52**, 41 (1986).

74. Y. A. Chao, C. W. Hu, and C. A. Suo, "A Theory of Fuel Management via Backward Diffusion Calculation," *Nucl. Sci. Eng.*, **93**, 78 (1986).

75. T. J. Downar and Y. J. Kim, "A Reverse Depletion Method for Pressurized Water Reactor Core Reload Design," *Nucl. Technol.*, **73**, 42 (1986).

76. R. Courant, *Calculus of Variations and Supplementary Exercises*, New York University, Institute of Mathematical Sciences (1961).

77. H. Taha, *Integer Programming - Theory, Applications, and Computations*, Academic Press Inc., New York (1975).

78. L. R. Foulds, *Optimization Techniques, An Introduction*, Springer-Verlag, New York (1981).

79. C. Cohen and J. Stein, "Multi-Purpose Optimization System User's Guide, Version 4," Volgelback Computing Center, Northwestern University (1978).

80. D. R. Vondy et al., "The BOLD VENTURE Computation System for Nuclear Reactor Core Analysis, Version III," ORNL-5711, Oak Ridge National Laboratory (1981).

81. D. M. Chapman, "GPT-Based Fuel Management Optimization," Master's Thesis, Nuclear Engineering Dept., University of Lowell (1985).

82. J. Lewins, "The Time-Dependent Importance of Neutrons and Precursors," *Nucl. Sci. Eng.*, **7**, 268 (1960).

83. J. Lewins, "Variational Representations in Reactor Physics Derived from a Physical Principle," *Nucl. Sci. Eng.*, **8**, 95 (1960).

84. J. Lewins, *Importance: The Adjoint Function*, Pergamon Press, Oxford (1965).

85. J. Lewins, "Developments in Perturbation Theory," *Adv. in Nucl. Sci. Technol.*, **4**, 309 (1968).

86. N. Usachev, *J. Nucl. Energy, Part A/B*, **18**, 571 (1963).

87. A. Gandini, "A Perturbation Method for Analysis of Neutron Source Worth Experiments in Nuclear Reactors," *Nucl. Sci. Eng.*, **30**, 451 (1967).

88. A. Gandini, "A Generalized Perturbation Method for Bilinear Functionals of the Real and Adjoint Neutron Fluxes," *J. Nucl. Energy, Part A/B*, **21**, 755 (1967).

89. A. Gandini, *Nucl. Sci. Eng.*, **57**, 248 (1975).

90. G. Pomraning, "Variational Principle for Eigenvalue Equations," *J. Math Phys.*, **8**, 149 (1967).

91. G. Pomraning, "A Derivation of Variational Principles for Inhomogeneous Equations," *Nucl. Sci. Eng.*, **29**, 220 (1967).

92. R. Saito and S. Katsuraghi, "Higher Order Perturbation Method in Reactor Calculation," *J. Nucl. Sci. Technol.*, **6**, 303 (1969).

93. R. Saito, "Numerical Study of Higher Order Perturbation Theory," *J. Nucl. Sci. Technol.*, **6**, 359 (1969).

94. R. Saito, "Modal Peturbation Method Applied to Diffusion Equation," *J. Nucl. Sci. Technol.*, **7**, 371 (1970).

95. W. M. Stacey, Jr., "Variational Estimates and Generalized Peturbation Theory for the Ratio of Linear and Bilinear Functionals," *J. Math. Phys.*, **13**, 1118 (1972).

96. W. M. Stacey, Jr., *Variational Methods in Nuclear Reactor Physics*, Academic Press, New York (1974).

97. A. Gandini, "Perturbation Methods in Nuclear Reactors from the Importance Conservation Principle," *Nucl. Sci. Eng.*, **35**, 141 (1969).

98. A. Gandini, "A Method of Correlation of Burnup Measurements for Physics Prediction of Fast Power-Reactor Life," *Nucl. Sci. Eng.*, **38**, 1 (1969).

99. M. Komata, "New Interpertations for the Usachev-Gandini Perturbation Theory," *Nucl. Sci. Eng.*, **47**, 489 (1972).

100. A. Gandini, M. Salvatores, and L. Tondinelli, "New Developments in Generalized Perturbation Methods in the Nuclide Field," *Nucl. Sci. Eng.*, **62**, 339 (1977).

101. L. Tondinelli, "Sensitivity of Actinide Concentration During Burnup with Respect to Nuclear Data," CNEN RT/FI(76)1, CNEN, Rome (1976).

102. M. J. Bell, "ORIGEN - The ORNL Isotope Generation and Depletion Code," Oak Ridge National Laboratory, ORNL-4628 (1973).

103. J. M. Kallfelz, et al., "Burnup Calculations with Time-Dependent Generalized Perturbation Theory," *Nucl. Sci. Eng.*, **62**, 304 (1977).

104. W. B. Terney and E. A. Williamson, "The Design of Reload Cores Using Optimal Control Theory," *Trans. Am. Nucl. Soc.*, **27**, 361 (1977).

105. D. R. Harris and M. Becker, "Nonlinear Perturbation Technique for the Nuclear Fuel Cycle," *Trans. Am. Nucl. Soc.*, **23**, 534 (1976).

106. D. G. Cacuci, et al., "Developments in Sensitivity Theory," *ANS Topical Meeting 1980 Advances in Reactor Physics and Shielding*, Sun Valley, Idaho (1980).

107. D. G. Cacuci, et al., "Sensitivity Theory for General Systems of Nonlinear Equations," *Nucl. Sci. Eng.*, **75**, 88 (1980).

108. E. Greenspan, M. L. Williams, and J. H. Marable, "Time-Dependent Generalized Perturbation Theory for Coupled Neutron-Nuclide Problems," *Nucl. Sci. Eng.*, **73**, 210 (1980).

109. A. Gandini, "Higher Order Time-Dependent Generalized Perturbation Theory," *Nucl. Sci. Eng.*, **67**, 91 (1978).

110. A. Gandini, "On the Standard Perturbation Theory," *Nucl. Sci. Eng.*, **79**, 426 (1981).

111. A. Dubi and D. Dudziak, "Higher-Order Terms in Sensitivity Analysis Through a Differential Approach," LA-8813-MS, Los Alamos Scientific Laboratory (1981).

112. G. Palmiotti, "Use of the Explicit High-Order Perturbation Formulation," *Nucl. Sci. Eng.*, **83**, 281 (1983).

113. T. Takeda and T. Umano, "Burnup Sensitivity Analysis in a Fast Breeder Reactor - Part I: Sensitivity Calculation Method with Generalized Perturbation Theory," *Nucl. Sci. Eng.*, **91**, 1 (1985).

114. T. Kamei, et al., "Burnup Sensitivity Analysis in a Fast Breeder Reactor - Part II: Prediction Accuracy of Burnup Characteristics," *Nucl. Sci. Eng.*, **91**, 10 (1985).

115. S. M. Bowman, et al., "Implementation of Generalized Perturbation Theory into the 3-D Nodal Code SIMULATE," *Trans. Am. Nucl. Soc.*, **34**, 305 (1980).

116. S. M. Bowman, "The Development of Depletion Perturbation Theory for a Reactor Nodal Code," ORNL/TM-7589, Oak Ridge National Laboratory, (1981).

117. D. M. Ver Planck, et al., "SIMULATE-E: A Nodal Core Analysis Program for Light Water Reactors," EPRI NP-2792-CCM, (1983).

118. M. R. Wagner, "Current Trends in Multidimensional Static Reactor Calculations," *ANS Topical Conf. on Comp. Methods in Nuc. Eng.*, CONF-750413 (1975).

119. M. Mitani, "Higher Order Perturbation Method in Reactor Calculations," *Nucl. Sci. Eng.*, **51**, 180 (1973).

120. E. Greenspan, et al., "Second Order Generalized Perturbation Theory for Source-Driven Systems," *Nucl. Sci. Eng.*, **68**, 1 (1978).

121. A. Gandini, "Implicit and Explicit Higher Order Perturbation Methods for Nuclear Reactor Analysis," *Nucl. Sci. Eng.*, **67**, 347 (1978).

122. A. Dubi and D. Dudziak, "Higher-Order Flux Perturbations," *Nucl. Sci. Eng.*, **77**, 153 (1981).

123. J. R. White, B. R. Frank, and J. Pappas, "Analytic Solution for the Fundamental and Higher Harmonics of the 1-D Diffusion Equation," *Trans. Am. Nucl. Soc.*, **46**, 408 (1984).

124. J. R. White, T. J. Cahill, and B. R. Frank, "Exact Analytic Solution for the Generalized Flux in 1-D Cartesian Geometry," *Trans. Am. Nucl. Soc.*, **49**, 220 (1985).

125. R. L. Childs, "Generalized Perturbation Theory Using Two-Dimensional Discrete Ordinates Transport Theory," ORNL/CSD/TM-128, Oak Ridge National Laboratory (1980).

126. E. M. Oblow, "Sensitivity Theory from a Differential Viewpoint," *Nucl. Sci. Eng.*, **59**, 187 (1976).

127. P. Dennery and A. Krzywicki, *Mathematics for Physicists*, Harper & Row, New York, New York (1967).

128. W. Conley, *Computer Optimization Techniques*, Petrocelli Books, Inc., Princeton (1980).

APPENDIXES

APPENDIX A DERIVATION OF SECOND-ORDER GPT USING A DIFFERENTIAL APPROACH

The purpose of this Appendix is to derive a formal second-order GPT formulation for the steady-state critical reactor problem. The development presented here follows Greenspan's derivation[120] of second-order GPT for a subcritical configuration with a fixed source. The functional derivative notation used is consistent with that of Oblow.[126] The matrix notation used in the earlier parts of this report is abandoned here in lieu of a more general operator notation (where the energy dependence is contained as part of the phase space variables).

A.1 The Response

The integral response of interest is first represented as

$$R = \int_{\rho} f[\psi(\rho), \Sigma(\rho)]\, d\rho \tag{A.1}$$

where $\psi(\rho)$ satisfies the forward diffusion equation

$$(L - \lambda F)\psi = 0 \tag{A.2}$$

and $\Sigma(\rho)$ represents the independent variables within the system (macro or micro cross sections, nuclide densities, etc.). If the independent variables are altered, the desired response is perturbed (becomes R') through direct effects and indirect flux effects. The perturbed response can be expanded in a functional Taylor series truncated to second-order, giving

$$R' = R + \sum_i \int_{\rho} \frac{\partial R}{\partial \Sigma_i(\rho)} \delta\Sigma(\rho) d\rho + \frac{1}{2} \sum_{ij} \int_{\rho} \int_{\rho'} \frac{\partial^2 R}{\partial \Sigma_j(\rho') \partial \Sigma_i(\rho)} \delta\Sigma_i(\rho) \delta\Sigma_j(\rho') d\rho d\rho' \tag{A.3}$$

Given eqn. (A.3), the task then becomes one of finding explicit formulations for $\partial R/\partial \Sigma_i$ and for $\partial^2 R/\partial \Sigma_i \partial \Sigma_j$.

A.2 First-Order Derivatives

To obtain the first-order terms, one can simply differentiate R with respect to $\Sigma_i(\rho)$ while noting that R is an explicit functional of $\Sigma_i(\rho)$ and that $\psi(\rho)$ is an implicit function of $\Sigma_i(\rho)$. Performing the indicated operations gives

$$\frac{\partial R}{\partial \Sigma_i(\rho)} = \frac{\partial f[\psi(\rho), \Sigma(\rho)]}{\partial \Sigma_i(\rho)} + \int_\eta \frac{\partial f[\psi(\eta), \Sigma(\eta)]}{\partial \psi(\eta)} \frac{\partial \psi(\eta)}{\partial \Sigma_i(\rho)} d\eta \tag{A.4}$$

where $\partial\psi/\partial\Sigma_i$ is defined by a formal differentiation of eqn. (A.2),

$$(L - \lambda F)\frac{\partial \psi(\eta)}{\partial \Sigma_i(\rho)} = -\frac{\partial}{\partial \Sigma_i(\rho)}(L - \lambda F)\psi(\eta) \tag{A.5}$$

Now, using the expression that defines the standard (no feedbacks) generalized adjoint flux,

$$(L - \lambda F)^* \Gamma^* = \frac{\partial f}{\partial \psi} \tag{A.6}$$

and the mathematical definition of an adjoint operator,[126] one can readily show that eqn. (A.4) is equivalent to

$$\frac{\partial R}{\partial \Sigma_i(\rho)} = \frac{\partial f[\psi(\rho), \Sigma(\rho)]}{\partial \Sigma_i(\rho)} - \int_\eta \Gamma^*(\eta) \frac{\partial}{\partial \Sigma_i(\rho)}(L - \lambda F)\psi(\eta) d\eta \tag{A.7}$$

This latter expression is the normal first-order GPT formulation which is typically written in shorthand form as

$$\frac{\partial R}{\partial \Sigma_i} = \frac{\partial f}{\partial \Sigma_i} - \langle \Gamma^* \frac{\partial}{\partial \Sigma_i}(L - \lambda F)\psi \rangle \tag{A.8}$$

A.3 Second-Order Derivatives

The second-order terms are derived in a similar manner. This time one formally differentiates $\partial R/\partial\Sigma_i(\rho)$ as given in eqn. (A.7) with respect to $\Sigma_j(\rho')$, giving

$$\frac{\partial R}{\partial \Sigma_j(\rho')\partial \Sigma_i(\rho)} = \int_\eta \frac{\partial^2 f(\eta)}{\partial \Sigma_j(\eta)\partial \Sigma_i(\eta)} \frac{\partial \Sigma_i(\eta)}{\partial \Sigma_i(\rho)} \frac{\partial \Sigma_j(\eta)}{\partial \Sigma_j(\rho')} d\eta \tag{A.9}$$

$$+ \int_\eta \frac{\partial^2 f(\eta)}{\partial \psi(\eta)\partial \Sigma_i(\eta)} \frac{\partial \psi(\eta)}{\partial \Sigma_j(\rho')} \frac{\partial \Sigma_i(\eta)}{\partial \Sigma_i(\rho')} d\eta$$

$$- \int_{\eta} \frac{\partial [\Gamma^*(\eta) B(\eta, \rho) \psi(\eta)]}{\partial \Sigma_j(\eta)} \frac{\partial \Sigma_j(\eta)}{\partial \Sigma_j(\rho')} d\eta$$

$$- \int_{\eta} \frac{\partial [\Gamma^*(\eta) B(\eta, \rho) \psi(\eta)]}{\partial \psi(\eta)} \frac{\partial \psi(\eta)}{\partial \Sigma_j(\rho')} d\eta$$

$$- \int_{\eta} \frac{\partial [\Gamma^*(\eta) B(\eta, \rho) \psi(\eta)]}{\partial \Gamma^*(\eta)} \frac{\partial \Gamma^*(\eta)}{\partial \Sigma_j(\rho')} d\eta$$

$$- \int_{\eta} \frac{\partial [\Gamma^*(\eta) B(\eta, \rho) \psi(\eta)]}{\partial \lambda} \frac{\partial \lambda}{\partial \Sigma_j(\rho')} d\eta$$

$$- \int_{\eta} \frac{\partial [\Gamma^*(\eta) B(\eta, \rho) \psi(\eta)]}{\partial (\partial \lambda / \partial \Sigma_i(\rho))} \frac{\partial (\partial \lambda / \partial \Sigma_i(\rho))}{\partial \Sigma_j(\rho')} d\eta$$

where we have let

$$B(\eta, \rho) = \frac{\partial}{\partial \Sigma_i(\rho)} \Big(L(\eta) - \lambda F(\eta) \Big)$$

Performing many of the indicated operations, such as

$$B = \frac{\partial}{\partial \Sigma_i} (L - \lambda F) = \frac{\partial L}{\partial \Sigma_i} - \lambda \frac{\partial F}{\partial \Sigma_i} - \frac{\partial \lambda}{\partial \Sigma_i} F$$

and

$$\frac{\partial B}{\partial \Sigma_j} = \frac{\partial}{\partial \Sigma_j \partial \Sigma_i} (L - \lambda F) = - \frac{\partial \lambda}{\partial \Sigma_i} \frac{\partial F}{\partial \Sigma_j}$$

where in the latter expression, the L and F operators are assumed to be linear with respect to Σ (Σ would represent the diffusion coefficient instead of the transport cross section within the L operator), and

$$\frac{\partial (\partial (L - \lambda F)/\partial \Sigma_i)}{\partial (\partial \lambda / \partial \Sigma_i)} = -F$$

and

$$\int_{\eta} (\Gamma^* F \psi) \frac{\partial^2 \lambda}{\partial \Sigma_j \partial \Sigma_i} d\eta = \frac{\partial^2 \lambda}{\partial \Sigma_j \partial \Sigma_i} \langle \Gamma^* F \psi \rangle = 0$$

one can reduce eqn. (A.9) to

$$\frac{\partial^2 R}{\partial \Sigma_j \partial \Sigma_i} = \frac{\partial^2 f}{\partial \Sigma_j \partial \Sigma_i} + \frac{\partial \lambda}{\partial \Sigma_i} \int_\eta \Gamma^* \frac{\partial F}{\partial \Sigma_j} \psi d\eta + \frac{\partial \lambda}{\partial \Sigma_j} \int_\eta \Gamma^* \frac{\partial F}{\partial \Sigma_i} \psi d\eta \tag{A.10}$$

$$+ \int_\eta \left(\frac{\partial^2 f}{\partial \psi \partial \Sigma_i} - \Gamma^* \frac{\partial}{\partial \Sigma_i} (L - \lambda F) \right) \frac{\partial \psi}{\partial \Sigma_j} d\eta - \int_\eta \frac{\partial \Gamma^*}{\partial \Sigma_j} \left(\frac{\partial}{\partial \Sigma_i} (L - \lambda F) \psi \right) d\eta$$

Finally, for the present work, we will assume that the Γ^* that appears in eqn. (A.7) is a given weight function independent of Σ_j. Thus, eqn. (A.10), with the last term set to zero, becomes the final form of the desired second-order derivatives. These terms, when utilized in eqn. (A.3), will give a second-order estimate of the perturbed response.

APPENDIX B LOCAL VERSUS GLOBAL EFFECTS

In choosing a scheme for computing the flux derivatives $\partial\psi(\eta)/\partial\Sigma(\rho)$, it should be noted that the intended use is to calculate a second-order correction term to first-order GPT. Therefore, the accuracy requirement on the flux derivatives is not severe, since any improvement in the first-order estimate will be helpful. Also, in many cases of interest, the second-order effects are desired where single large localized perturbations are made (as in rod ejection or insertion analysis).

The analysis of the higher-order contribution to the total ΔR_E has identified some characteristics that might be useful in the development of an approximate higher-order correction term. In particular, it is shown in eqn. (5.8) that the higher-order component ΔR_{HO} contains both local and global terms, where the local terms are integrated over only the perturbed region and the global contribution involves integration over the entire reactor.

The importance of the distinction between the local and global effects is that knowledge of the flux derivatives is required only over the range of integration. If the local terms (with no cross derivatives) are used, then the distribution of $\partial\psi(\eta)/\partial\Sigma(\rho)$ is needed only within the perturbed region. If the global term is treated, the complete $\partial\psi(\eta)/\partial\Sigma(\rho)$ profile over all space will be required. Experience in dealing with large individual perturbations suggests that the global component is small and that it may be sufficient to approximate only the local effects.

To test out this hypothesis, a brief study was initiated to quantify the relative magnitude of the global versus local higher-order terms. By using a combination of direct computations, exact perturbation theory, and first-order

GPT, the local and global higher-order terms were computed separately. The exact delta response due to a given perturbation can be calculated by direct means using eqn. (5.4). The total local and global components can also be computed via evaluation of the integrals in eqn. (5.5). Finally, the first-order local effect is determined from first-order GPT via eqn. (5.7).

Using this technique several computations were performed to numerically evaluate the individual components of the perturbed response. The 2-D 2-group IAEA PWR benchmark problem discussed in Section IV was also utilized here (with no feedbacks). The responses chosen for this study were the eigenvalue and two zone-averaged relative power density ratios (in Zones 11 and 14). These were chosen as representative global and local responses, respectively.

Two reference cases were used; an all-rods-out (ARO) case and an all-rods-in (ARI) model. Three different perturbations were made for each reference configuration. For the ARO reference core the first two perturbation cases modeled a control rod insertion in a single zone, Zone 1 and 41, respectively. Also, as a test of the coupled interaction of two large perturbations, a third case, which was the sum of the first two control rod insertions, was made. Since this coupled interaction may not be treated in some cases (if a full set of cross derivatives is not available), it was important to characterize this case as well as the single large localized perturbation.

For the ARI reference configuration, a similar analysis was performed. In these cases, the perturbations represented rod ejection simulations. The first two perturbed cases modeled individual rods being ejected from the core and a third case modeled the interaction resulting from the two rod ejections performed simultaneously.

The numerical results of this brief study are summarized in Tables B.1 and B.2 for the ARO and ARI reference configurations respectively. The data tabulated gives the delta response ΔR_E, the first-order GPT estimate ΔR_{FO}, and an approximation of the higher-order effects, denoted as ΔR_{HOA} (for Higher-Order Approximation). The ΔR_{HOA} term only includes the first-order term and the higher-order local component. The higher-order global contribution is not included. Also, for the coupled perturbation cases, the ΔR_{HOA} terms are simply the sum of the ΔR_{HOA} components for the individual Zone 1 and Zone 41 perturbations. This was done as a test to determine how important cross derivative terms were in multiple perturbation cases.

Analysis of Tables B.1 and B.2 shows that the original hypothesis was correct. The local higher-order terms do indeed dominate the global terms for the single perturbation cases. The absolute error columns show a drastic decrease in error when the higher-order local contribution is added to the first-order GPT estimate. These data also show that first-order GPT, by itself, is totally unacceptable for perturbations of this magnitude. However, when the local higher-order contribution is treated, extremely good agreement is obtained. In fact, these data show that the global term plays a relatively small role for large localized perturbations in 2-D geometry.

For the multiple perturbation cases, the interaction between the two perturbations plays a more significant role. Here one sees that the higher-order global term is not negligible. However, even in these coupled cases, the ΔR_{HOA} estimates were an improvement over first-order GPT (in most cases).

In summary, it should be noted that the above evaluation has had two major effects on this overall study of higher-order GPT. First, it has shed some light on the relative magnitude of the higher-order components (local versus

TABLE B.1 GPT Estimates for Several Responses for the Rod-Insertion Problem in the 2-D IAEA Configuration

Response	ΔR_E	ΔR_{FO}	Abs. Error First-Order	ΔR_{HOA}	Abs. Error Higher-Order
Case 1 (Zone 1)					
P-11/P-Ave	-0.331	-0.846	0.515	-0.312	0.019
P-14/P-Ave	0.023	0.063	0.040	0.023	0.000
λ (PCM)	244.	646.	402.	244.	0.
Case 2 (Zone 41)					
P-11/P-Ave	0.265	0.622	0.357	0.240	0.025
P-14/P-Ave	0.089	0.220	0.131	0.085	0.004
λ (PCM)	359.	951.	194.	357.	2.
Case 3 (Zones 1 & 41)					
P-11/P-Ave	-0.124	-0.224	0.100	-0.072	0.052
P-14/P-Ave	0.129	0.284	0.155	0.108	0.021
λ (PCM)	683.	1597.	914.	601.	82.

Note: Rod Insertion +53% change in Σ_{a2}

Reference Responses P-11/P-Ave = 1.527
P-14/P-Ave = 1.203
λ = 0.95607

global) for various situations. Secondly, the quantitative comparisons clearly show that only the local terms are important for large individual perturbations. Depending on the intended use of the second-order derivatives, this fact may significantly reduce the cost of generating the diagonal terms of the full cross derivative matrix, $\partial^2 R/\partial\Sigma_i\partial\Sigma_j$ (where the diagonal terms are $\partial^2 R/\partial\Sigma_j^2$). In fact, it was this behavior that led to the investigation of the Green's Function Perturbation Method (as discussed in Section V).

TABLE B.2 GPT Estimates for Several Responses for the Rod-Ejection Problem in the 2-D IAEA Configuration

Response	ΔR_E	ΔR_{FO}	Abs. Error First-Order	ΔR_{HOA}	Abs. Error Higher-Order
Case 1 (Zone 1)					
P-11/P-Ave	0.516	0.197	0.319	0.563	0.047
P-14/P-Ave	-0.039	-0.012	0.023	-0.033	0.002
λ (PCM)	-425.	-155.	270.	-427.	2.
Case 2 (Zone 41)					
P-11/P-Ave	-0.295	-0.128	0.167	-0.335	0.040
P-14/P-Ave	-0.097	-0.039	0.058	-0.103	0.006
λ (PCM)	-579.	215.	364.	-583.	4.
Case 3 (Zones 1 & 41)					
P-11/P-Ave	0.122	0.069	0.053	0.229	0.106
P-14/P-Ave	-0.114	-0.051	0.063	-0.137	0.023
λ (PCM)	-866.	-369.	497.	-1010	144.

Note: Rod Ejection -35% change in Σ_{a2}

Reference Responses P-11/P-Ave = 1.531
P-14/P-Ave = 1.111
λ = 0.97161

APPENDIX C VERIFICATION OF GREEN'S FUNCTION PERTURBATION METHOD

A small test program was written to validate the Green's Function Perturbation Method as presented in Section V of this report. The model utilized in this code is a five-region 1-group 1-D Cartesian geometry configuration. The reference core is homogeneous so the ΔL operator [see eqn. (5.24)] is zero for this case. The Green's functions for this simple situation are:

Finite Green's Function

$$G_{>}(x,x') = \frac{1}{2D\kappa} \frac{\sinh \kappa(x_1 - x)}{\cosh \kappa(x_1 - x')} \qquad \text{for } x > x'$$

$$G_{<}(x,x') = \frac{1}{2D\kappa} \frac{\sinh \kappa(x_0 - x)}{\cosh \kappa(x_0 - x')} \qquad \text{for } x < x'$$

Infinite Green's Function

$$G_{>}(x,x') = \frac{1}{2D\kappa} \exp\Big(-\kappa(x - x')\Big) \qquad \text{for } x > x'$$

$$G_{<}(x,x') = \frac{1}{2D\kappa} \exp\Big(\kappa(x - x')\Big) \qquad \text{for } x < x'$$

where $\kappa^2 = \Sigma_a/D$ and $x_0 = 0.0$ and x_1 = length of 1-D configuration. Using these expressions, the code evaluates eqns. (5.31)-(5.37) to obtain an estimate of $\partial\psi(\eta)/\partial\Sigma(\rho)$ for several perturbations. Several cases were run and the zone-averaged values of $\Delta\psi/\psi$ for these cases were compared with direct computations.

Summary results from one particular example are given in Tables C.1 and C.2. This case models a control rod inserted into the central zone of the reactor. Table C.1 shows how the delta zone-averaged flux (in the zone of the perturbation) varies with the magnitude of $\Delta\Sigma_a/\Sigma_a$. It also compares direct

TABLE C.1 Comparison of Delta Flux Predictions for Rod Insertion in Central Zone of Simple 1-D Model

$\%\Delta\Sigma_a/\Sigma_a$	Average Percent $\Delta\psi/\psi$ in Central Region		
	Direct	GF Finite	GF Infinite
1.0	-1.2	-1.2	-1.3
5.0	-5.8	-6.0	-6.6
10.0	-11.3	-12.0	-13.2
20.0	-21.4	-24.0	-26.5
40.0	-38.0	-47.9	-53.0

Note that the Green's Function (GF) results used 15 terms.

computations with the Green's function method developed here. Table C.1 also contrasts the new method with the finite versus infinite Green's functions. Table C.2 illustrates the behavior of the Green's function technique with respect to the number of terms used in the series expansion.

Several interesting observations can be made from the data contained here. For this model, the $\Delta\psi/\psi$ variation is nearly linear up to around 20% $\Delta\Sigma_a/\Sigma_a$. This result means that the first-order estimate of the perturbed flux will be accurate over a wide range. Also of major importance is the benchmarking of the basic approach. The main reason for using the finite Green's function is that, for this case, the predicted $\Delta\psi$ should be exact for small material perturbations and a large number of terms in the series expansion. As seen in Table C.1, this result has been achieved for the 1% perturbation case. Thus, the methodology is theoretically sound. Once the method has been verified, one can begin making approximations to the original theoretical foundation.

TABLE C.2 Delta Flux Convergence Rates for Rod Insertion in Central Zone of Simple 1-D Model

Number of Terms	Average Percent $\Delta\psi/\psi$ in Central Region for 5% $\Delta\Sigma_a/\Sigma_a$	
	GF Finite	GF Infinite
1	-1.8	-1.8
2	-3.0	-3.1
3	-3.8	-4.0
4	-4.4	-4.6
5	-4.9	-5.1
6	-5.2	-5.5
7	-5.4	-5.8
8	-5.6	-6.0
9	-5.7	-6.2
10	-5.8	-6.3
15	-6.0	-6.6

Two such approximations are addressed in Tables C.1 and C.2; the use of the infinite Green's function and the reduction in the number of expansion terms. For a given number of terms, the runtime with the finite Green's function was about three times longer than with the infinite Green's function (because the exponential function is easier to evaluate than the cosh and sinh functions). Even with this approximation, the infinite Green's function results are quite good for the case at hand. Thus, it appears that the use of the infinite Green's function will not cause major problems. In addition, Table C.2 shows that convergence is quite rapid. It only takes about 5-6 terms to get to 80% of

the final predicted $\Delta\psi/\psi$, and a 20% error in $\Delta\psi/\psi$ should be acceptable for estimating the second-order response derivatives for most applications.

The above results are quite encouraging. They show that the Green's function approach is feasible from basic principles, that the use of the infinite Green's function does not introduce significant error, and that the series solution technique converges to an acceptable level with only a few terms. However, one must keep in mind the simplicity of the model used in the above computations. Thus, the method appears to have considerable potential, but further work is required before the real benefits of this new technique can be fully evaluated.

VITA

John Richard White was born in Millinocket, Maine on April 19, 1951. He attended elementary schools in that town and graduated from Stearns High School in June 1969. He spent his first year of college at the University of Maine, Orono. In May 1971, the author joined the United States Air Force and worked as an electronics technician for three years.

In the fall of 1974, the author started his sophomore year at the University of Lowell and in 1977 he graduated with two Bachelor degrees; one in Nuclear Engineering and the other in Electrical Engineering. He then was employed for almost six years at Oak Ridge National Laboratory where he was involved in reactor physics methods development work. During that time, he attended the University of Tennessee, Knoxville and received his Master's degree in Nuclear Engineering in March 1980.

He continued his graduate studies at the University of Tennessee and after completing all course work (in 1982) he began teaching in the Nuclear Engineering Department at the University of Lowell in Lowell, Massachusetts. He completed his Doctoral Dissertation and received the Doctor of Philosophy degree with a major in Nuclear Engineering in the spring of 1987.

His immediate plans are to continue his research and teaching career as a professor in the Nuclear Engineering Department at the University of Lowell.